

MAX-PET:

Demonstration of a novel PET concept

Chiara Casella, ETH Zurich

DPNC - Université de Genève, March 14th 2012

Outline

AX-PET : AXial Positron Emission Tomography (PET)

- **Brief introduction about PET** (Positron Emission Tomography)
- **Axial concept**
 - What is it ? Why?
- **AX-PET detector**
 - choice of the detector elements
 - AX-PET modules
 - “demonstrator” for a PET scanner
- **AX-PET detector performance**
 - from characterization measurements with ^{22}Na sources
- **Simulations**
- **Tomographic image reconstruction**
 - description of the reconstruction methods
 - measurements campaigns with phantoms and radiotracers
 - reconstructed images
- **Perspectives**
 - preliminary results with **Digital Si-PM** as alternative photodetectors
- **Conclusions**

AX-PET in the context of HEP

- ▶ Long tradition of using technologies from High Energy Physics into other fields, and particularly medical applications.
- ▶ AX-PET : small size calorimeter, using scintillating crystals, WLS, photodetectors “borrowed” from HEP

Selection of most relevant AX-PET papers :

Novel Geometrical Concept of a High Performance Brain PET Scanner Principle, Design and Performance Estimates

J. Seguinot et al, Nuovo Cimento C Vol 29, No 4, pp 429-463 (2006)

axial concept,

Hybrid Photo Diodes (HPD)
readout

High precision axial coordinate readout for an axial 3-D PET detector module using a wave length shifter strip matrix

A. Braem et al, NIM A 580 (2007), 1513-1521

WLS strips

Wavelength shifter strips and G-APD arrays for the read-out of the z-coordinate in axial PET modules

A. Braem et al, NIM A 586 (2008), 300-308

G-APD as photodetectors

The AX-PETdemonstrator—Design, construction and characterization

P. Beltrame et al, NIM A 654 (2011) 546-559

Characterization
& performance

The AX-PET Concept: New Developments And Tomographic Imaging

P.Beltrame et al, 2011 IEEE NSS Conference Record MIC 22-5

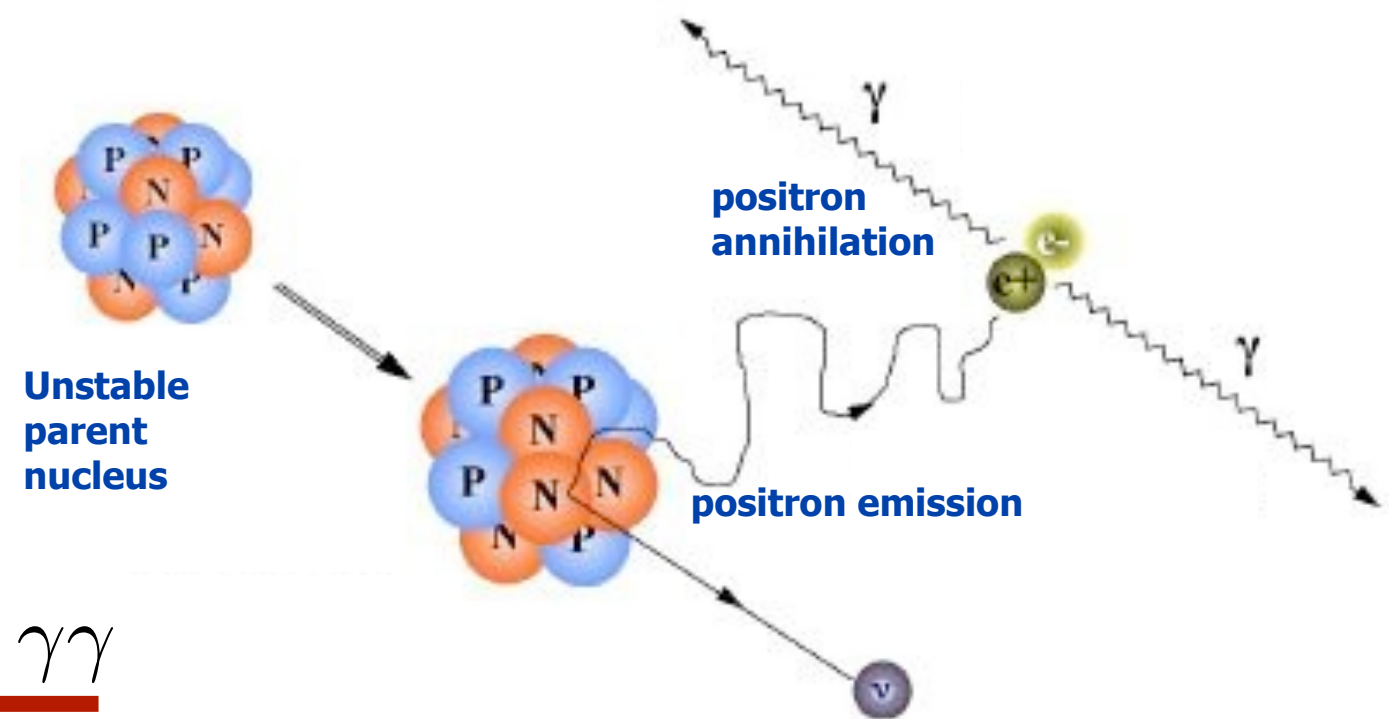
Tomographic images

for more details : <https://twiki.cern.ch/twiki/bin/view/AXIALPET/WebHome>

Positron emission / annihilation

- basis of the PET system **Positron Emission :** $p \rightarrow n + e^+ + \nu_e$
- β^+ decay of different radionuclides

Radionuclide	Half life	Emax_e+(MeV)
¹¹ C	20.4 min	0,96
¹⁵ O	122 sec	1,73
¹⁸ F	109,8 min	0,63
²² Na	2.6 years	0,55



- **Positron Annihilation :** $e^+ e^- \rightarrow \gamma\gamma$

2 photons emitted

► “back - to - back”

► $E\gamma = 511 \text{ keV}$

Physics of the positron annihilation => fundamental limits to the spatial resolution of PET

► Finite positron range (ρ)

annihilation position \neq emission point

ρ depends on the energy of the positron (i.e. on the radioisotope)

► Non-collinearity of the 2 photons

residual momentum of the e^+e^- at the annihilation

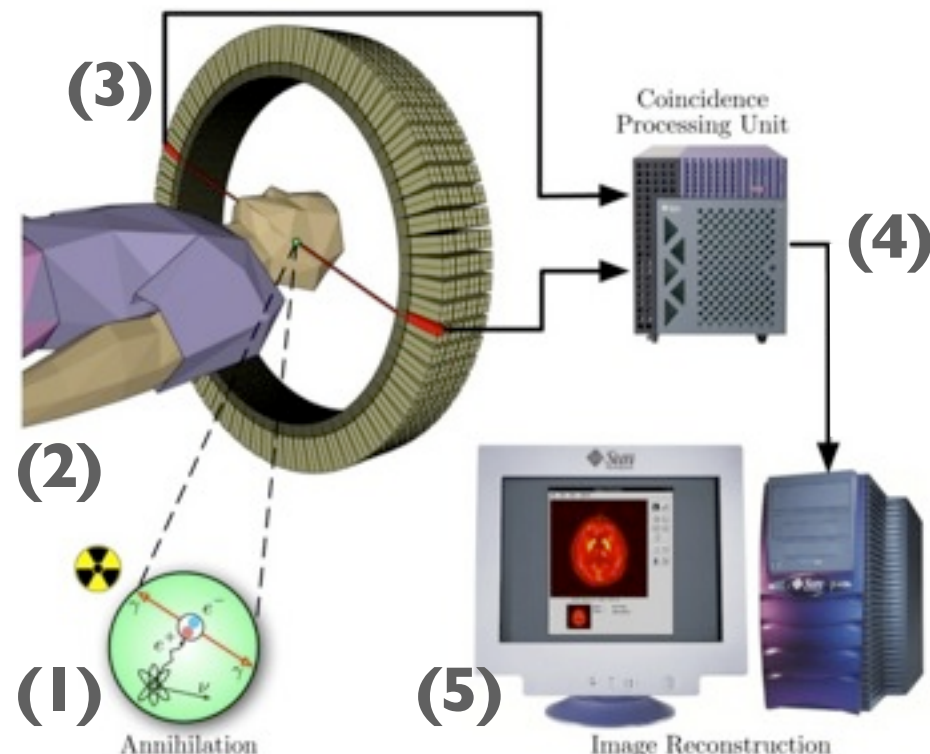
the 2 photons are emitted with a small deviation from 180° ($\Delta\theta \sim 0.5^\circ$)

blurring of the spatial resolution $R_{FWHM} \sim 0.0022 \times D [\text{mm}]$

Positron Emission Tomography : General principles

PET detector principle :

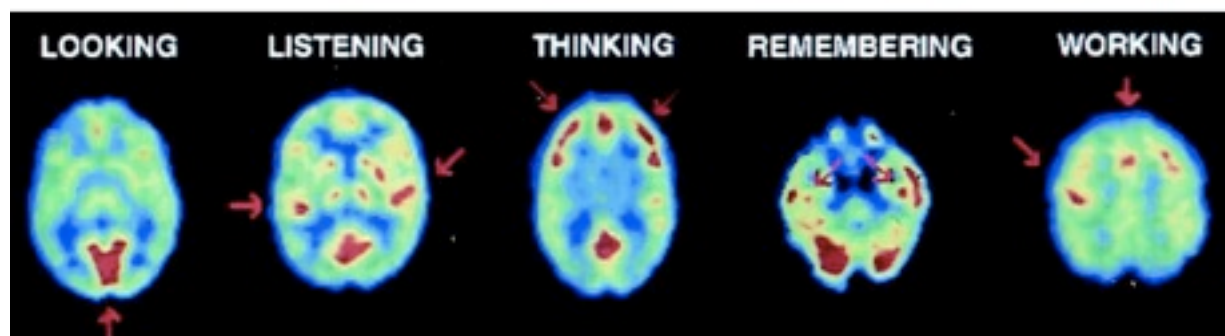
coincidence of 2 photons of defined energy (511 keV) and emitted on the same line (“back to back”)



- (1) Inject the **radiotracer into the body**
- (2) Wait for uptaking period
- (3) Start the acquisition (i.e. **detection of coinc. events**)
- (4) Feed the data into the reconstruction algorithms
- (5) **image of the activity concentration**

full body / brain scanners

- ▶ clinical applications
 - ▶ oncology (tumor diagnosis)
 - ▶ neurology (e.g. brain disease diagnosis)
 - ▶ map normal human brain / heart functions

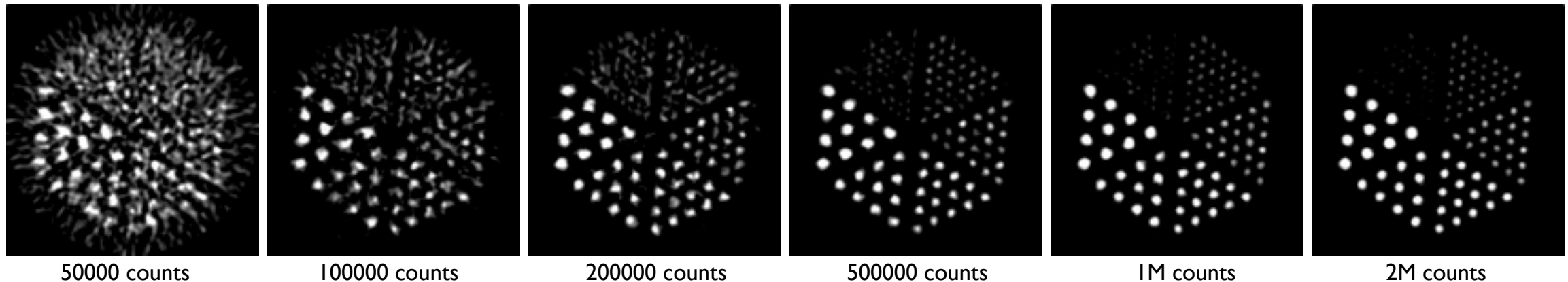


small animal scanners

- ▶ pre-clinical studies
 - ▶ cancer research
 - ▶ new tracers development
 - ▶ pharmacokinetics

Requirements for an ideal PET

number of counts does matter !!!

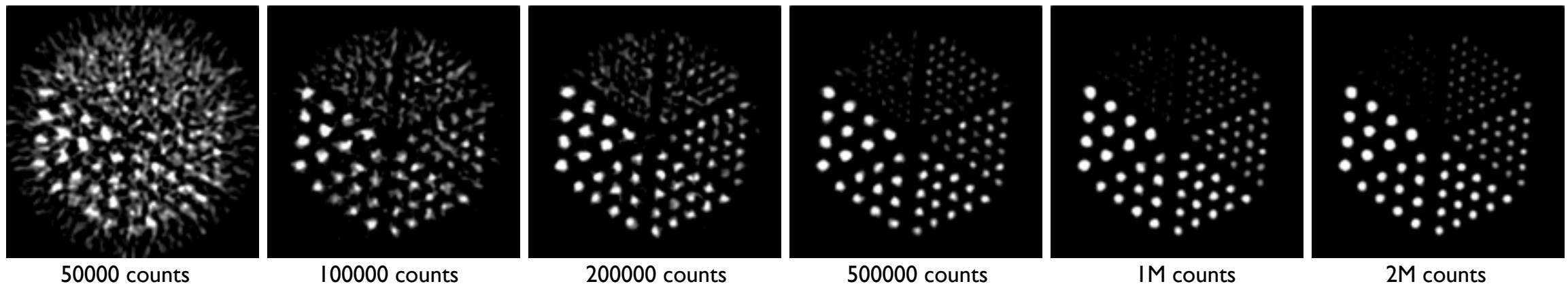


A.Del Guerra, CERN Academic Training 2009

- ▶ how to improve counting statistics ?
 - ▶ increase radio-tracer concentration
 - ▶ extend the scan duration time
- ▶ **OPTIMIZED DETECTOR SENSITIVITY**
(geometry / materials)
- ▶ **HIGH SPATIAL RESOLUTION** (=> be able to resolve small structures)
- ▶ **GOOD TIMING RESOLUTION** (small coincidence window => reduce random coincidences)
- ▶ **GOOD ENERGY RESOLUTION** (=> reject scattering events in the body)

Requirements for an ideal PET

number of counts does matter !!!

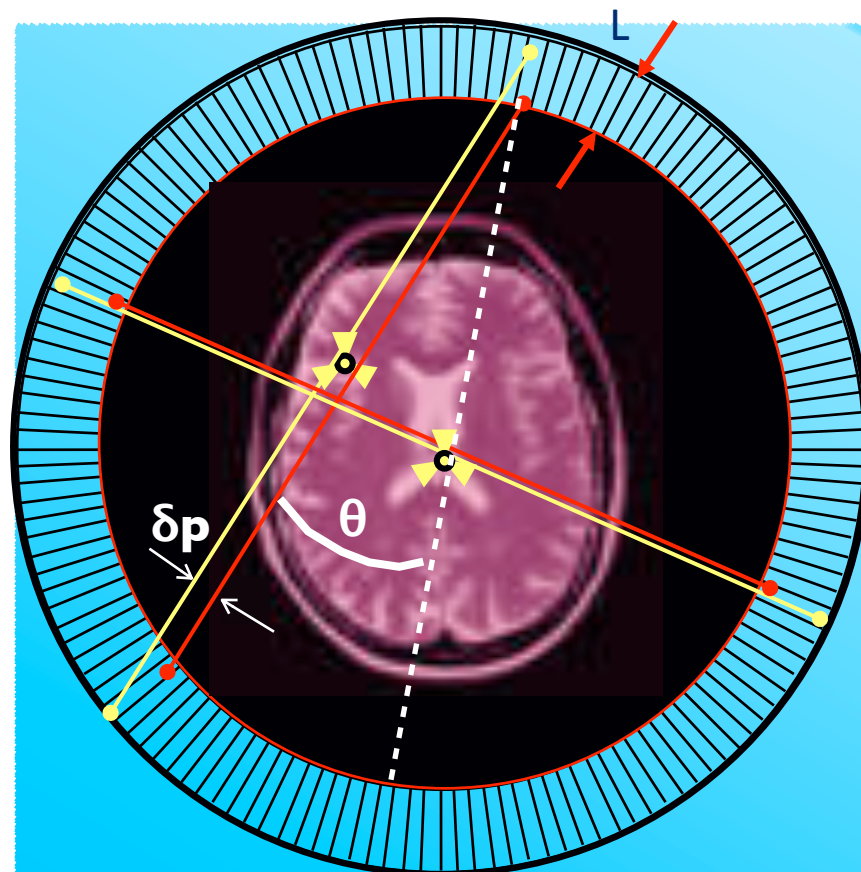


A.Del Guerra, CERN Academic Training 2009

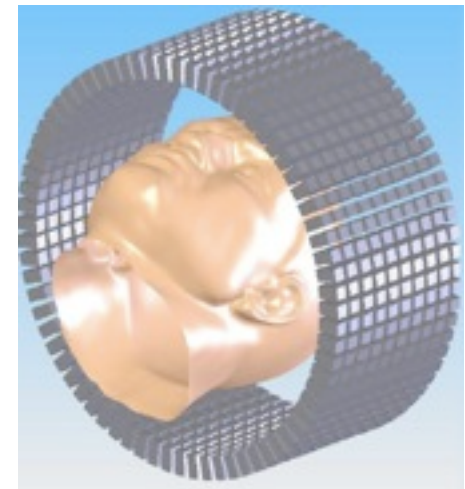
- ▶ how to improve counting statistics ?
 - ▶ increase radio-tracer concentration
 - ▶ extend the scan duration time
- ▶ **OPTIMIZED DETECTOR SENSITIVITY**
(geometry / materials)
- ▶ **HIGH SPATIAL RESOLUTION** (=> be able to resolve small structures)
- ▶ **GOOD TIME RESOLUTION** (small coincidence window => reduce random coincidences)
- ▶ **GOOD ENERGY RESOLUTION** (=> reject scattering events in the body)

High resolution vs high sensitivity

in “conventional”
PET scanners :



scintillator based
radial arrangement



$$\epsilon = 1 - e^{-\mu \cdot L}$$

max interaction efficiency,
long L

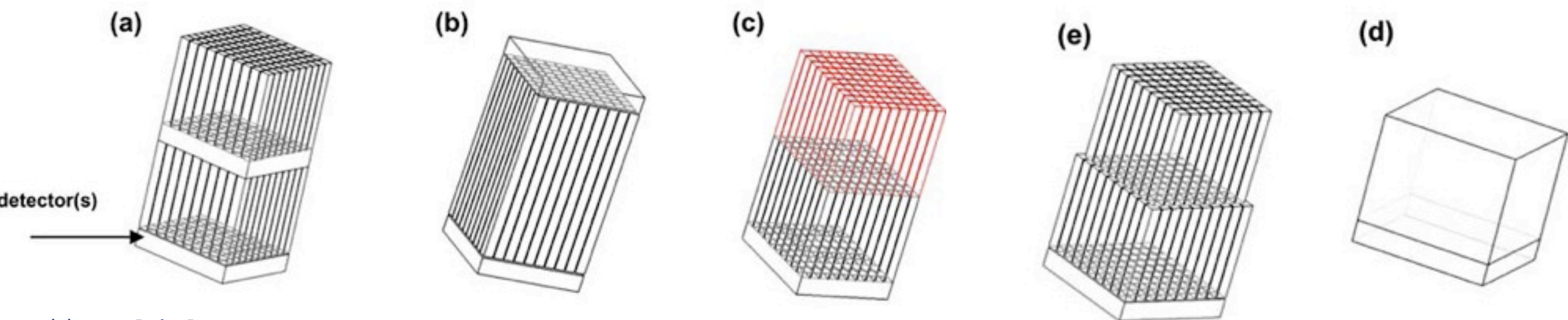
$$\delta p = L \cdot \sin \theta$$

min parallax error
- deterioration of the spat. resol.
- non uniformity in the field of view
short L

- ▶ always a compromise between
- ▶ good spatial resolution (small L, small δp)
- ▶ good detection efficiency (long L)
- ▶ solution : add DOI (Depth Of Interaction) information
 - ▶ several attempts / different strategies

Conventional PET schemes

DOI attempts :



(a) multiple
crystals/
photodetector
layers

(b) dual-ended
photodetectors
DOI from the ratio of
the 2 PD responses

(c) Phoswich design
different types of
crystals with diff decay
times
=> DOI from pulse
shape discrimination

(d) monolithic. Iterative stat.
models with DOI from light output
intensity and/or light spread profiles

(e) dual layer offset
position.
DOI from different light output
profiles

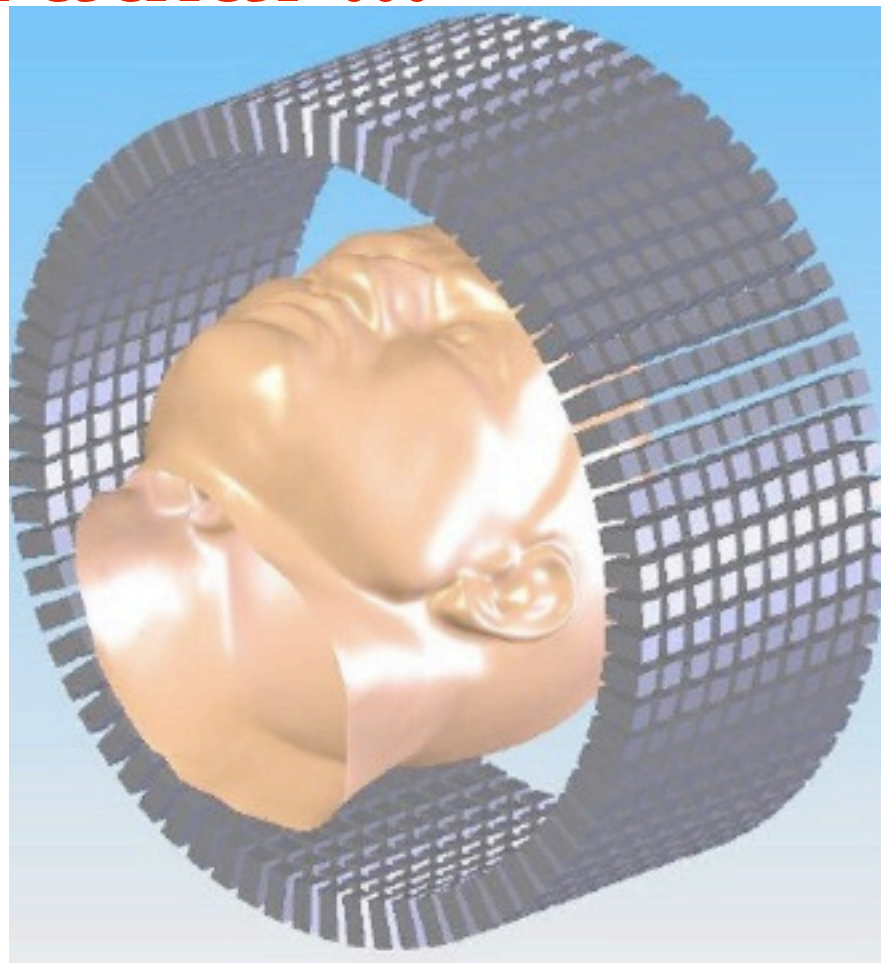
only partial DOI information !

need a precise 3D identification of the photon interaction point

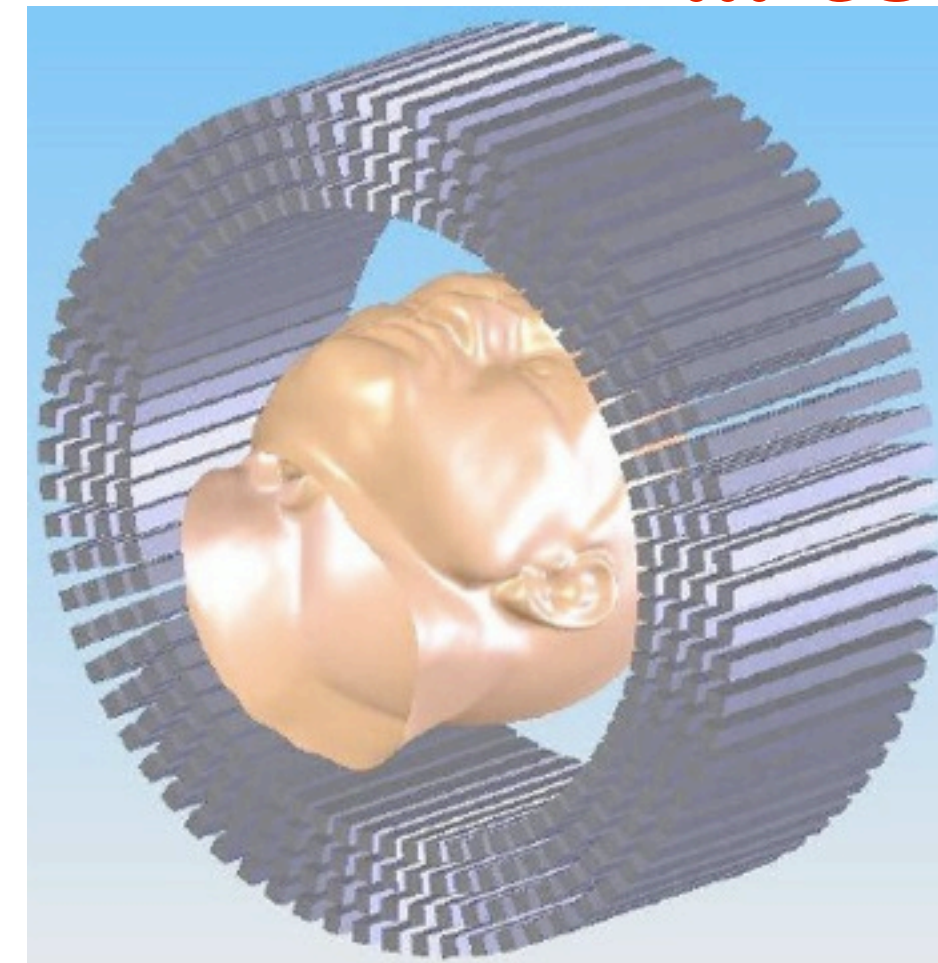
The AXIAL concept

AX-PET approach to the DOI problem : **change the geometry !**

from radial ...



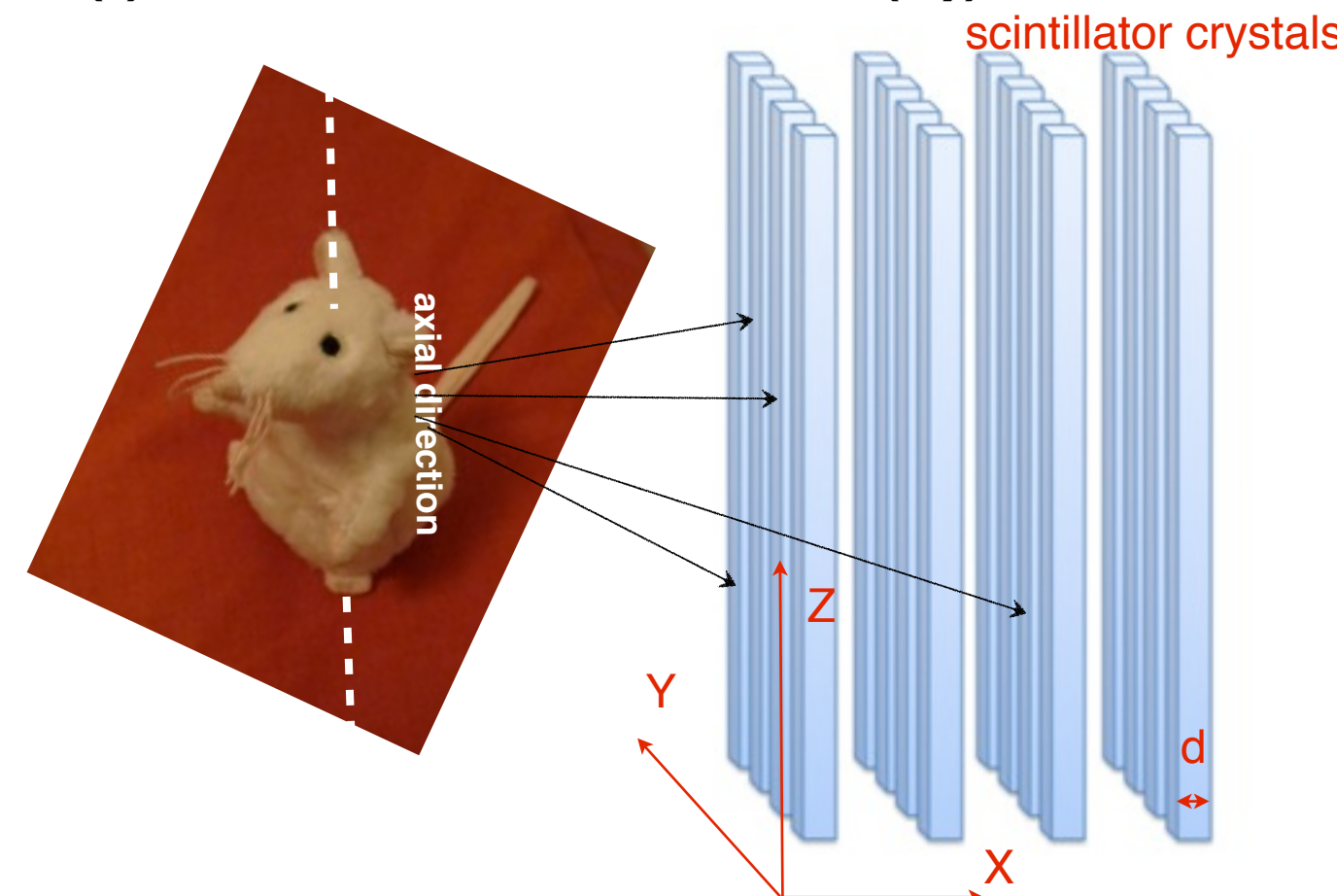
... to axial !



- ▶ long and axially oriented crystals
- ▶ DOI information = position of the hit crystal

The detector concept

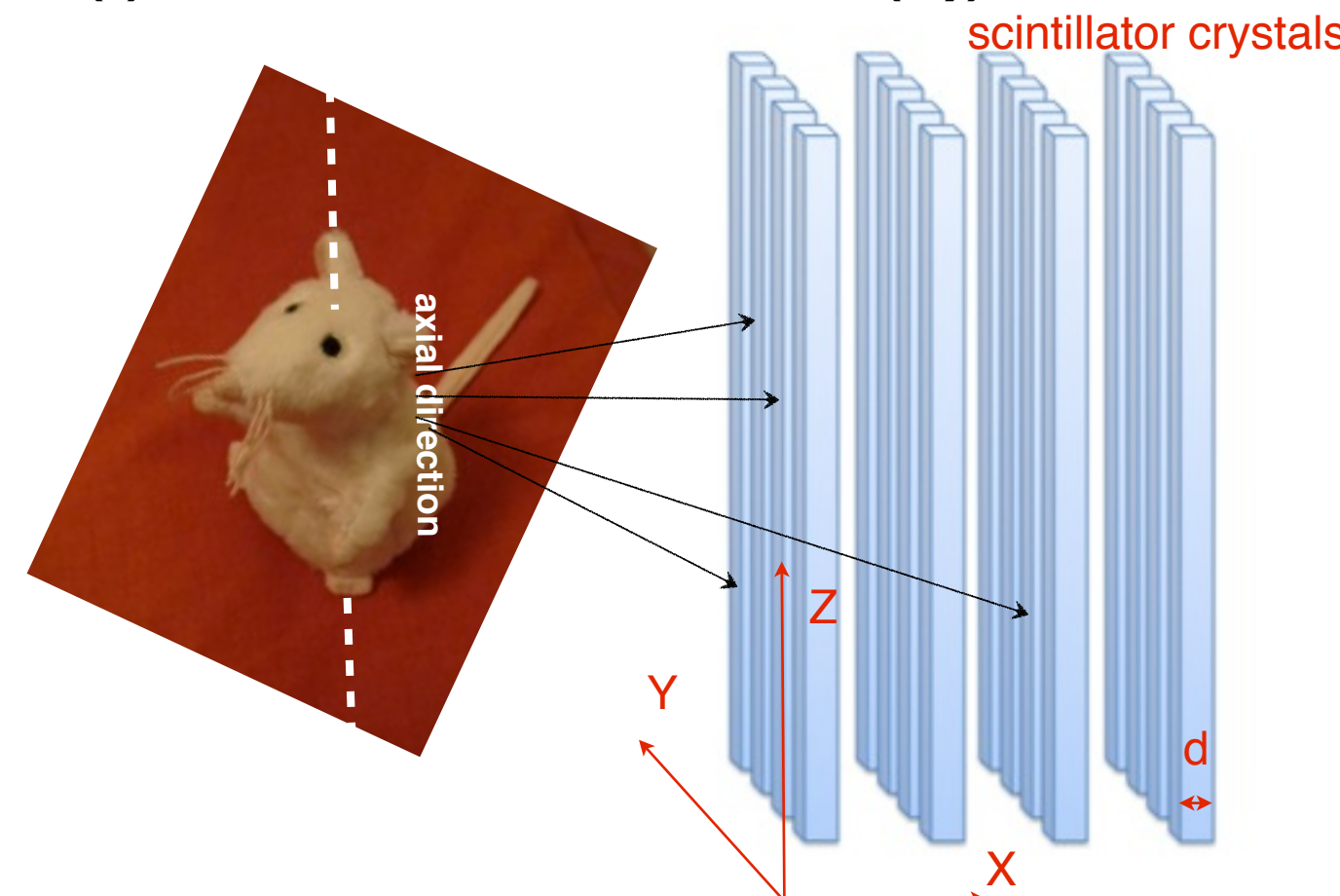
(I) TRANSAXIAL COORDINATE (x,y)



- Transaxial coordinate: from position of the hit crystal
- Transaxial resolution = $d/\sqrt{12} \text{ FWHM}$
- To **increase spatial resolution** => Reduce crystals size (d)
- To **increase sensitivity** => Add additional layers

The detector concept

(1) TRANSAXIAL COORDINATE (x,y)



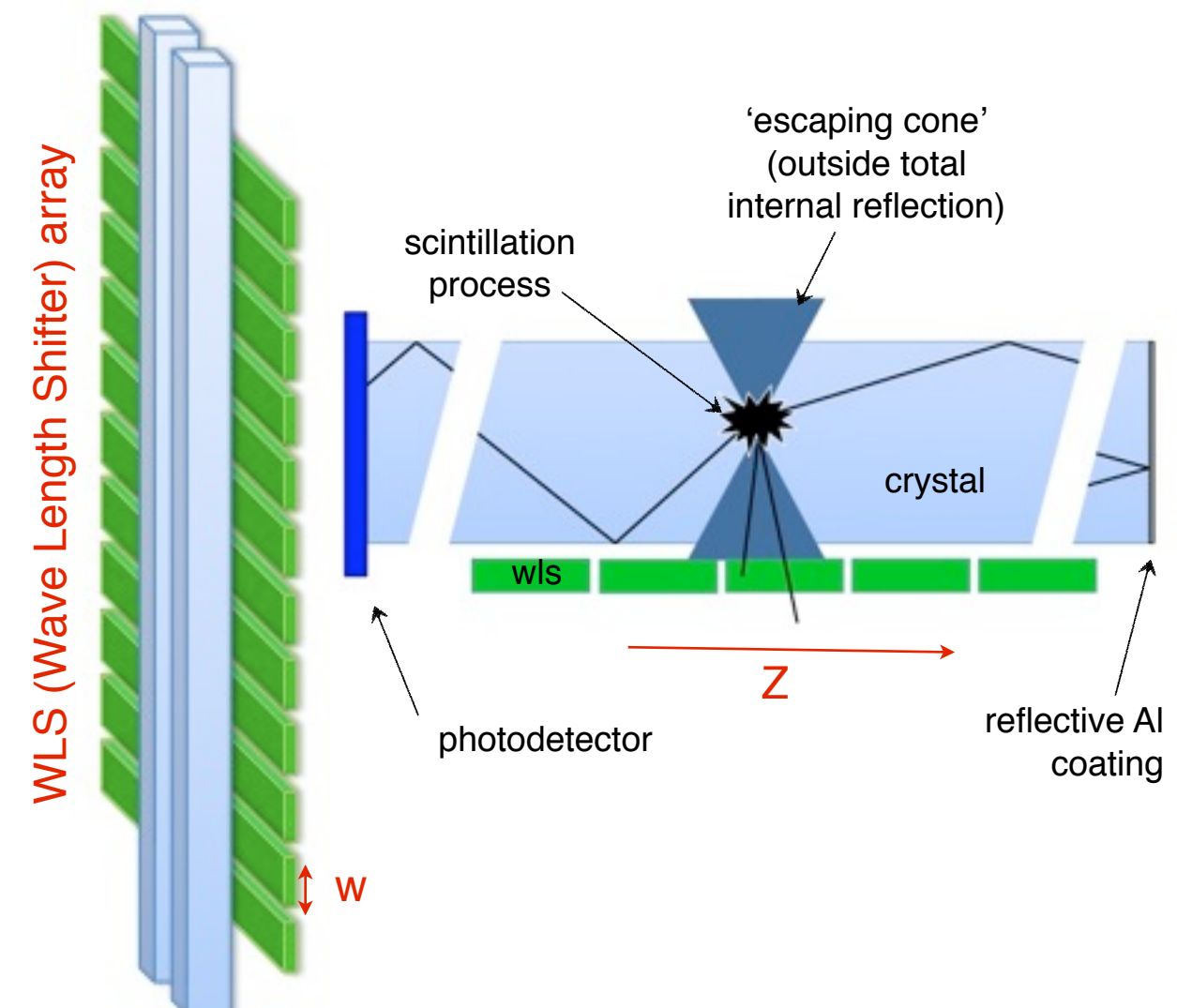
- Transaxial coordinate: from position of the hit crystal

- Transaxial resolution = $d/\sqrt{12}$ FWHM

- To increase spatial resolution => Reduce crystals size (d)

- To increase sensitivity => Add additional layers

(2) AXIAL COORDINATE (z)

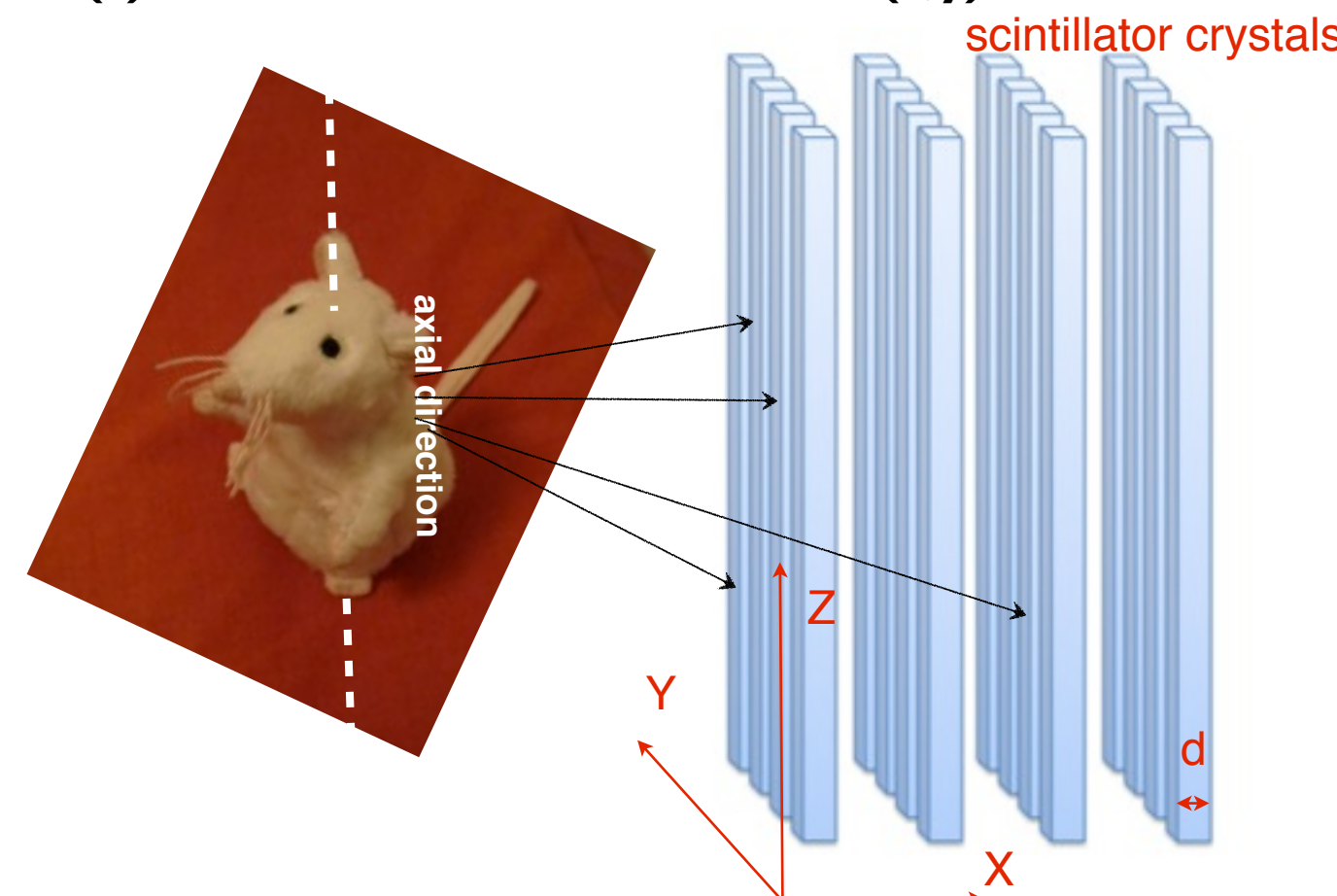


- Axial coordinate : center of gravity method

- Axial resolution < w

The detector concept

(1) TRANSAXIAL COORDINATE (x,y)



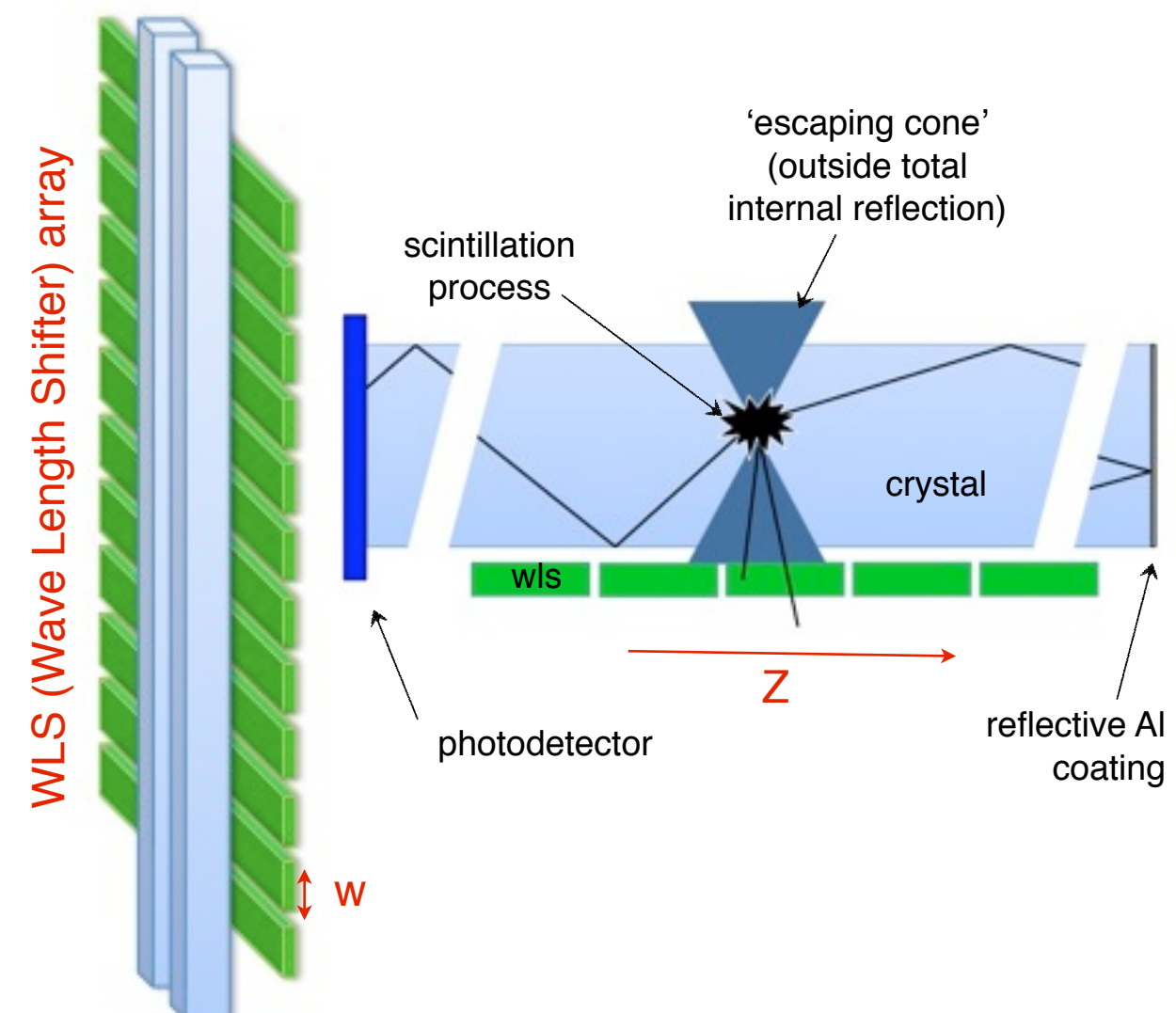
- Transaxial coordinate: from position of the hit crystal

- Transaxial resolution = $d/\sqrt{12}$ FWHM

- To increase spatial resolution => Reduce crystals size (d)

- To increase sensitivity => Add additional layers

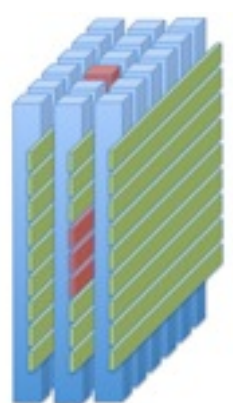
(2) AXIAL COORDINATE (z)



- Axial coordinate : center of gravity method

- Axial resolution < w

**3D localization of the photon interaction point
without compromising between spatial resolution and sensitivity**



AX-PET Collaboration



Instituto Nazionale di Fisica Nucleare (INFN)
Sezione di Bari, I-70122 Bari, Italy



Università and INFN Cagliari
Cagliari, Italy



Ohio State University (OSU)
Columbus, Ohio 43210, USA



European Organization for Nuclear Research (CERN)
PH Department, CH-1211 Geneva, Switzerland



University of Michigan
Ann Arbor, MI 48109 USA



University of Oslo
NO-0316 OSLO, Norway

Instituto Nazionale di Fisica Nucleare (INFN)
Sezione di Roma, University of Rome, La Sapienza, 00185, Italy



Instituto de Física Corpuscular (IFIC)
University of Valencia, 46071, Spain



Tampere University of Technology
FI-33100 Tampere, Finland

AX-PET GOAL : PET demonstrator

Goal of the AX-PET collaboration:

Build and fully characterize a “**demonstrator**” for a PET scanner based on the axial concept. Assess its performances.

Demonstrator =>

Two identical AX-PET modules, used in coincidence

Characterization / Performance =>

- test each individual module in a dedicated setup
- characterization in the coincidence setup
- reconstruction of the images of extended objects
- simulations



Detector choice: Scintillator

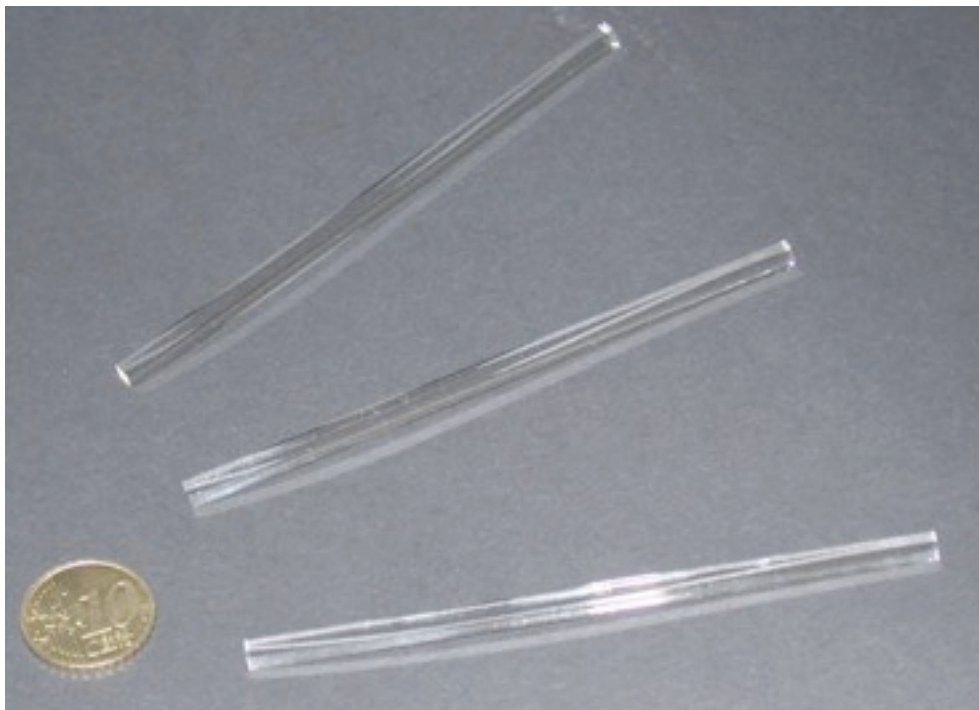
detect photons, $E_\gamma = 511 \text{ keV}$

- => • inorganic scintillator
• high Z , high ρ

bare scintillating crystals with escaping light =>

- non hygroscopic
- nude crystals (i.e. unwrapped, uncoated)
- perfectly polished surfaces ; sharp edges

LYSO crystals ($\text{Lu}_{1.8}\text{Y}_{0.2}\text{SiO}_5$: Ce) Prelude 420 from Saint Gobain :



$Z_{\text{Lu}} = 71$	
Properties –	
Density [g/cm ³]:	7.1
Hygroscopic	no
Attenuation length for 511keV (cm):	1.2
Wavelength of emission max.[nm]	420
Refractive index@emission max.	1.81
Decay time [ns]:	41
Energy resolution [%]:	8.0
Light yield [photons/keV γ]:	32
Average temperature coefficient from 25 to 50° C (%/°C):	-0.28
Photoelectron yield [% of NaI(Tl)] (for γ -rays)	75

- lyso bars : **3 x 3 x 100 mm³** each
- Al coated on the non-readout face ($R \sim 80-85\%$)
- measured : $\lambda_{\text{opt}} = (412 \pm 31) \text{ mm}$; $(\Delta E/E)_{\text{intr}} = (8.3 \pm 0.5) \text{ \% FWHM}$, @511 keV

^{176}Lu is a naturally radioactive β emitter:
($A \sim 39 \text{ Bq/g}$; β -decay followed by a γ -cascade)
useful for the calibration

Detector choice:WLS strips

- requirement : high absorption of the crystal scintillation photons (blue)

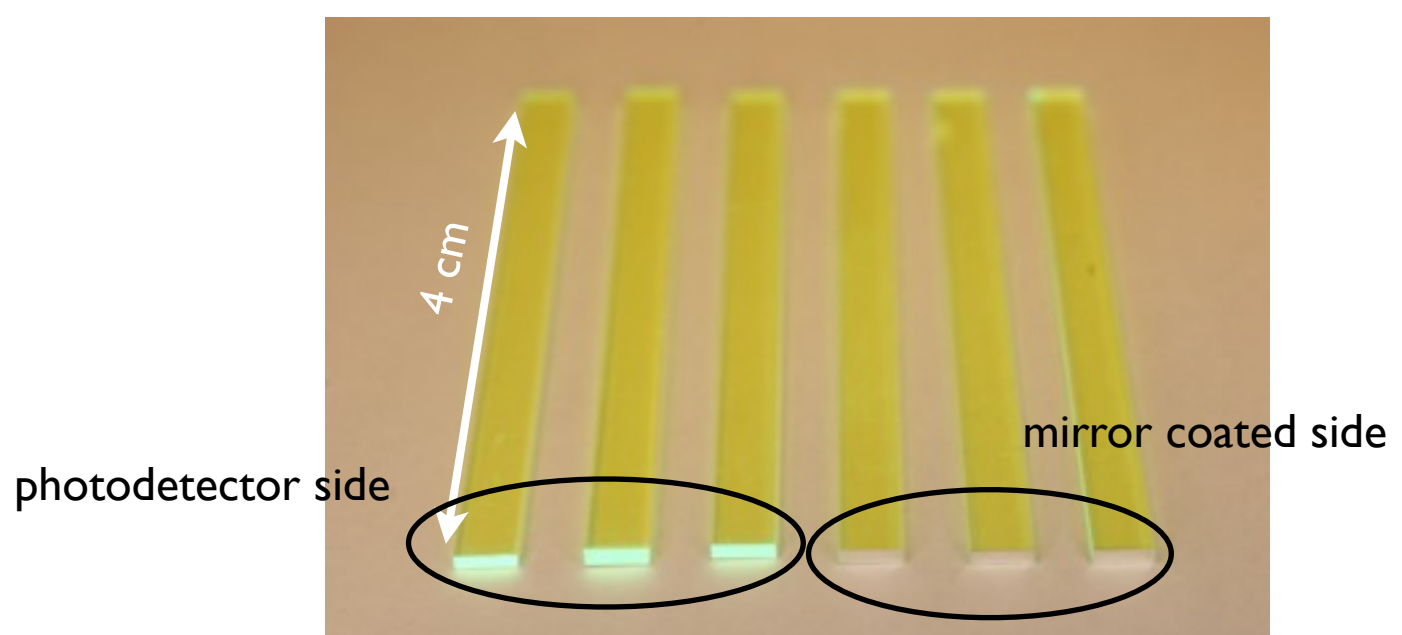
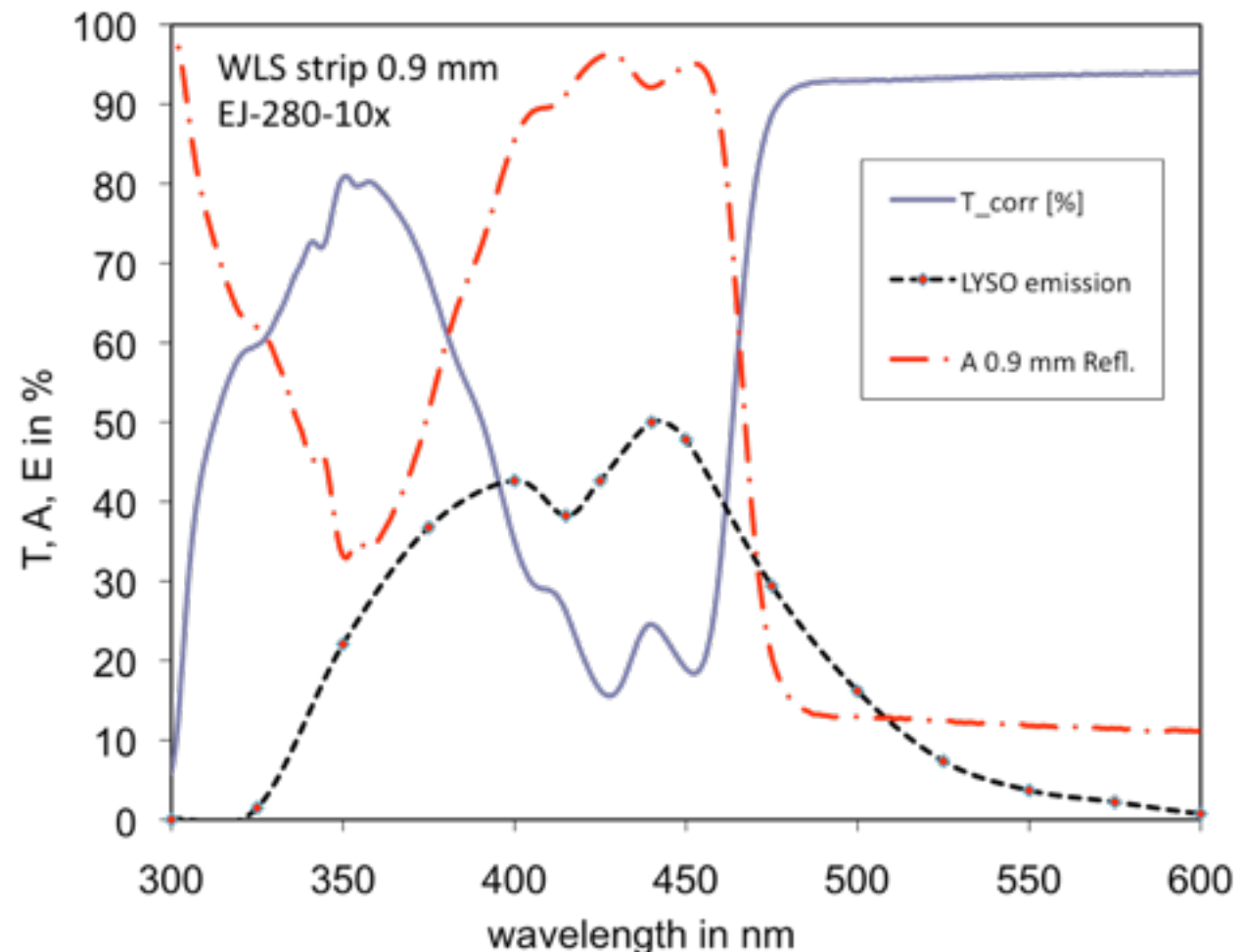
- **EJ-280-10x from Eljen Technology**

- blue to green WLS
- highly doped ($\times 10$ higher dye concentration than standard) to maximize the absorption (absorption length _ blue light ~ 0.4 mm)

- each WLS strip : **$3 \times 0.9 \times 40$ mm 3**

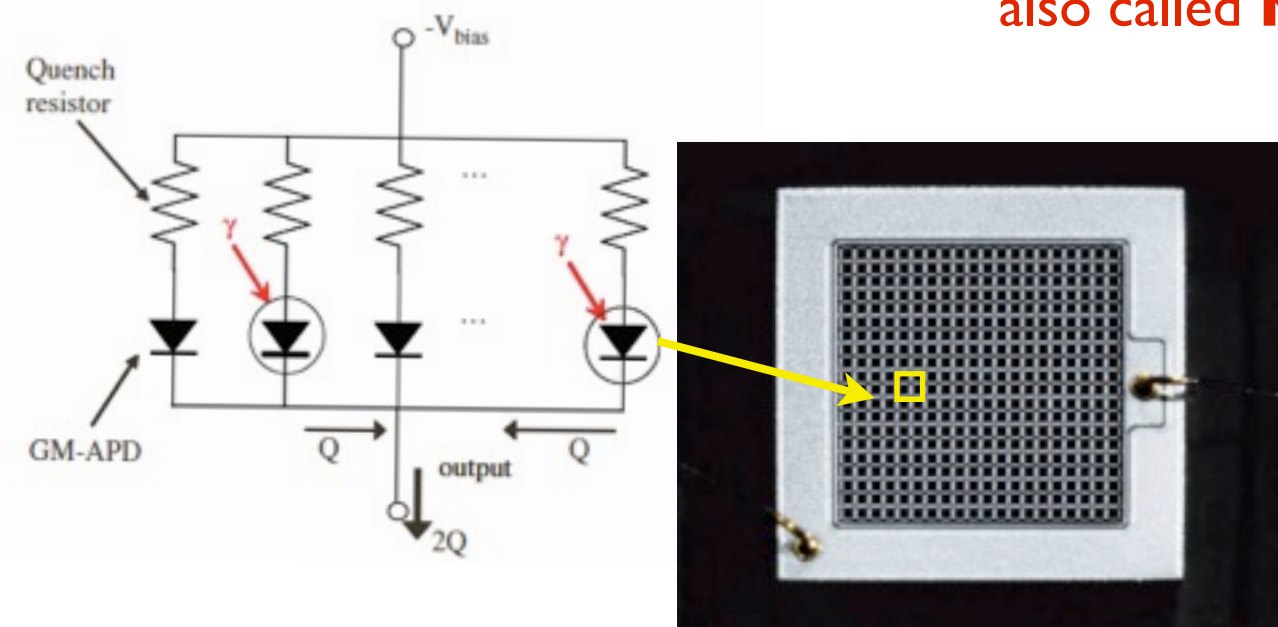
- decay time = 8.5 ns

- measurements : $\lambda_{\text{opt}} = (188 \pm 36)$ nm

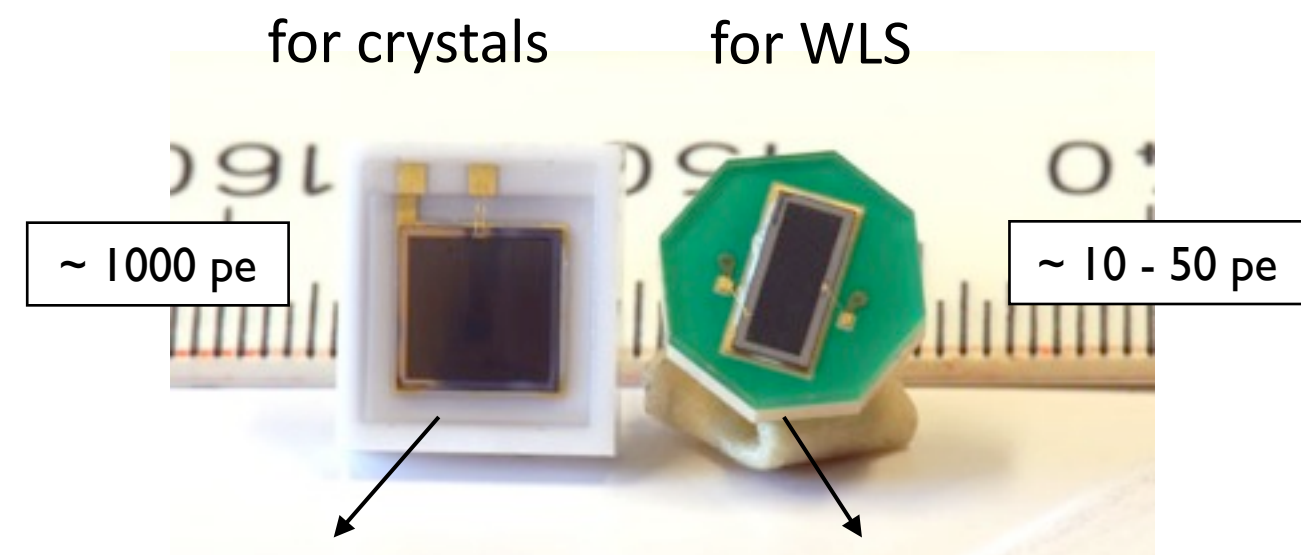


Detector choice: Photodetectors

- ▶ newest frontier in photo-detection: **SiPM** (Si photomultipliers)
also called **G-APD** (Geiger-mode APD)
also called **MPPC** (Multi Pixel Photon Counter) - from Hamamatsu



- ▶ array of commonly biased APD used in Geiger mode
- ▶ output : analogue sum of all the firing APD cells
- ▶ excellent photon counting capabilities ✓
- ▶ high gain (10^5 to 10^6) at low bias V (~ 70V) ✓
- ▶ advantages of a Si sensor:
 - ▶ high QE ✓
 - ▶ compactness ✓
 - ▶ insensitive to magnetic field (MRI comp.) ✓
 - ▶ temperature dependent ✓
 - ▶ dark rate (~ 1 MHz @ thr = 0.5 pe) ✓

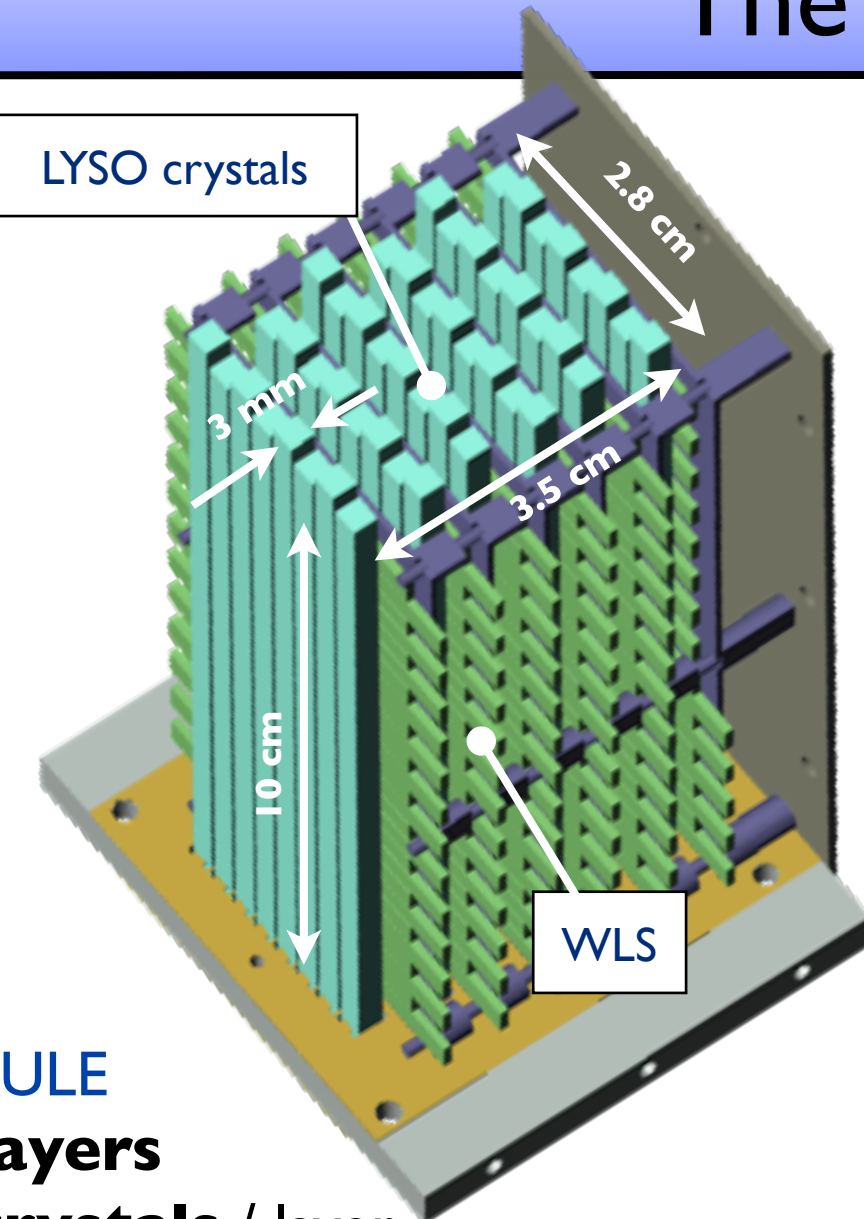


- MPPC S10362-33-050C :**
- 3x3 mm² active area
 - 50 μm x 50 μm pixel
 - 3600 pixels
- MPPC 3.22×1.19 Octagon-SMD :**
- 1.2 x 3.2 mm² active area
 - 70 μm x 70 μm pixel
 - 782 pixels
 - custom made units

	crystal MPPC	WLS MPPC
type	S10362-33-050c	custom tailored
charge gain G	$6 \cdot 10^5$	$1 \cdot 10^6$
dG/dV	$55 \cdot 10^4 \text{ V}^{-1}$	$110 \cdot 10^4 \text{ V}^{-1}$
noise rate at 0.5 pe	4.7 MHz	3.2 MHz
noise rate at 1.5 pe	0.9 MHz	0.5 MHz

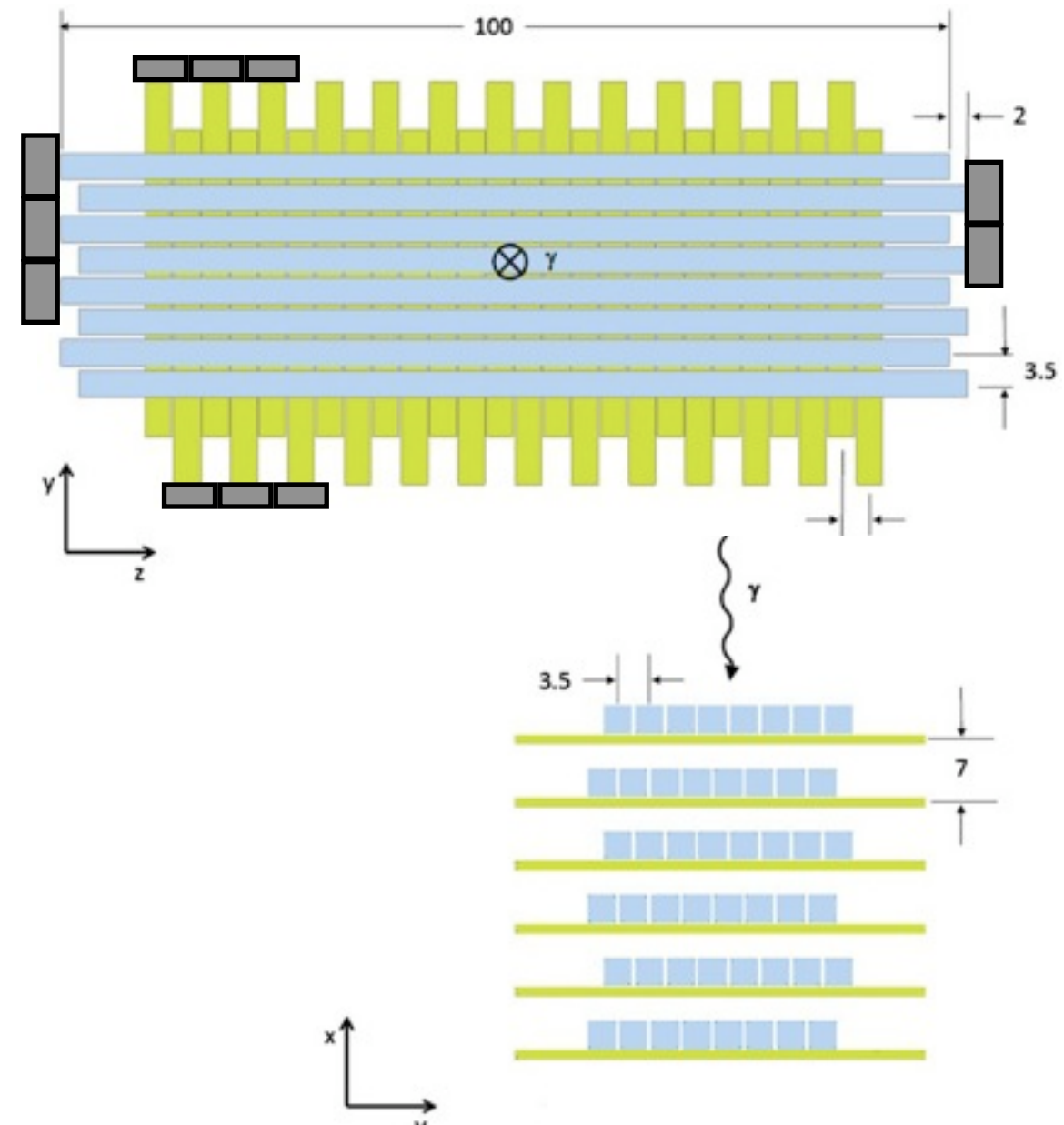
Table 1: Main characteristics of the MPPCs. Gain and noise rates refer to temperature of 25°C.

The AX-PET module

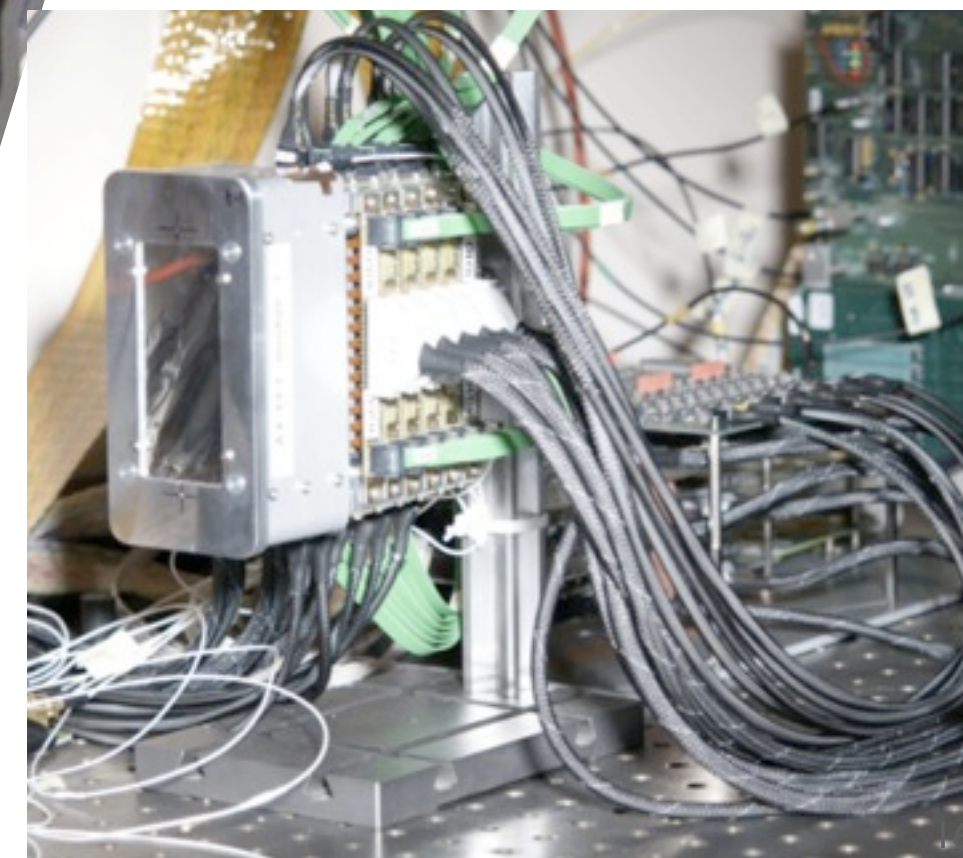
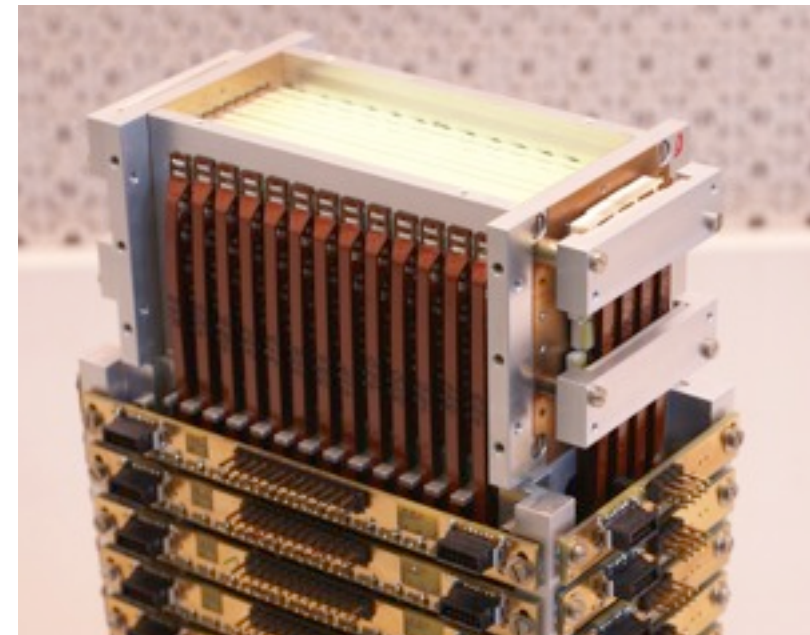
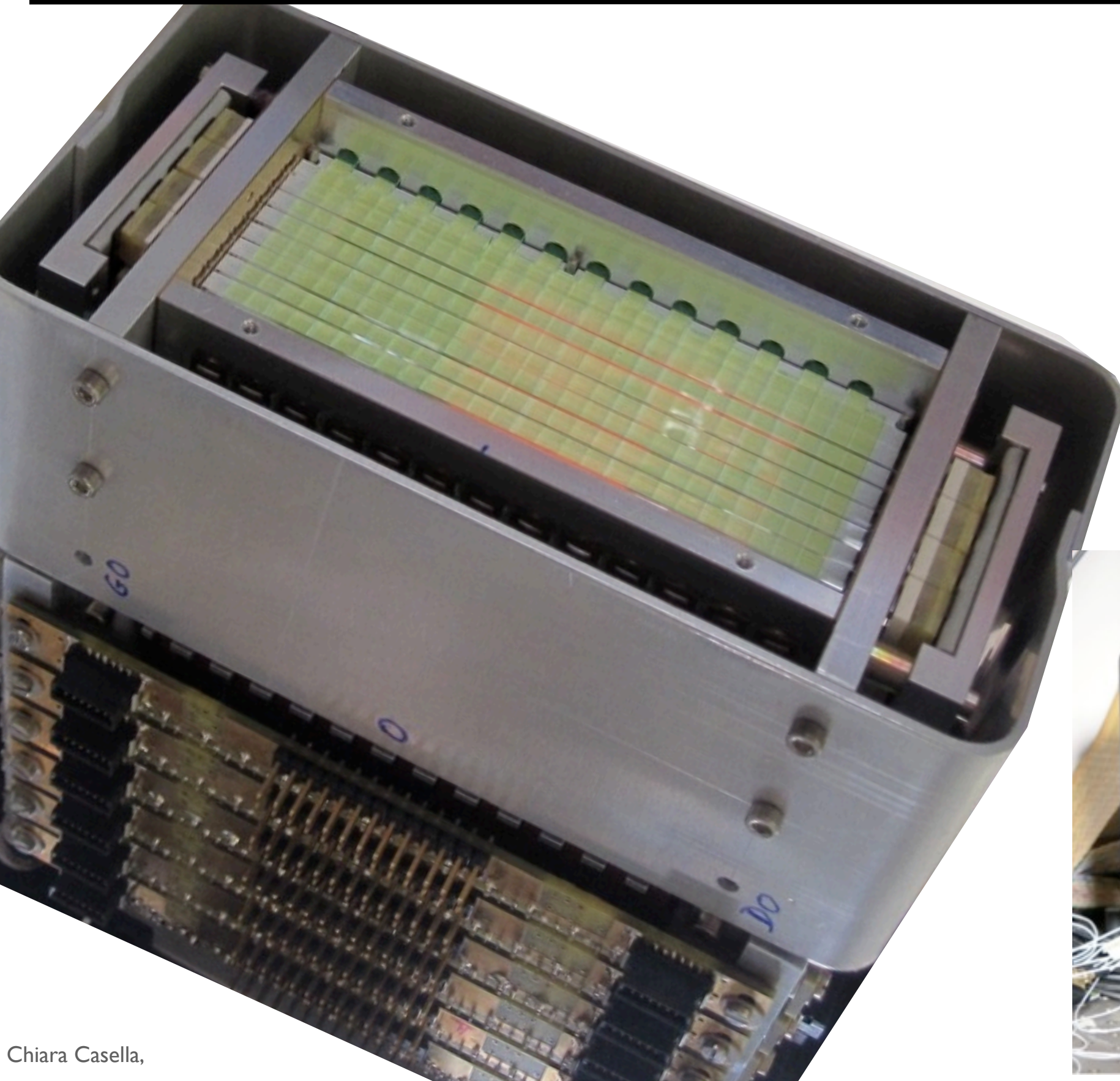


MODULE

- **6 layers**
- **8 crystals / layer**
- **26 WLS / layer**
- **48 crystals + 156 WLS = 204 channels**
- staggering in the crystals layout to optimize photon interaction probability
- optical separation between layers
- each crystal and WLS strip individually coupled to its photodetector
- crystals / WLS strips readout on alternate sides (to optimize packing density)



The AXPET module

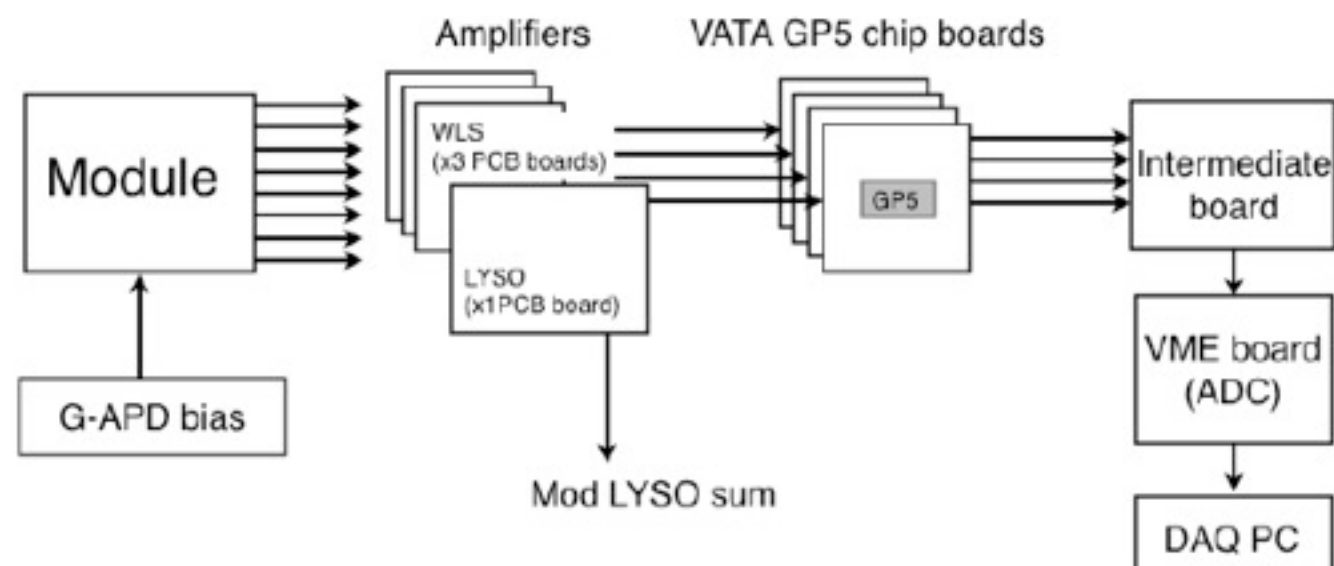
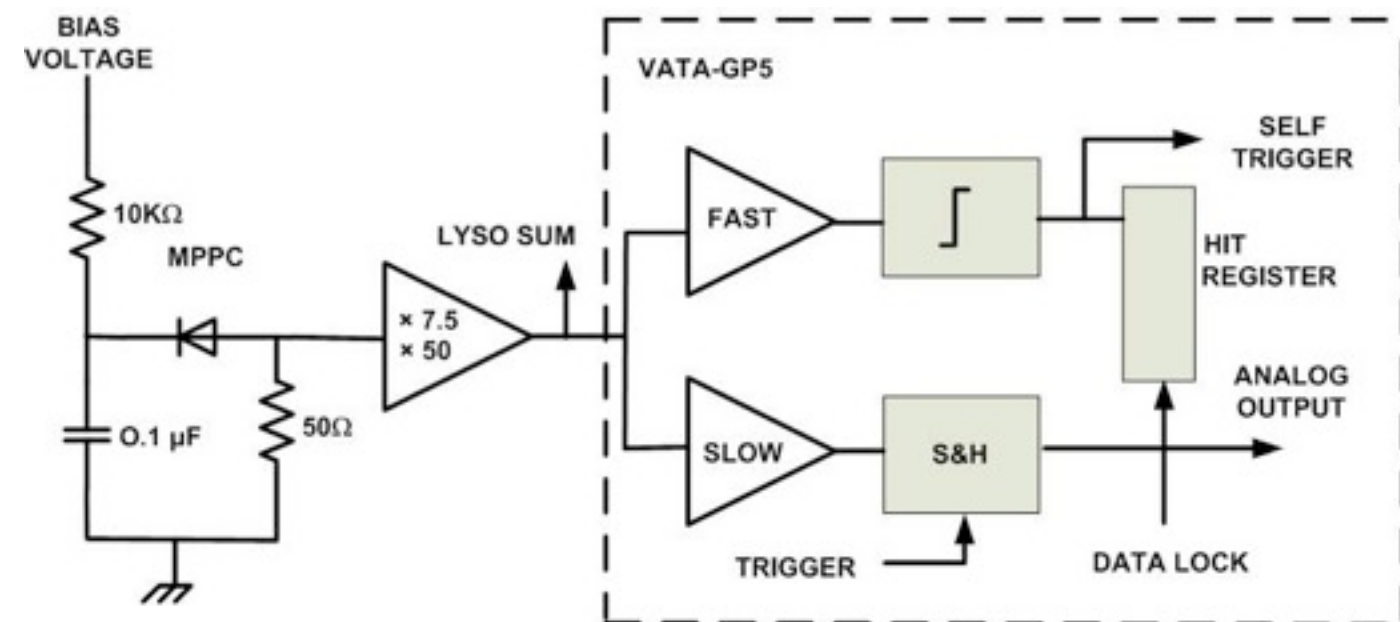


Readout & DAQ

Individual analogue readout of MPPC output

Custom designed DAQ system

- ▶ **fully analogue** readout chain
- ▶ **not optimized** at all for this specific application
- ▶ **Amplifiers:** OPA486 (Lyo) / OPA487 (WLS)
- ▶ Fast **energy sum** for all the crystals in the module
- ▶ **VATA GP5 chip**
 - 128 ch charge sensitive integrating
 - fast ($\sim 50\text{ns}$ shaper + discriminator) / slow ($\sim 250\text{ns}$ shaper) branches
 - **sparse readout** mode: only the channels above thr are multiplexed into the output
- ▶ analogue info processed by custom made VME **ADC**



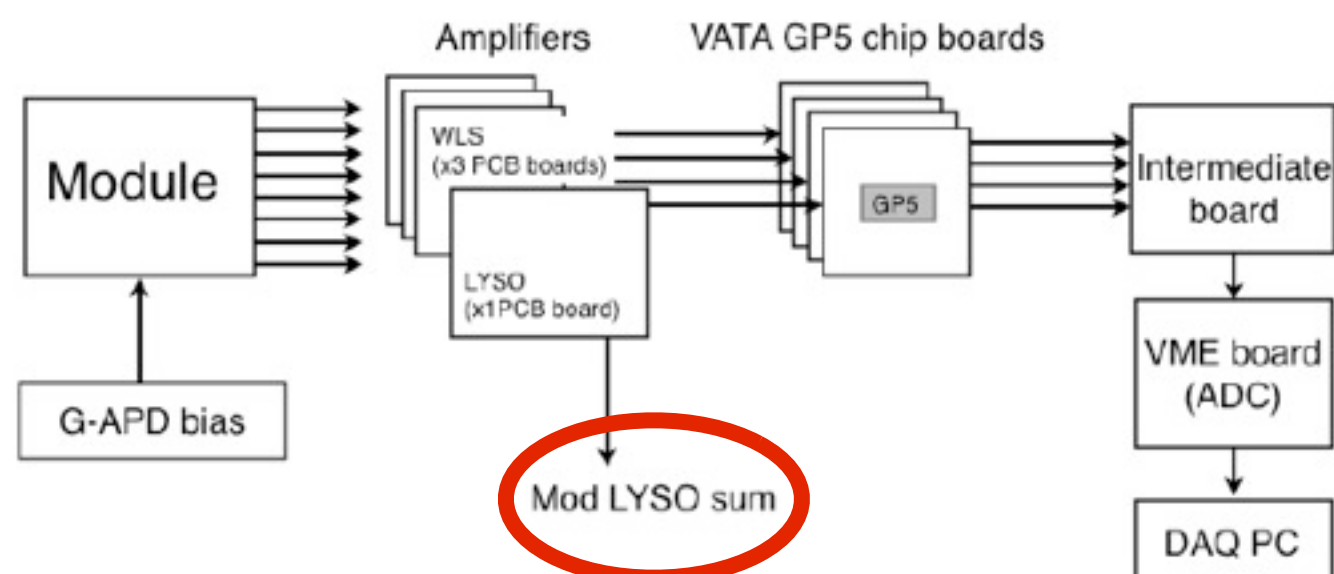
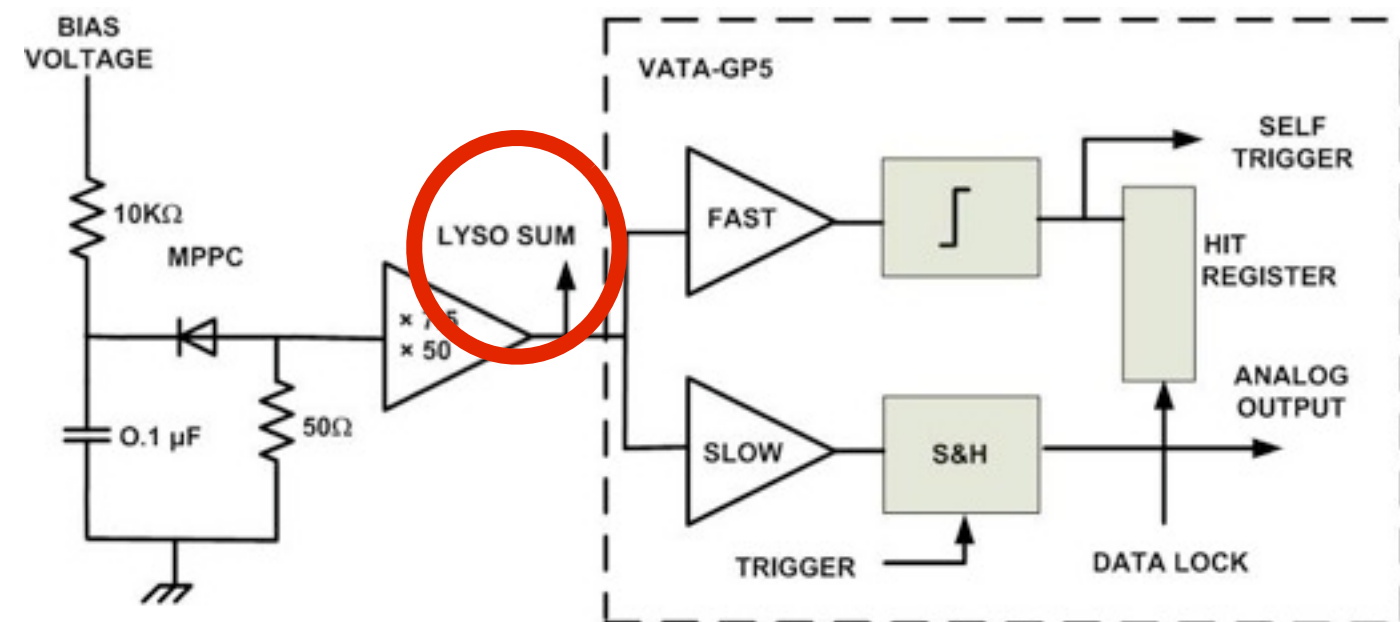
Readout & DAQ

Individual analogue readout of MPPC output

Custom designed DAQ system

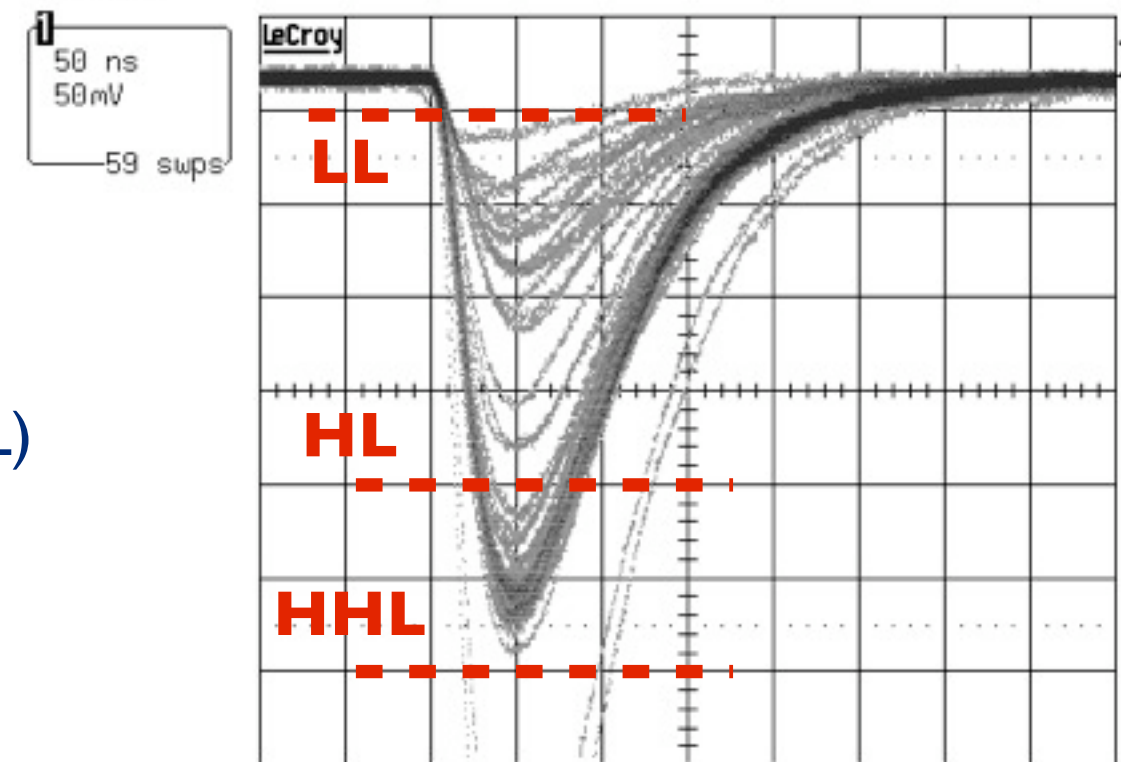
- ▶ **fully analogue** readout chain
- ▶ **not optimized** at all for this specific application

- ▶ **Amplifiers:** OPA486 (Lyo) / OPA487 (WLS)
- ▶ Fast **energy sum** for all the crystals in the module
- ▶ **VATA GP5 chip**
 - 128 ch charge sensitive integrating
 - fast (~ 50ns shaper + discriminator) / slow (~ 250ns shaper) branches
 - **sparse readout** mode: only the channels above thr are multiplexed into the output
- ▶ analogue info processed by custom made VME **ADC**



Fast energy sum & Trigger

- ▶ analogue sum of the whole module
(i.e. total energy over 48 crystals)
- ▶ with a proper threshold choice (LL x HL X notHHL)
=> select only events with **511 keV total energy deposition**



TRIGGER



TRIGGER = 2 modules

- each one discriminated @ 511 keV energy sum
- used in coincidence

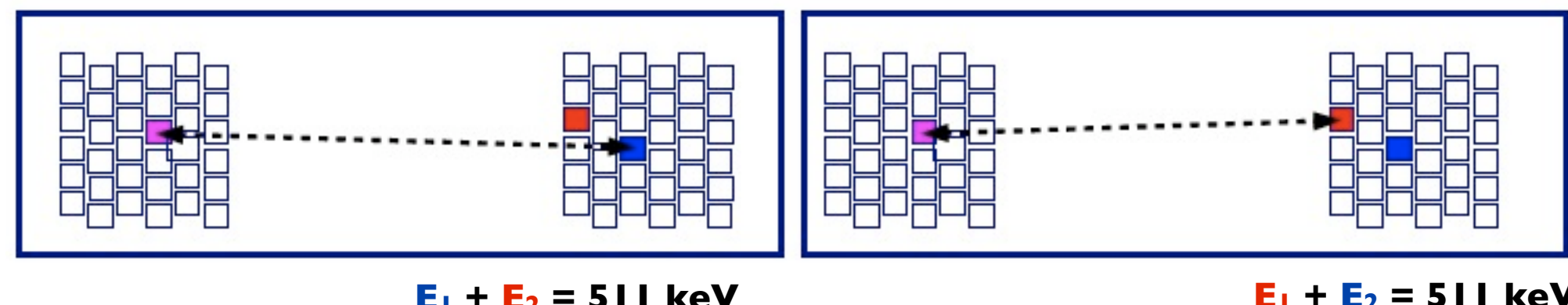
=> Selection of the good events

Compton scattering

Compton scattering in the detector

- ▶ fast energy sum & trigger
- ▶ high granularity in the module
- ▶ good energy resolution

} Possibility to tag Compton scattered events
in the detector
“Inter-Crystal Scattering” events (ICS)



if the event is :

- correctly identifiable (e.g. Compt. kinematics)
=> the event can be included in the reconstruction
- ambiguous (1-2 OR 2-1 ?)
=> the event is rejected

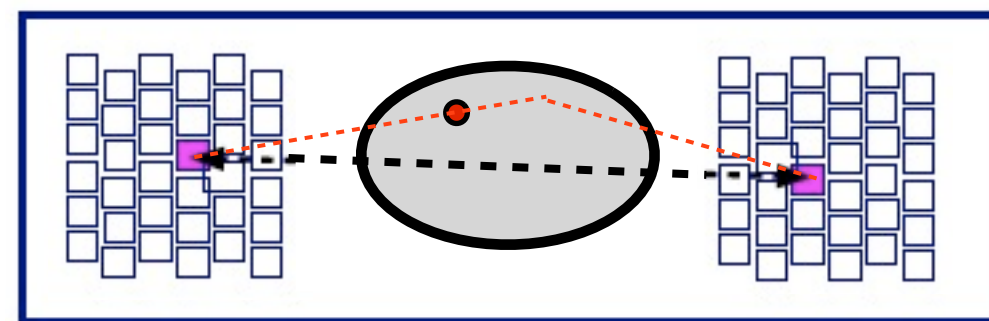
=> **improved sensitivity**

=> **improved resolution**

win - win situation !

Compton scattering in the body

Events killed by the trigger !



$E_{\text{sum}} = 511 \text{ keV}$

$E_{\text{sum}} < 511 \text{ keV}$

AX-PET inspired other developments

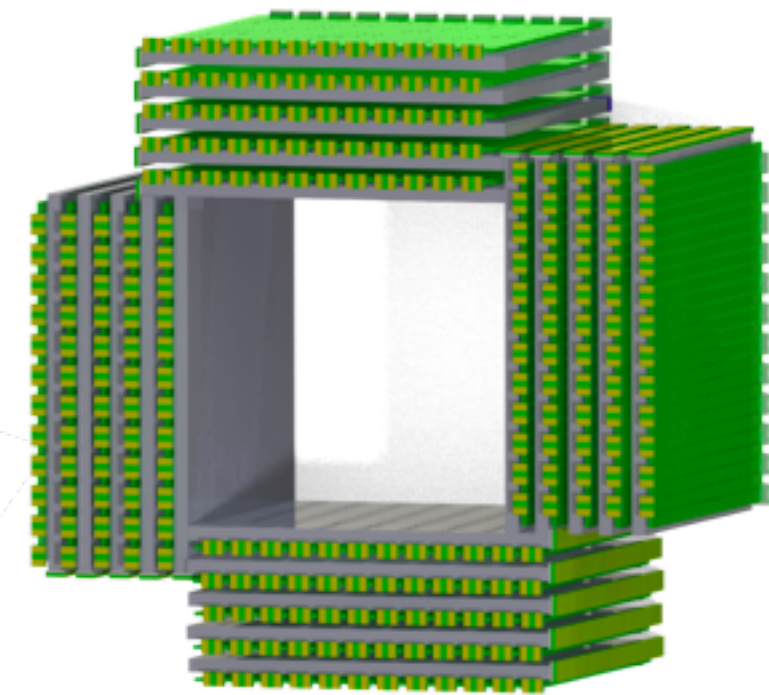
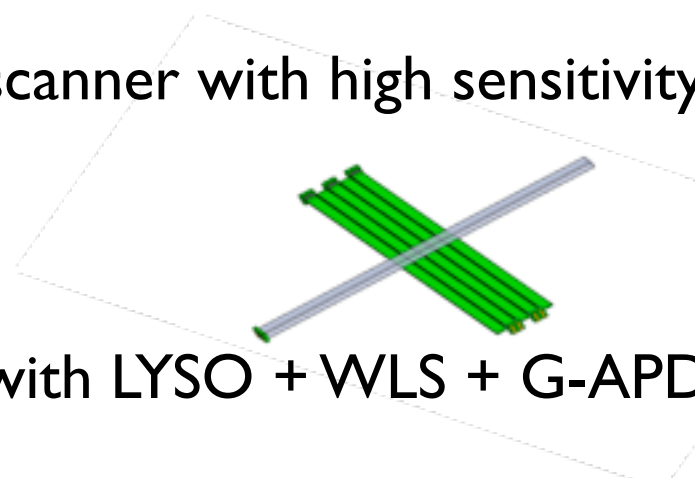
COMPET :

University of Oslo, Norway - E. Bolle et al.

research project for a pre-clinical PET scanner with high sensitivity, high resolution. MRI compatible

- no axial geometry
- 3D reco of photon interaction point with LYSO + WLS + G-APD

E. Bolle et al, NIM A 648(2011) S93-S95



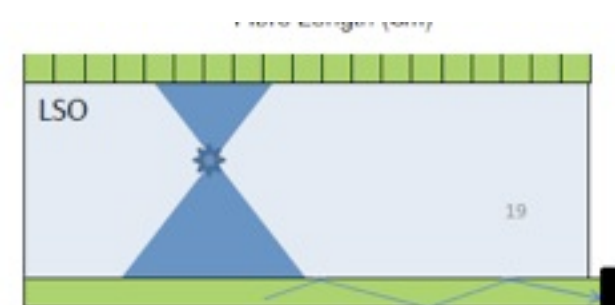
Tampere University (Finland) :

build a small specific scanner based on AX-PET (toward possible commercialization...)

Low cost planar detector for PET

Triumph, Canada - F. Retiere et al.

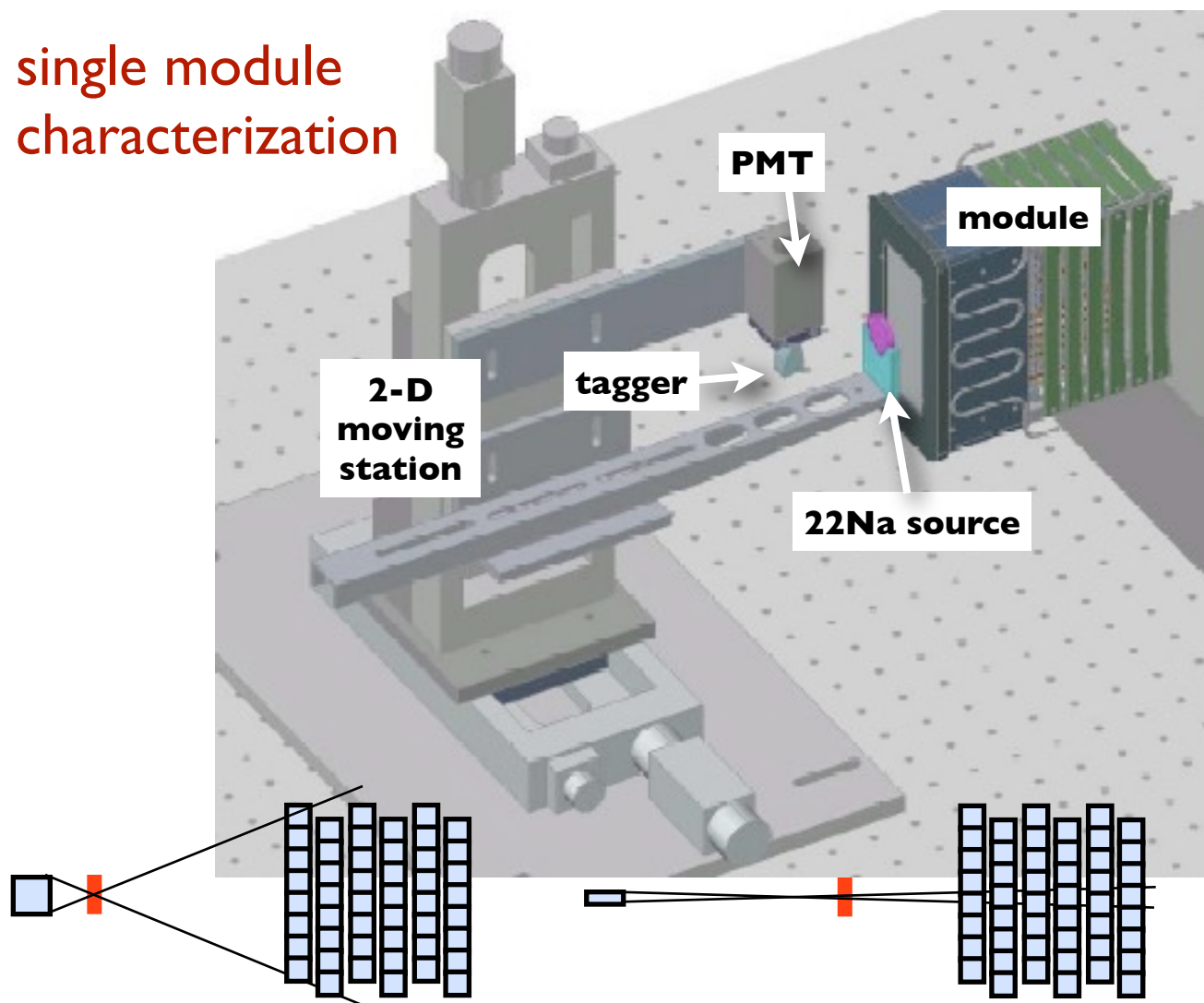
F. Retiere, NIM A (2011) doi:10.1016/j.nima.2011.12.084



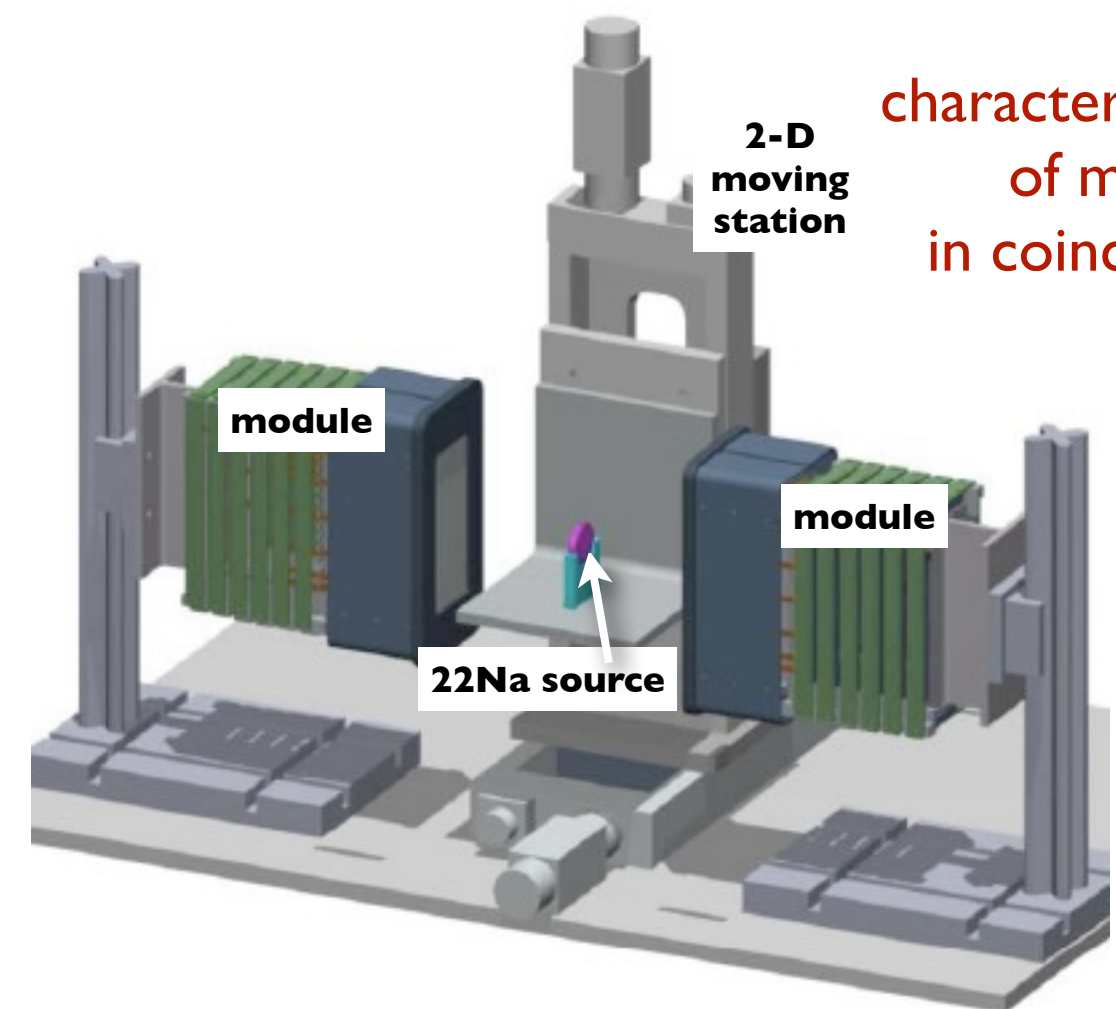
Characterization measurements

with point-like **^{22}Na source** (diam = 0.25 mm, A~900 kBq) , @ CERN

single module characterization



characterization of modules in coincidence



- two different taggers
 - different distances tagger / source / module
- => both uniform illumination of the module and precisely collimated beam spot

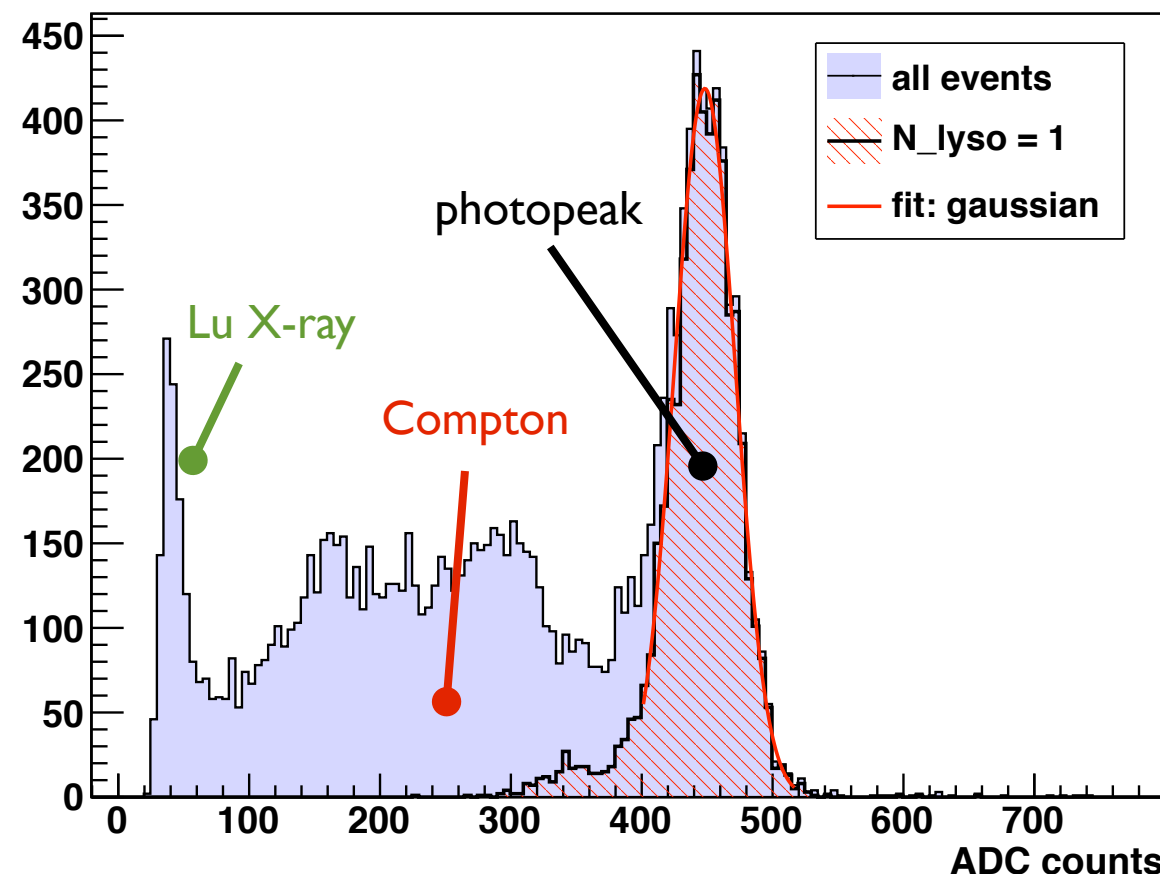
AX-PET performance:

NIM A 654 (2011) 546-559

1. Energy measurement / energy calibration => LYSO response
2. Position measurement / spatial resolution => WLS response

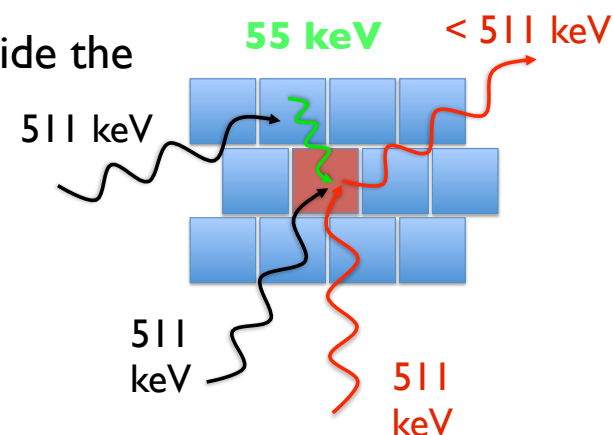
LYSO energy response

LYSO No. 21 - ^{22}Na coinc. trigger



typical energy spectrum of one LYSO inside the module :

- ▶ photopeak (511 keV)
- ▶ Compton continuum (0 - 340 keV)
- ▶ Lu X-ray peak (~ 55 keV)



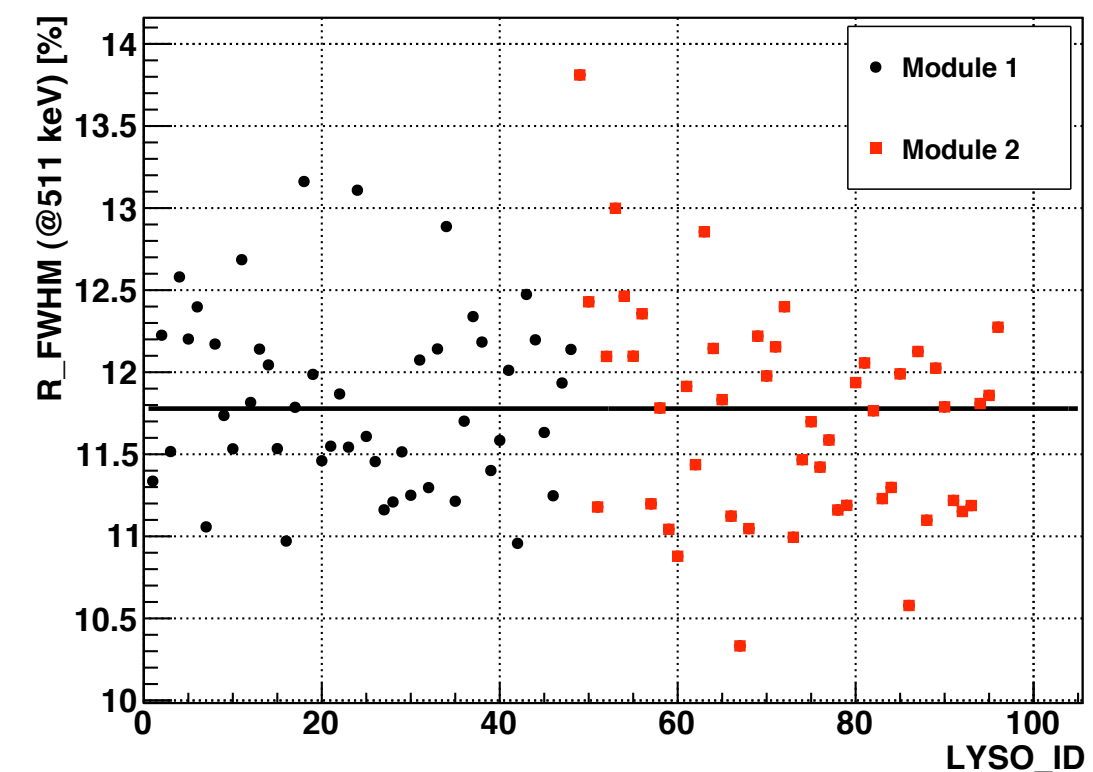
Light yield at 511 keV ~ 1000 pe

(from independent calibration measurements)

Energy resolution

- ▶ from gaussian fit of the photopeak
- ▶ AFTER ENERGY CALIBRATION

Energy resolution

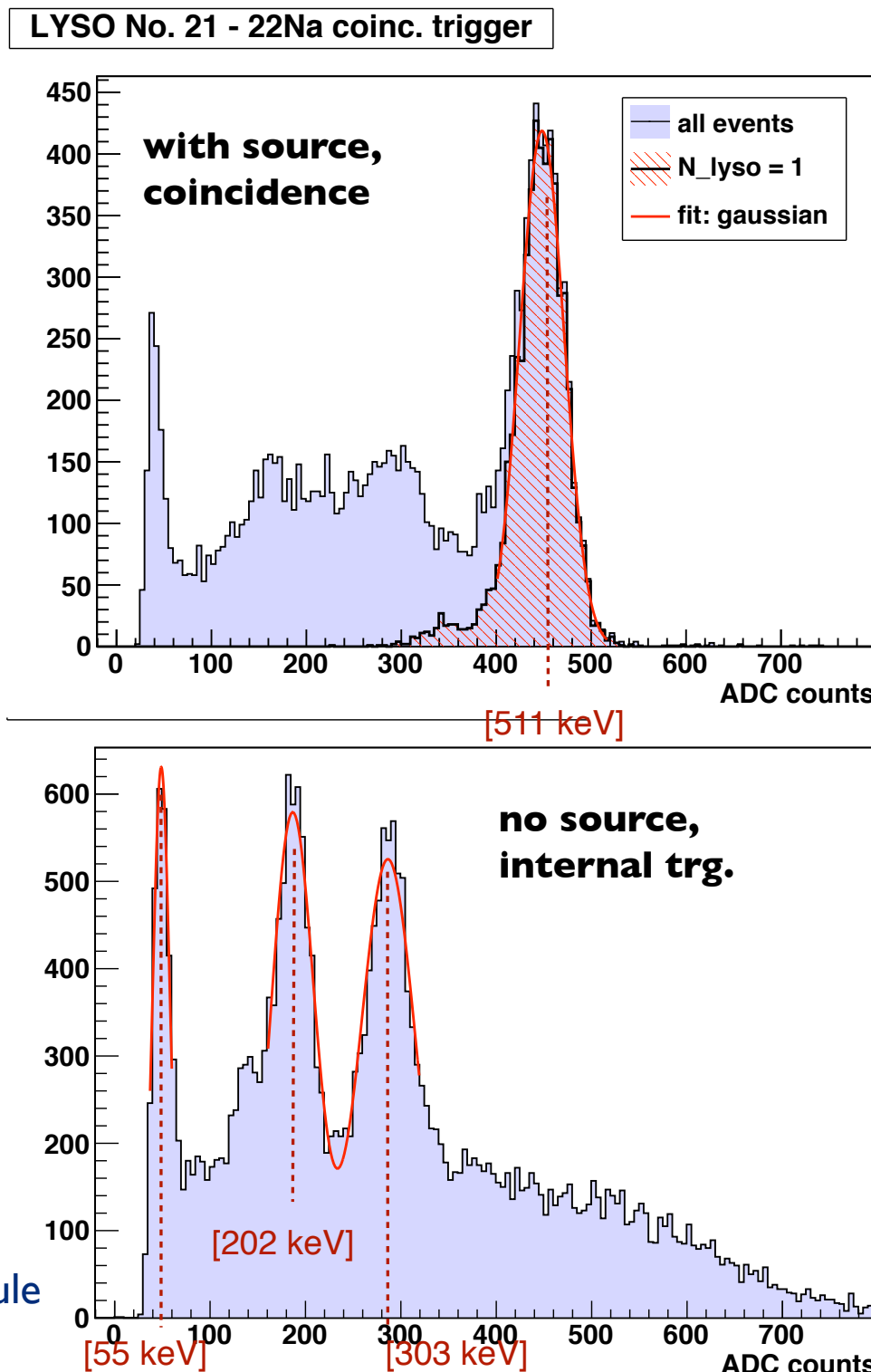


$\langle R_{\text{FWHM}} \rangle \sim 11.8\% @511 \text{ keV}$

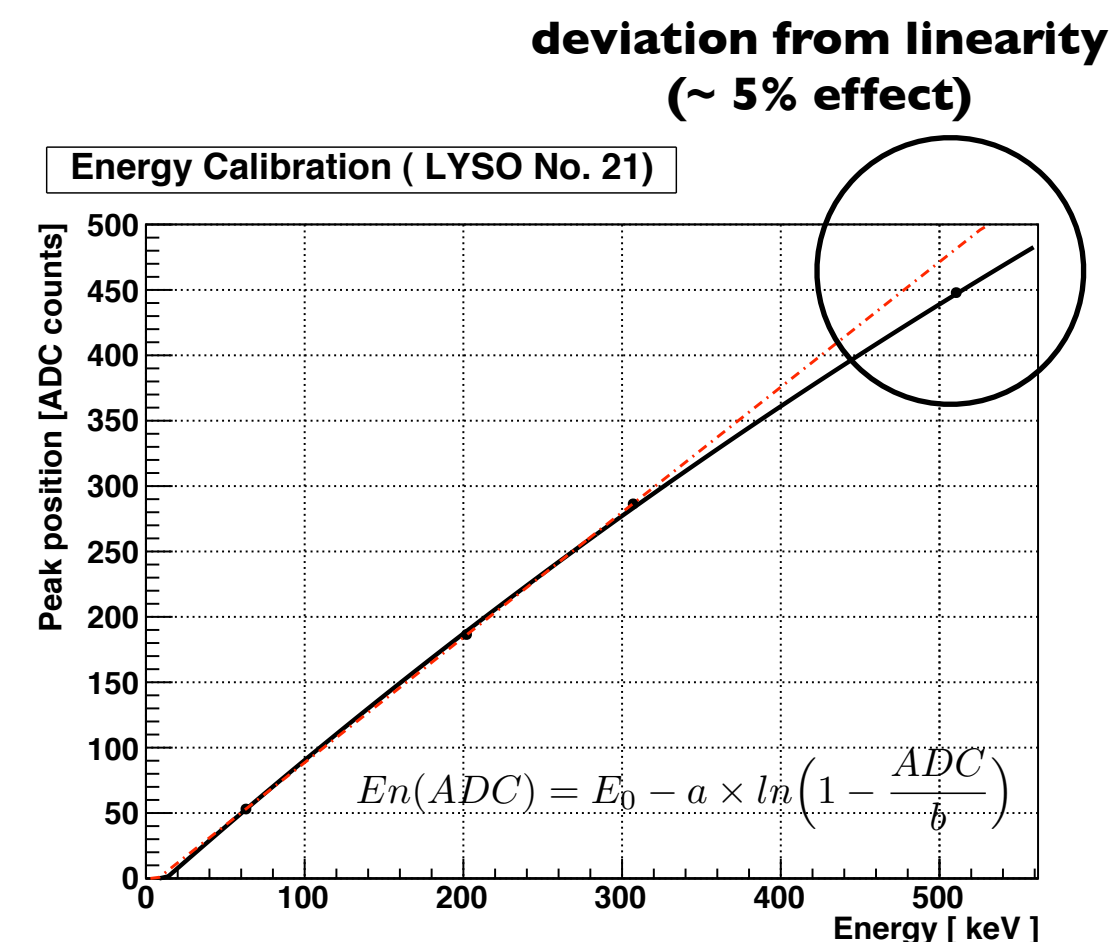
(averaged on 96 LYSO crystals)

LYSO energy calibration

Photopeak + Intrinsic Lu radioactivity: very good tool for the energy calibration



same procedure applied identically for every channel



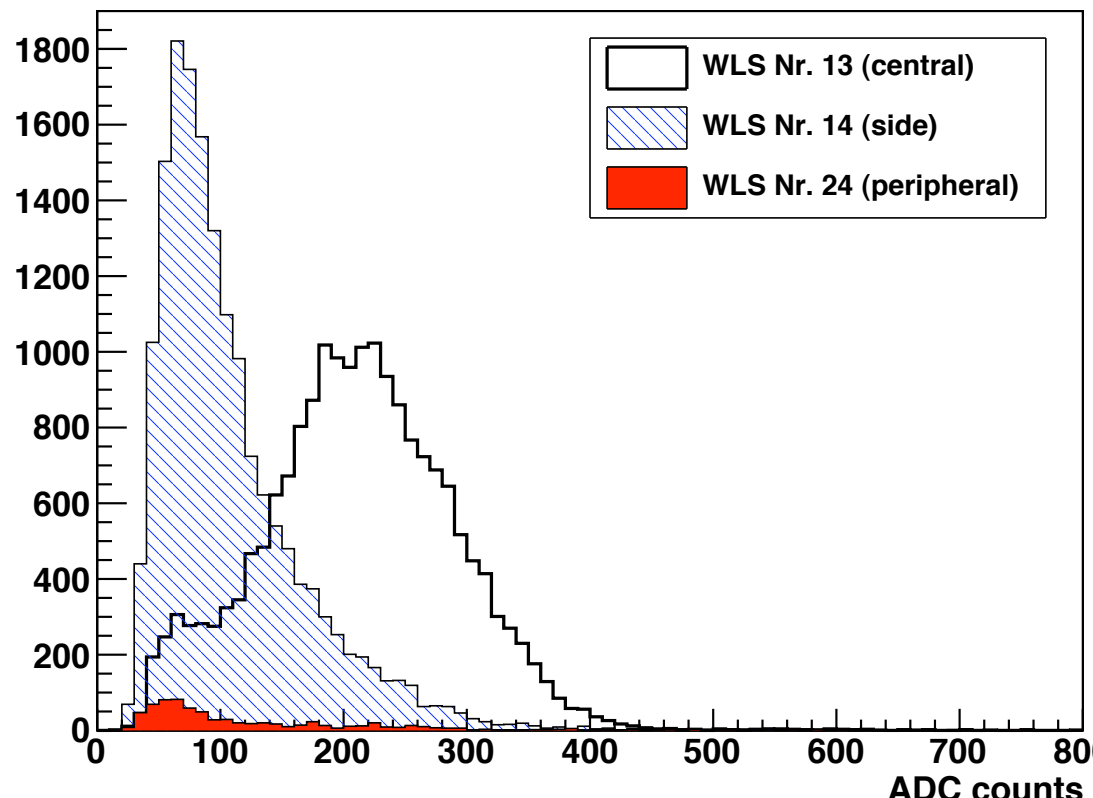
MPPC saturation. Due to:
- limited nr of cells in the MPPC (3600)
- important light yield in the scintillator (~1000).

WLS response

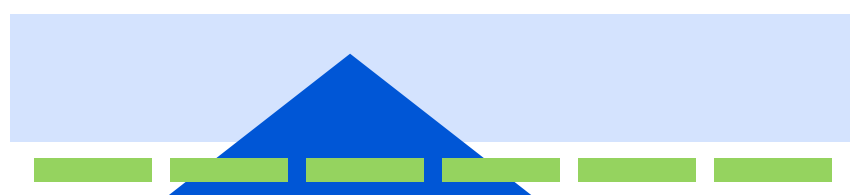
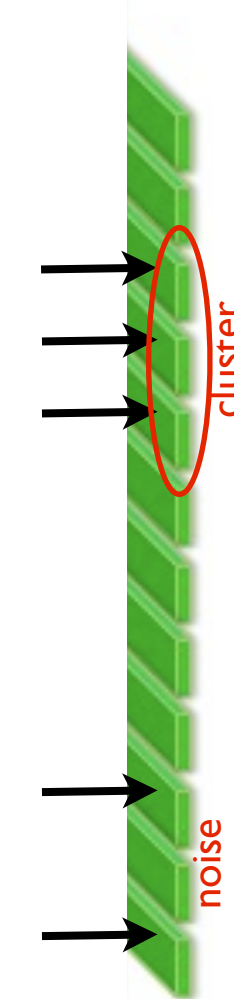
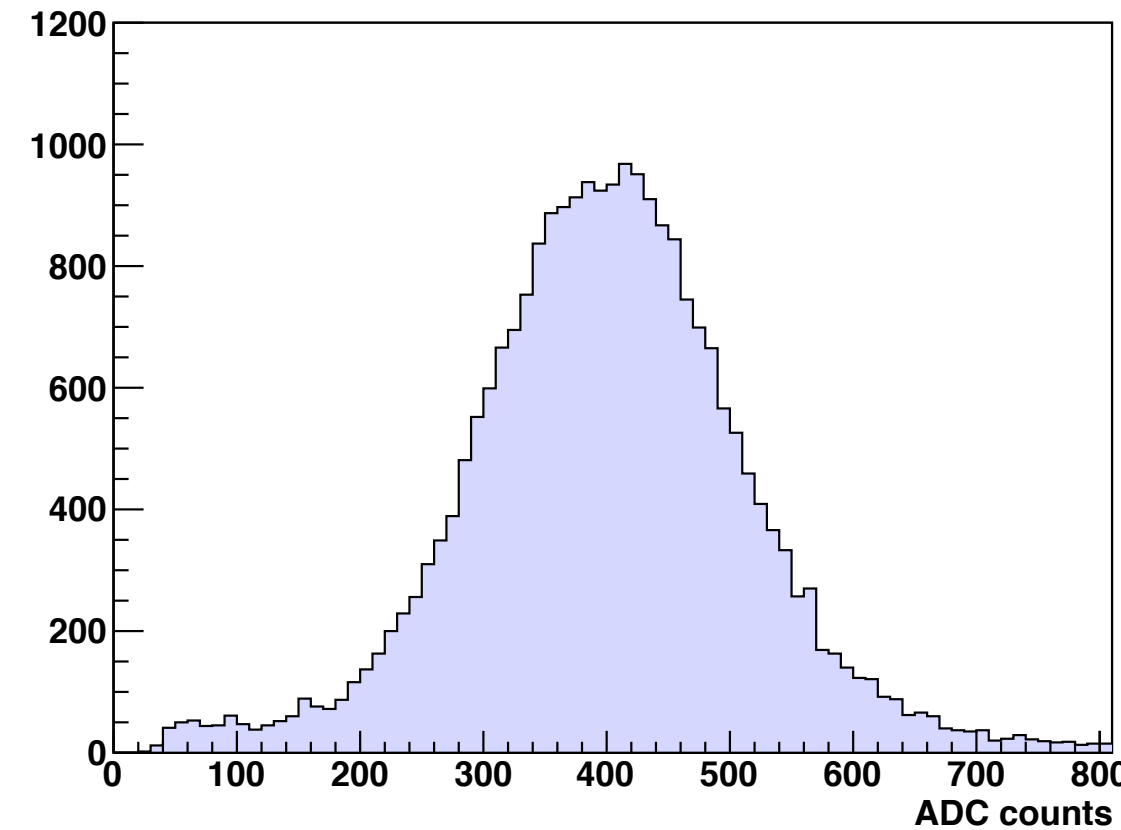
typical integrated raw spectra of few WLS strips

- beam spot collimated at the center of the module (WLS 13)
- 511 keV energy deposition in the LYSO

Collimated beam spot, WLS response



WLS cluster: Summed ADC counts



- more than 1 WLS participate to the event (typically 2-4)
- noise should not be included

Light yield in WLS cluster ~ 100 pe

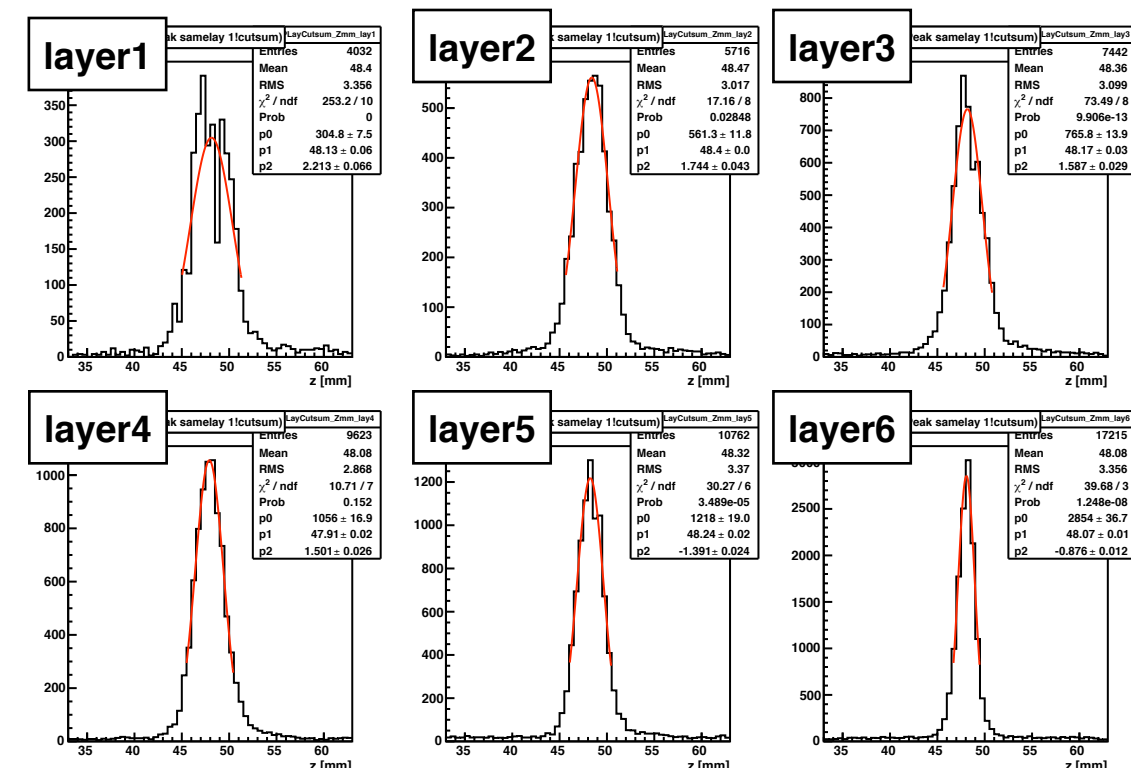
@511 keV LYSO energy deposition

(from independent calibration measurements: 1 pe ~ 4 ADC)

axial coordinate :
derived from center of gravity method
from all the WLS participating to the cluster

Axial spatial resolution

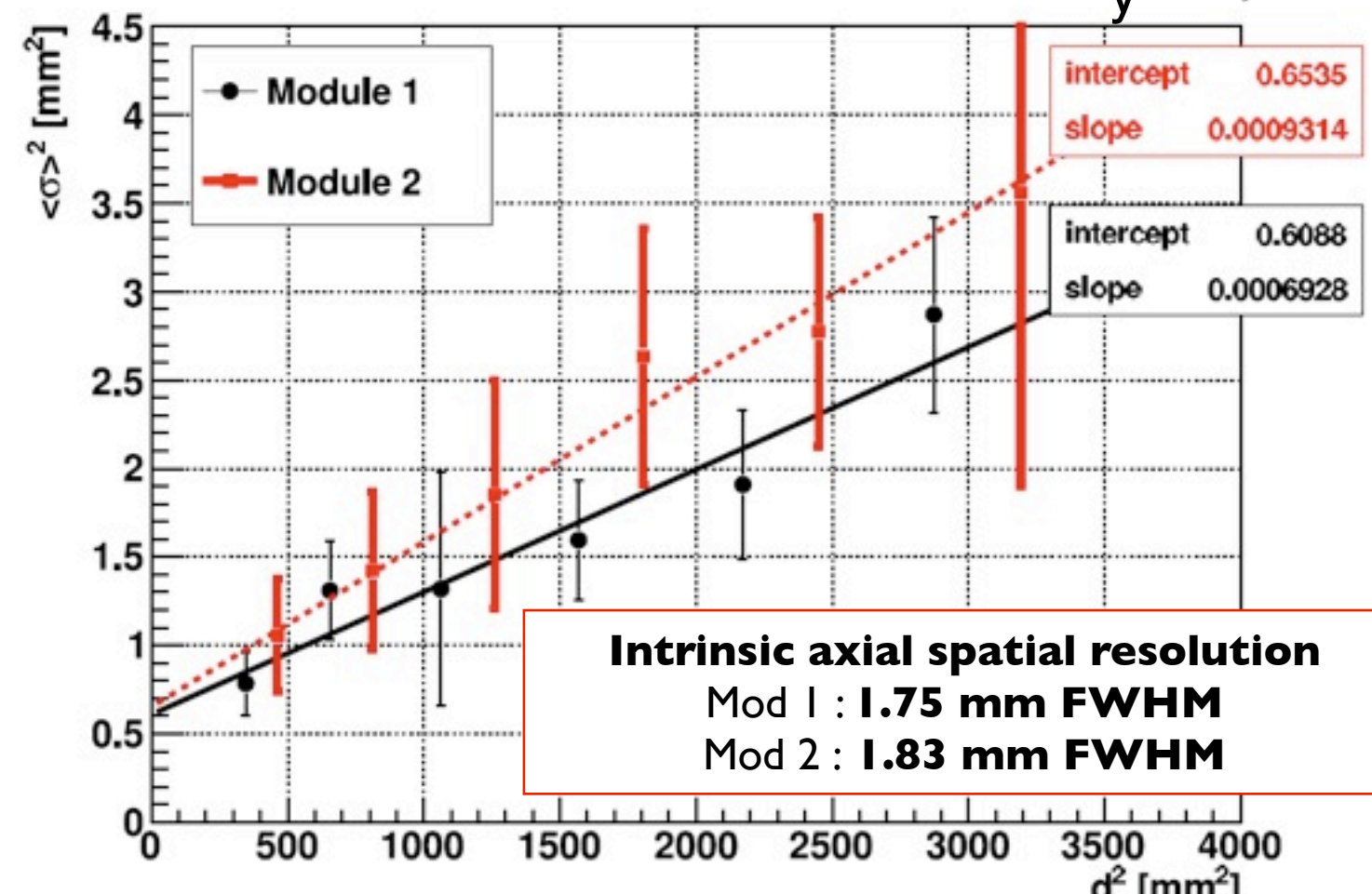
z coordinate (COG) :



each measured σ_z includes :

- intrinsic spatial resolution
- positron range ($\rho \sim 0.54 \text{ mm}$)
- non collinearity ($\div d$)
- beam divergency ($\div d$)
- (source dimensions; $\phi=250\mu\text{m}$)

Axial resolution



Intrinsic axial spatial resolution

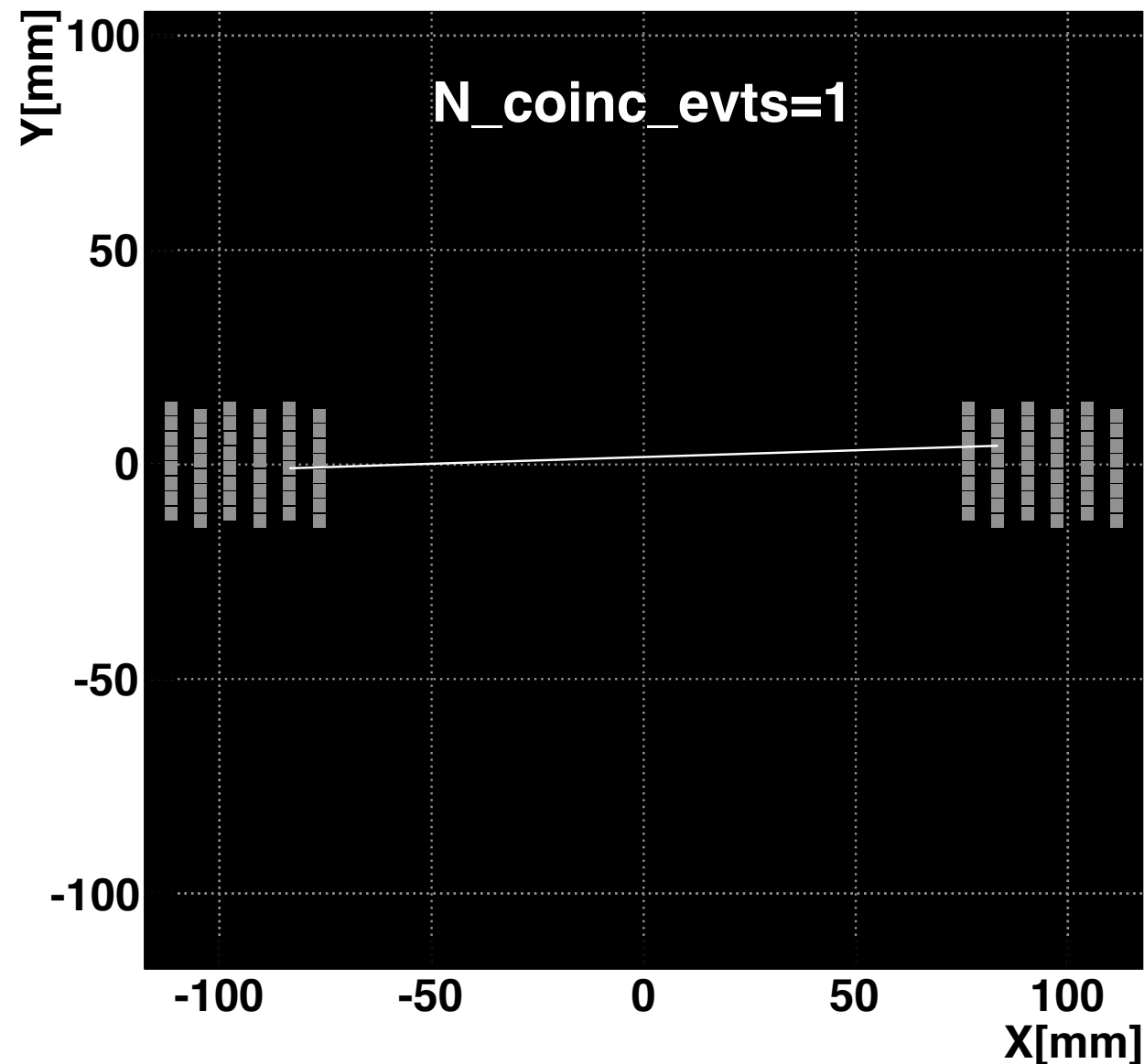
Mod 1 : **1.75 mm FWHM**
Mod 2 : **1.83 mm FWHM**

Trans-axial spatial resolution

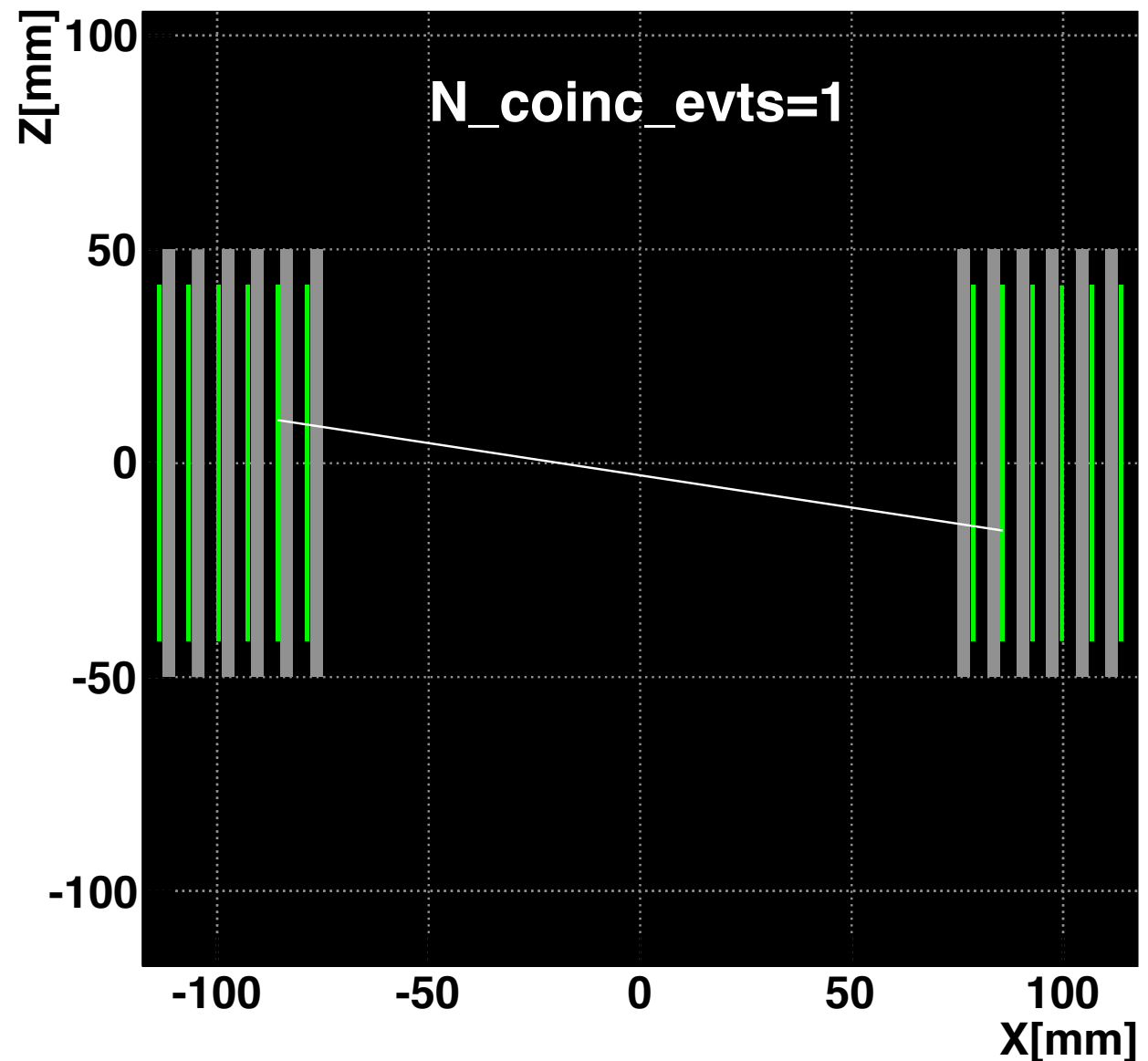
- $\langle \sigma_x \rangle = d/\sqrt{12} = 0.87 \text{ mm}$ (**digital**) ; **FWHM ~ 2 mm**
- $\langle \sigma_y \rangle = d/\sqrt{12} = 0.87 \text{ mm}$ (**digital**) ; **FWHM ~ 2 mm**

Two modules coincidences

TOP View - $d(\text{Mod1}, \text{Mod2}) = 150 \text{ mm}$



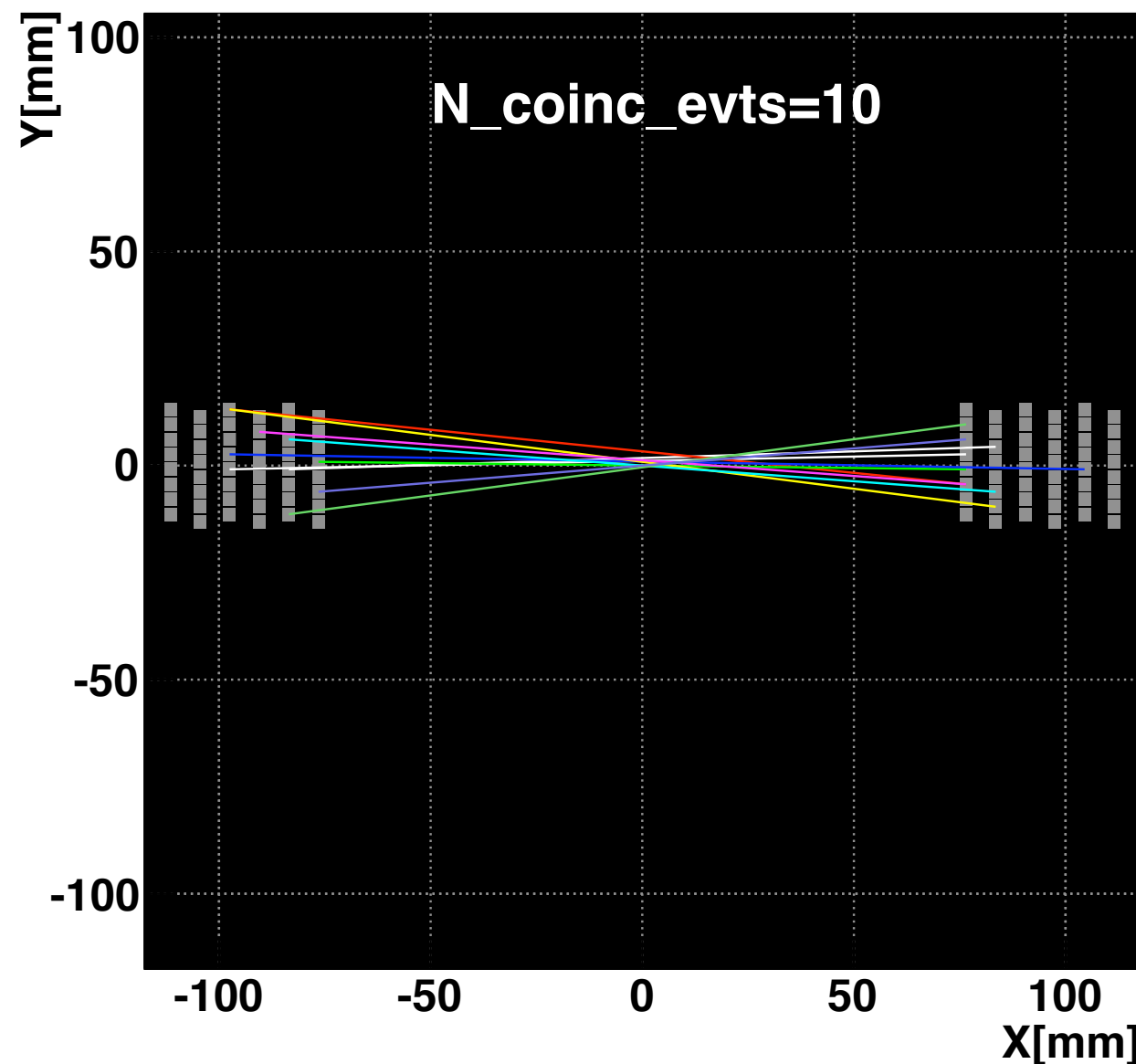
SIDE View - $d(\text{Mod1}, \text{Mod2}) = 150 \text{ mm}$



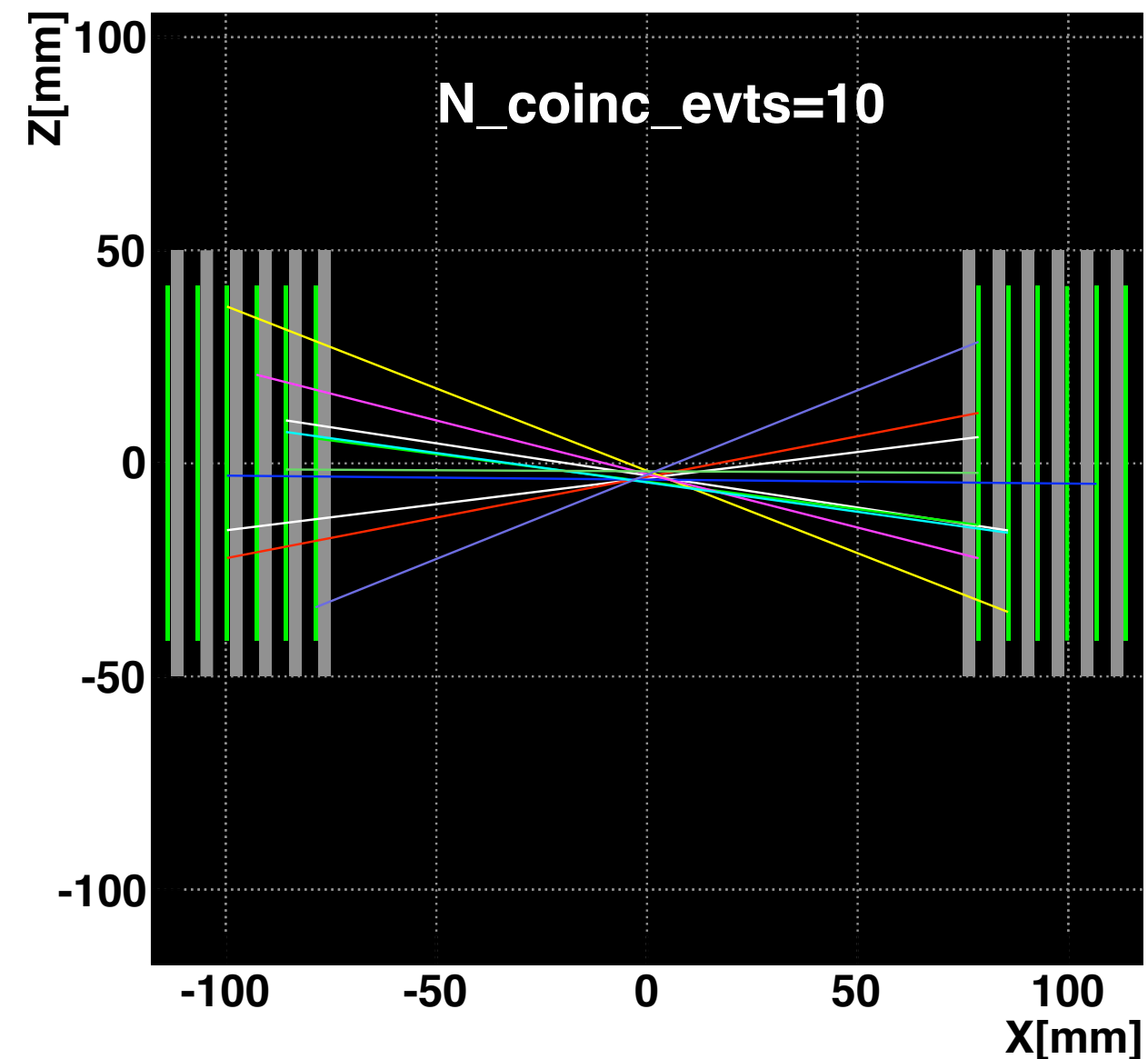
AX-PET very first coincidence event !

Two modules coincidences

TOP View - $d(\text{Mod1}, \text{Mod2}) = 150 \text{ mm}$

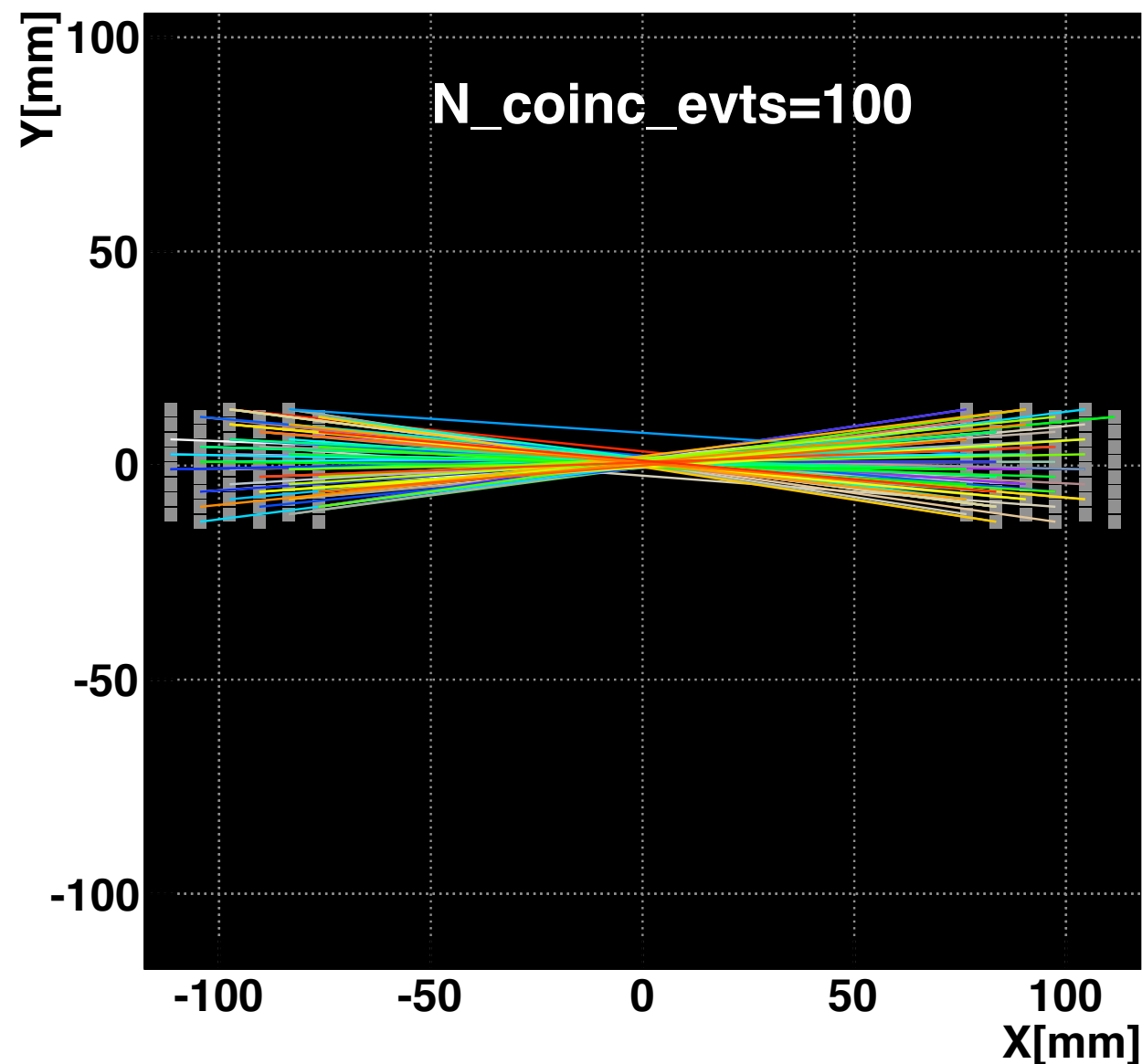


SIDE View - $d(\text{Mod1}, \text{Mod2}) = 150 \text{ mm}$

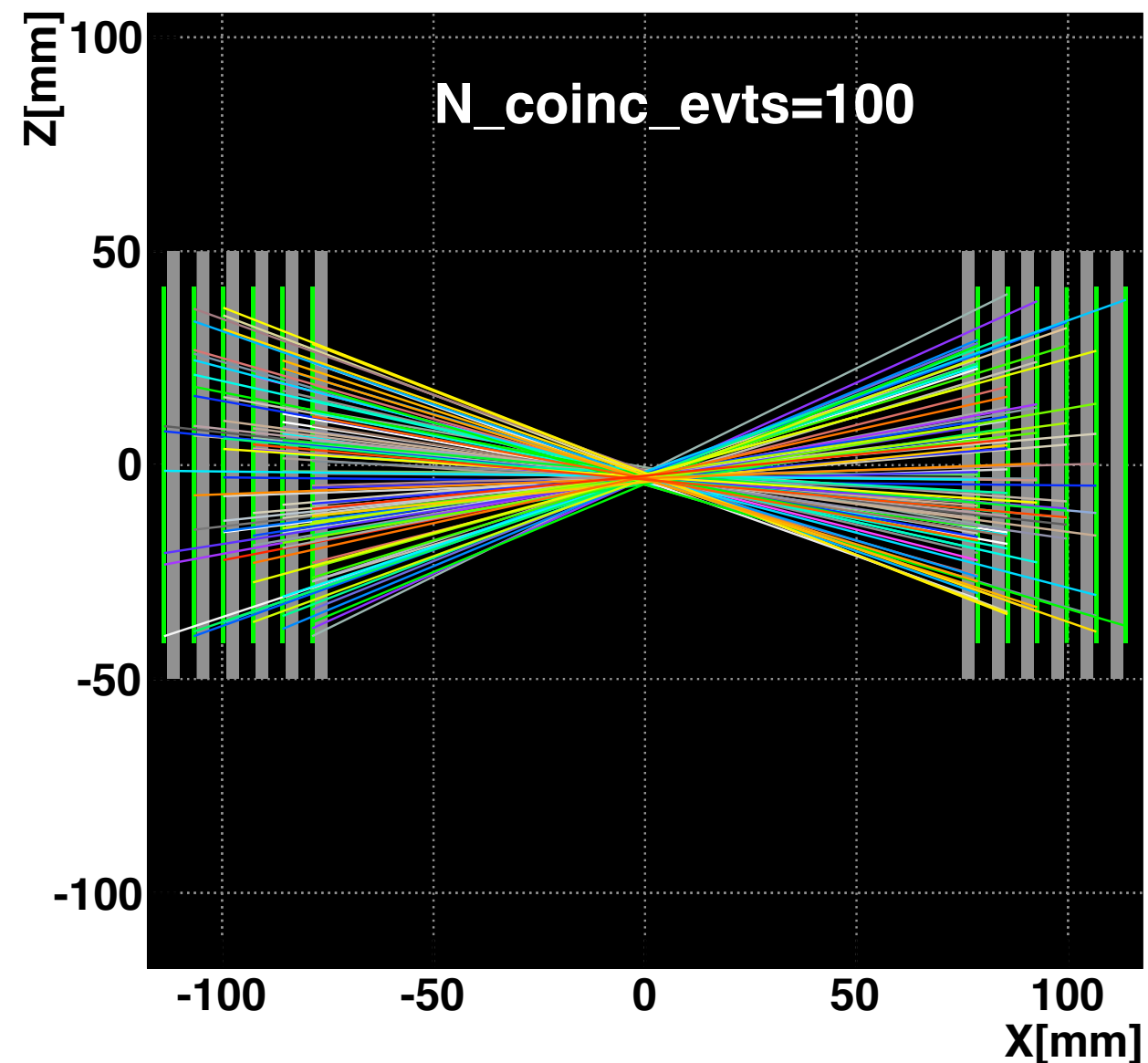


Two modules coincidences

TOP View - $d(\text{Mod1}, \text{Mod2}) = 150 \text{ mm}$



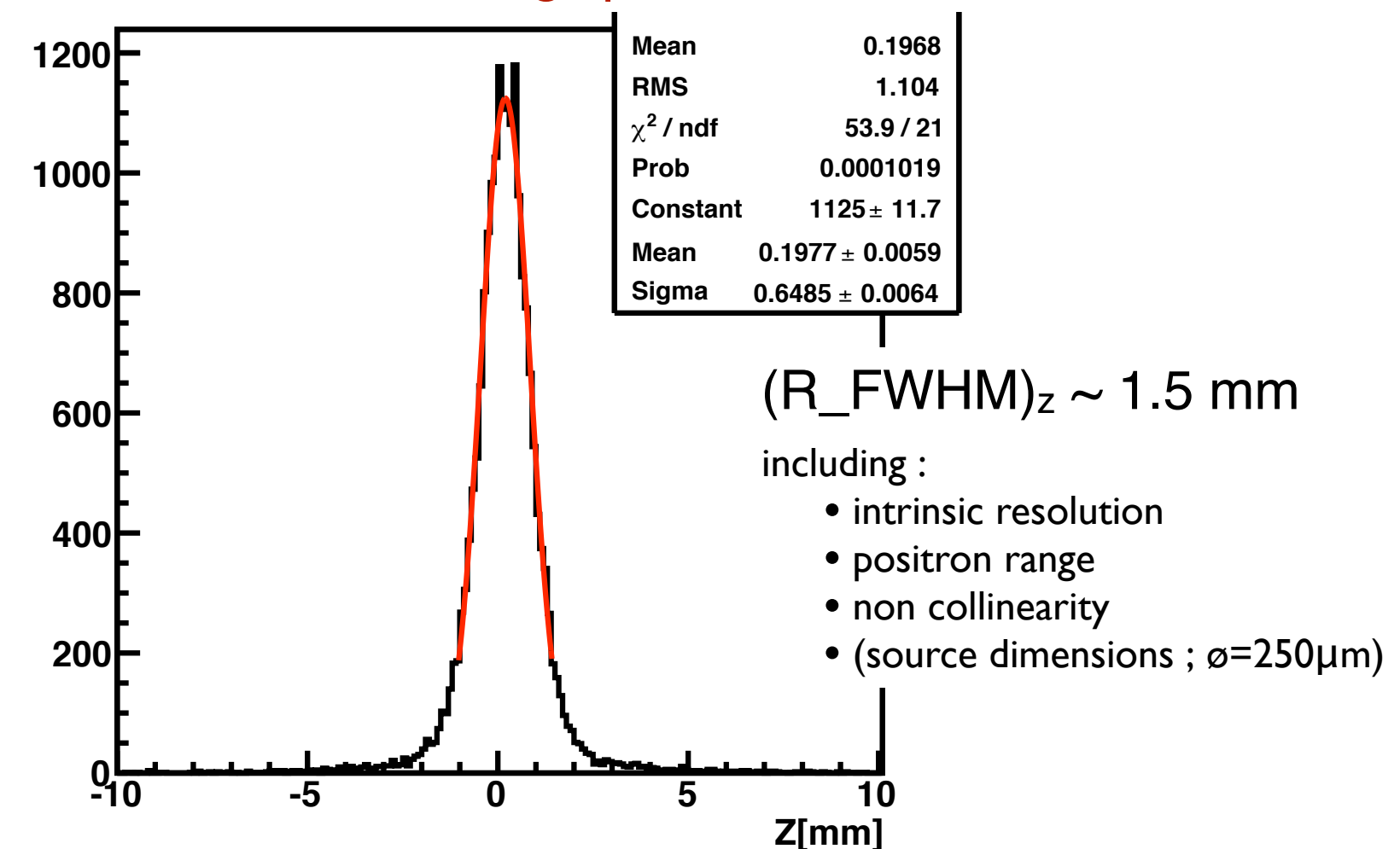
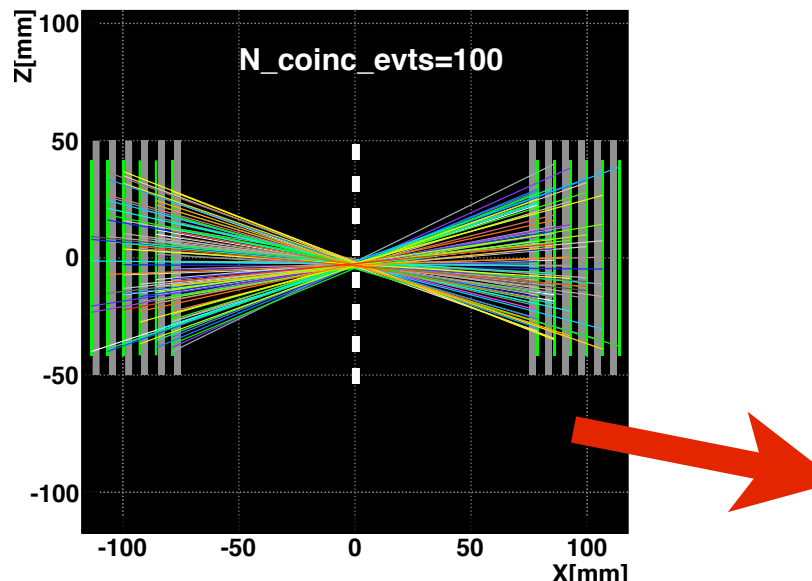
SIDE View - $d(\text{Mod1}, \text{Mod2}) = 150 \text{ mm}$



Axial resolution

Intersection of LOR with central plane
no tomographic reconstruction !!!

SIDE View - $d(\text{Mod1,Mod2}) = 150 \text{ mm}$

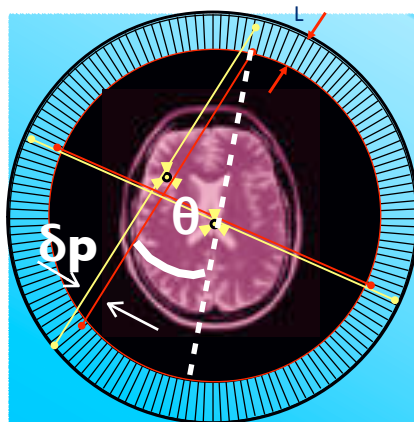


$$R_{intr} = \sqrt{R_{meas}^2 - R_\rho^2 - R_{180}^2} \approx 1.35 \text{ mm}$$

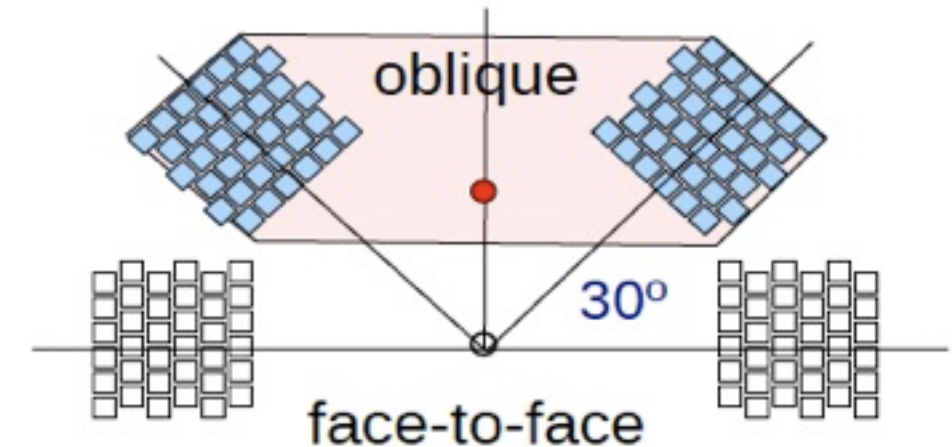
$\sim \left(\frac{(R_{FWMH})_z \text{ SingleMod}}{\sqrt{2}} \right)$

Arrows point from the equation to the terms $(0.54 \text{ mm})^2$ and $[0.0022 \times \text{Diam} = 0.33 \text{ mm}]^2$.

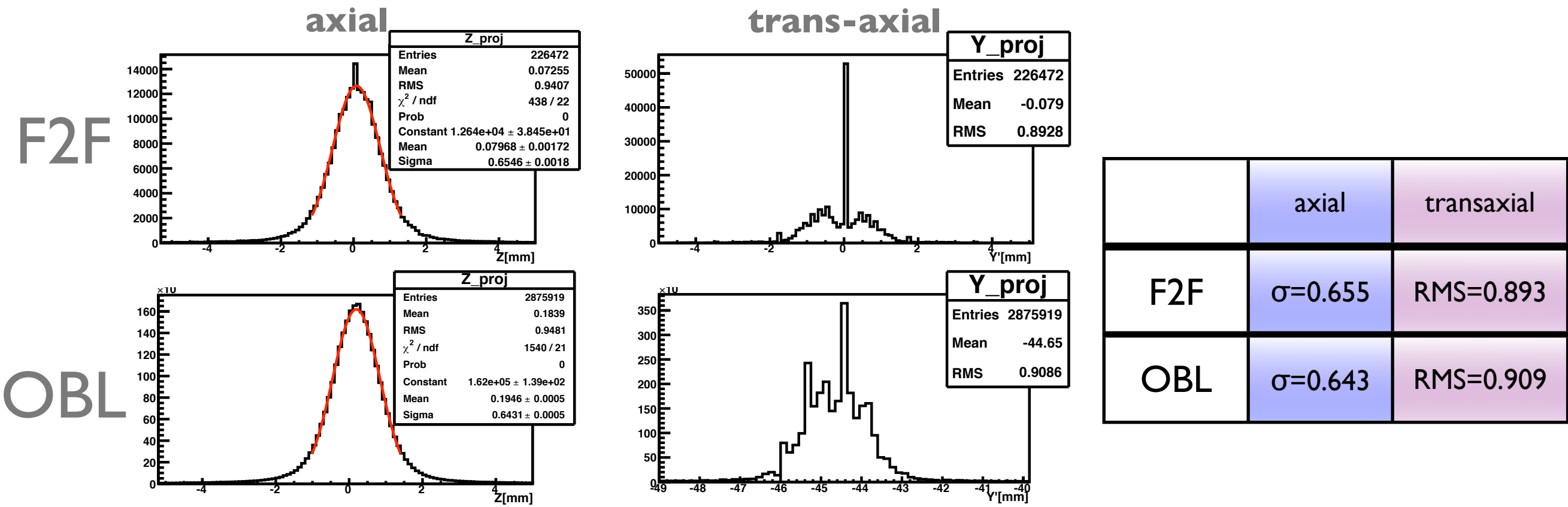
Parallax free demonstration



parallax error is more and more important outside the center of the FOV



intersection of LORs with the plane containing the source



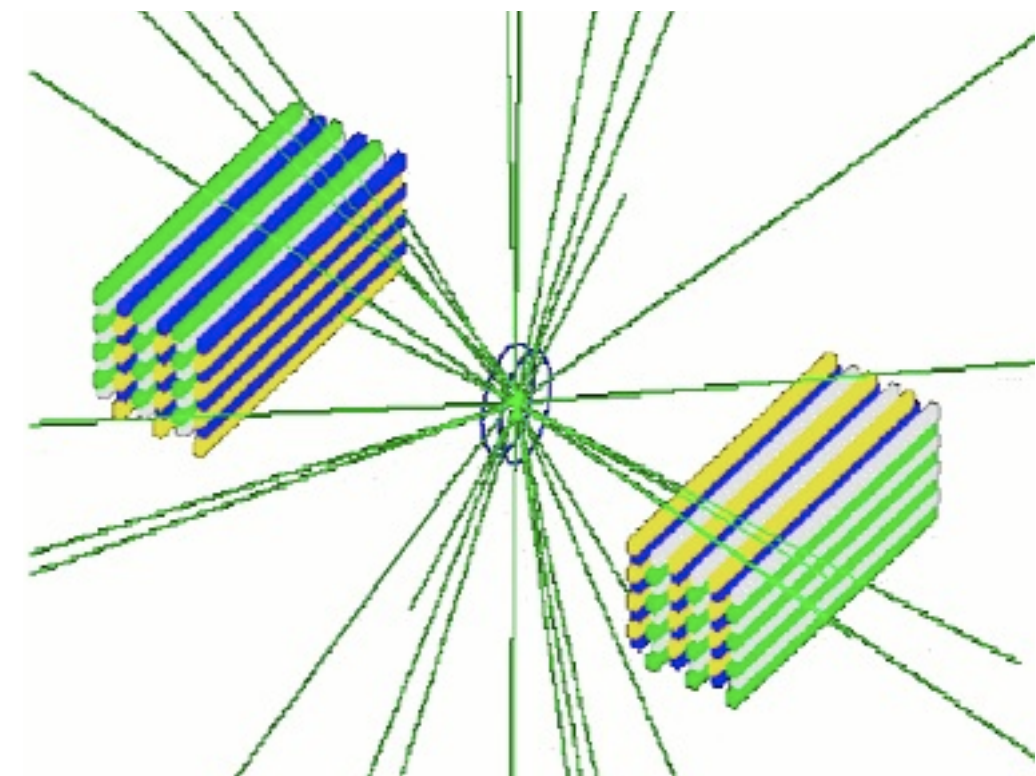
Intrinsic resolution is **not degraded by parallax effects**, even in very oblique configuration !

Simulations

AX-PET is a fully simulated system

Dedicated Monte Carlo simulations for AX-PET .

- Why?
- (1) get a better understanding of the detector
 - (2) train Compton reconstruction algorithms
 - (3) support image reconstruction
 - (4) simulate an hypothetical full ring scanner
and estimate its potential performance



GATE simulation package (Geant4 application for tomographic emission)

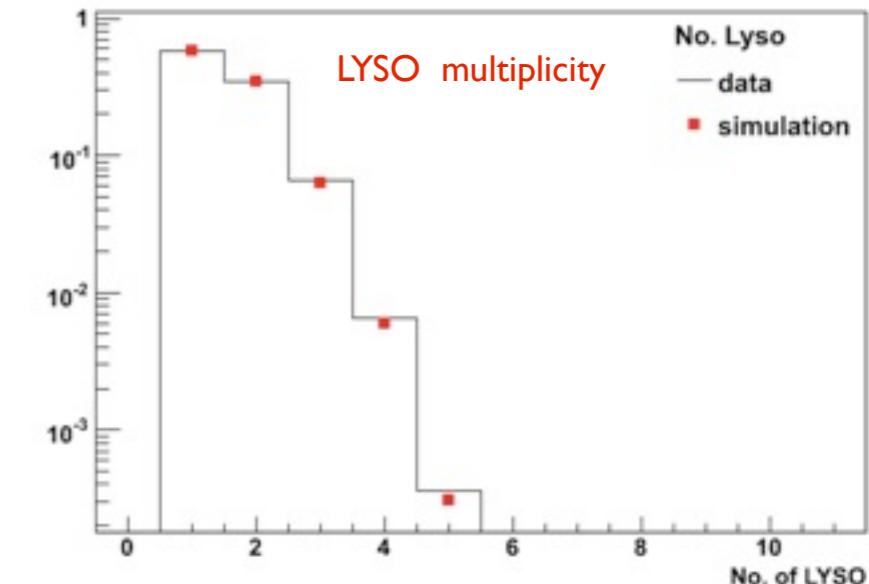
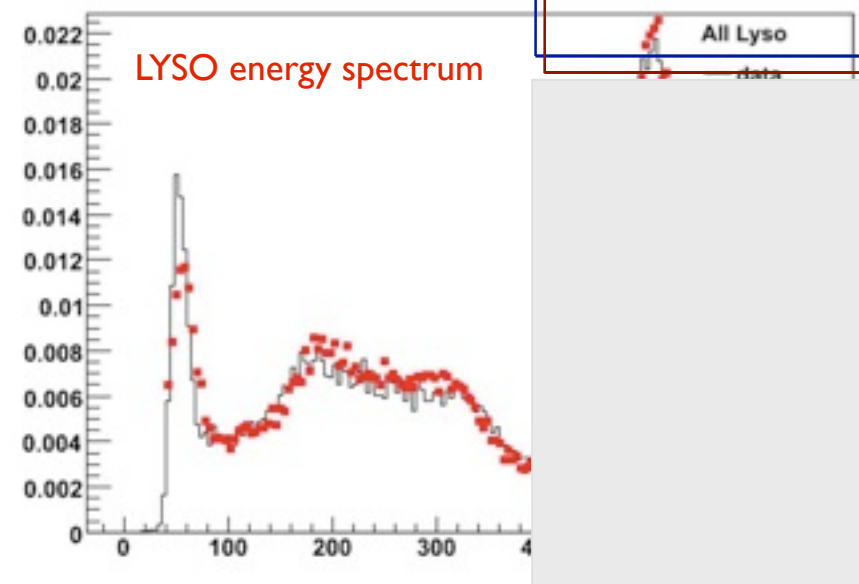
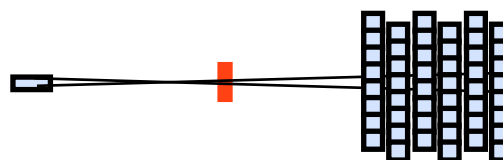
Non conventional nature of AX-PET

- => several challenges for simulations (standard templates could not be applied)
- **geometry (axial; staggering; layered structure)**
 - **WLS modeling**
 - **dedicated sorter for the coincidences
(module sum; trigger logic... up to DAQ rate modeling)**

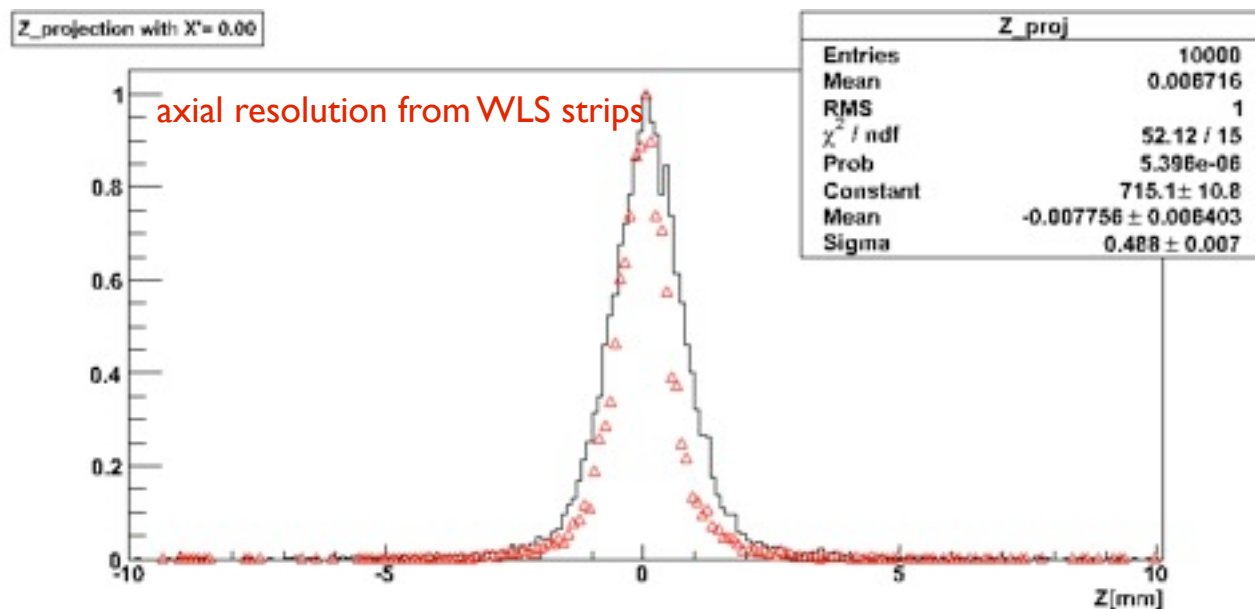
Simulations: some results

Excellent agreement data / simulations :

One AXPET Module
illuminated by a collimated
511 keV gamma beam :
Data and Simulations



Two AXPET Modules in coincidences



Inter-Crystal Scattering (ICS)

- identify ICS events before image reconstruction.
- several identification algorithms tested

Max. E	Compton K.	Klein-Nishina	Neural Networks
61%	65%-66%	61%-63%	75%

- identification rate for ICS ~ 60%

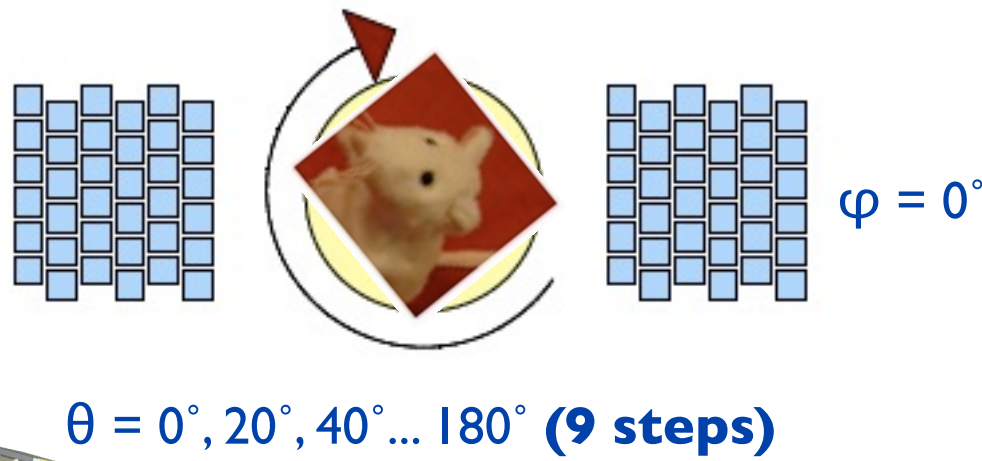
very incomplete collection of results here !
simulations paper is in preparation !

Towards a tomographic reconstruction...

How to mimic a full scanner with 2 modules only available?

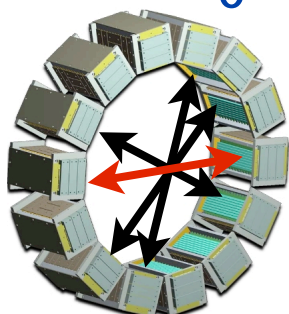
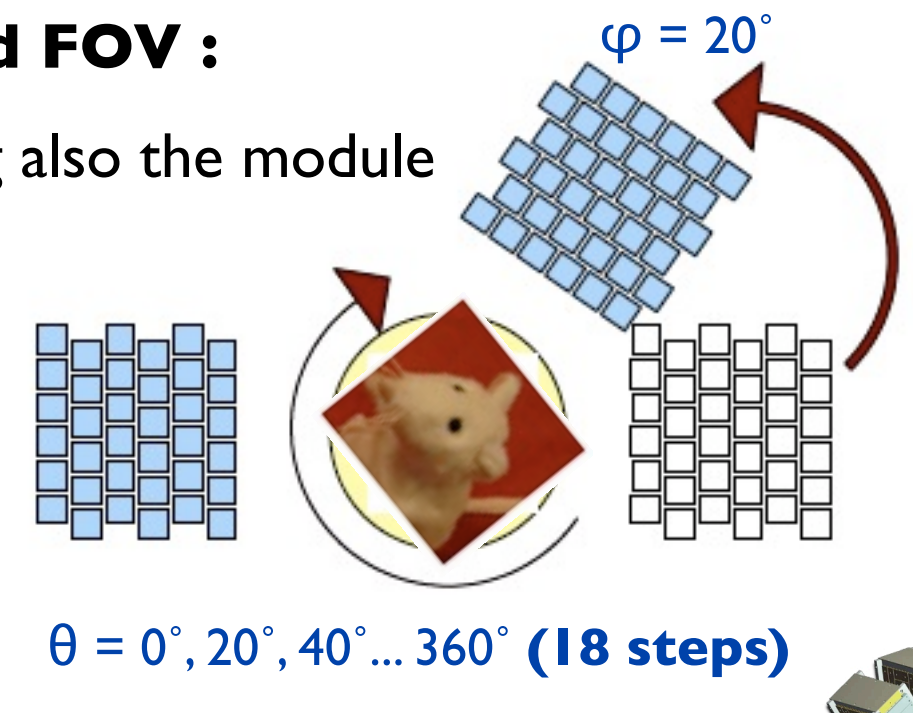
Central FOV :

rotating the phantom...

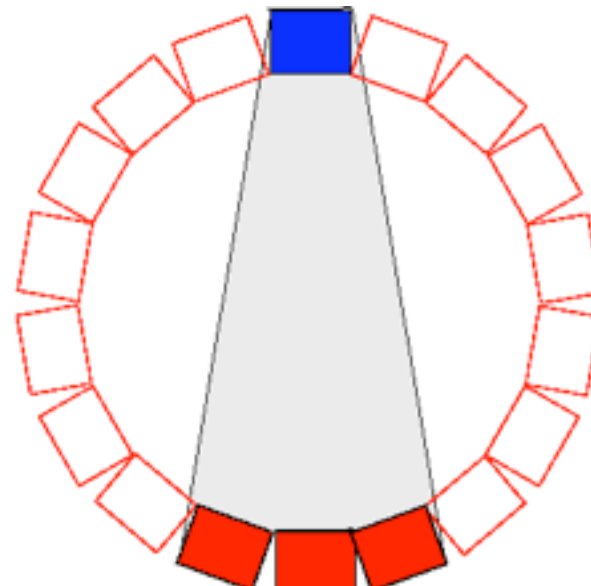


Extended FOV :

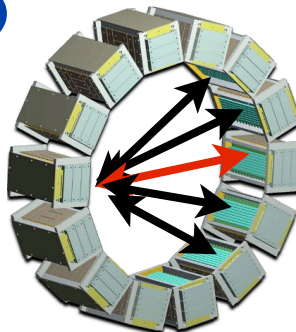
...and rotating also the module



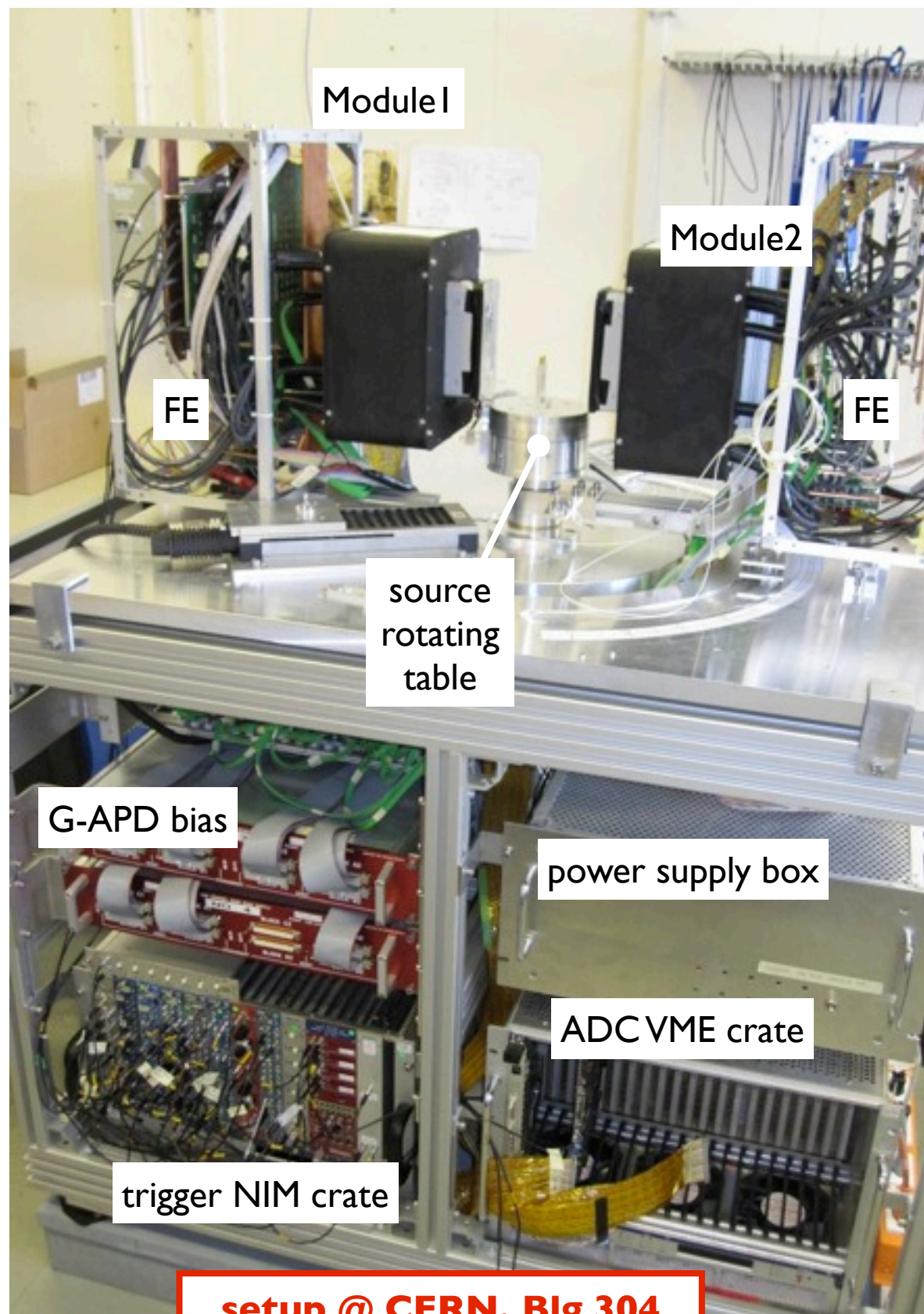
1 tomographic acquisition
= 27 steps acquisition



mimics a 18-modules ring, with coincidences between face-to-face ± one adjacent modules

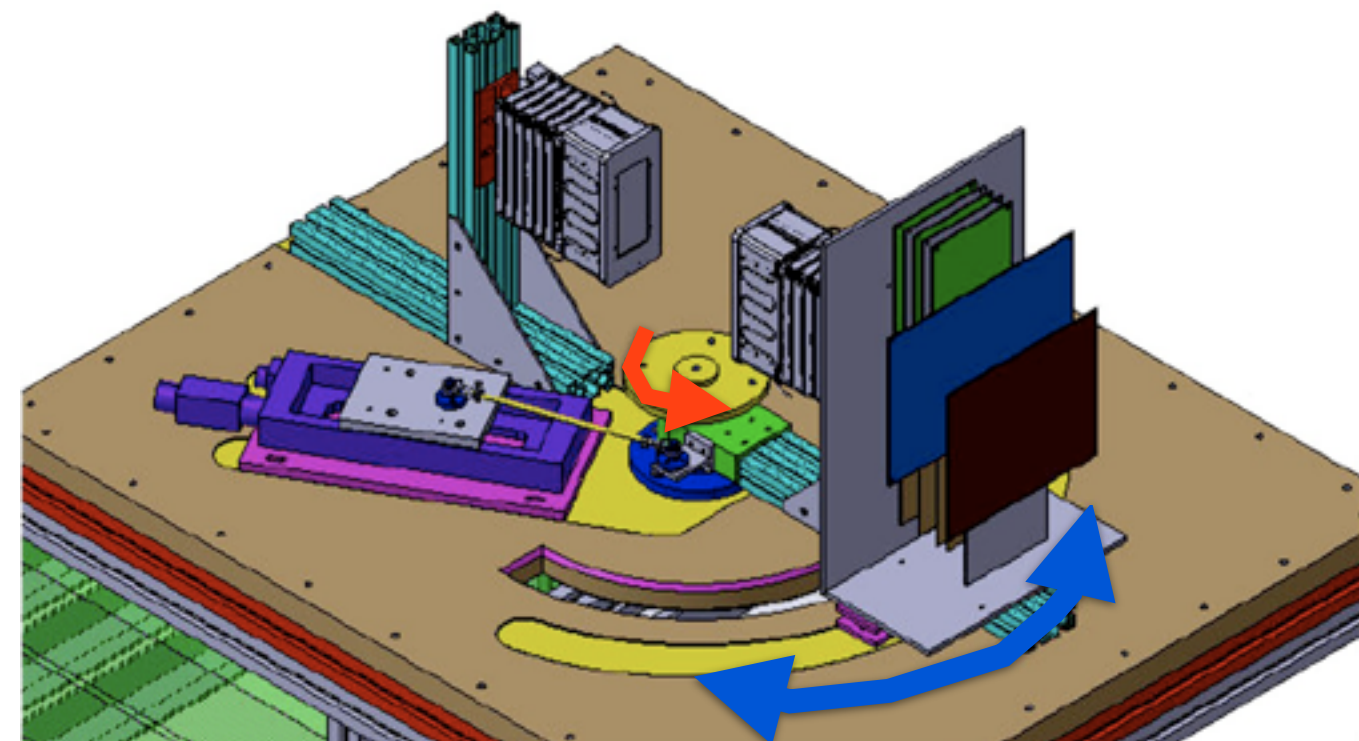


Setup for tomographic reconstruction



The two modules are mounted on top of a portable platform, which houses also the electronics, power supply, etc...

- One rotating motor for the source / phantom
- One module fixed (Mod1); the other rotating (Mod2)



Measurements with phantoms

Three different measurement campaigns :

@ ETH Zurich (CH), Radio-Pharmaceutical Institute - Apr 2010

@ AAA (Advanced Acceleration Applications) St. Genis-Pouilly (FR) - July 2010

@ AAA (Advanced Acceleration Applications) St. Genis-Pouilly (FR) - July 2011

in-situ cyclotron production of the radiotracer.

- Phantoms filled with **F-18** based **tracers** (F-18 in water solution)
- **$t_{1/2} \sim 110$ mins**
- Concentration diluted in water; **A_0 : few MBq up to ~ 100 MBq**

Measurements with phantoms

Three different measurement campaigns :

@ ETH Zurich (CH), Radio-Pharmaceutical Institute - **Apr 2010**

- very first measurements with high activity and extended objects
- limited to the **central FOV** (i.e. fixed modules, rotating source)

@ AAA (Advanced Acceleration Applications) St. Genis-Pouilly (FR) - **July 2010**

- **extended FOV** coverage (one module rotating, rotating source)
- larger phantoms / placed off-centered phantoms

@ AAA (Advanced Acceleration Applications) St. Genis-Pouilly (FR) - **July 2011**

- **extended FOV** as before
- **improved DAQ** performance
- improved acquisition methods

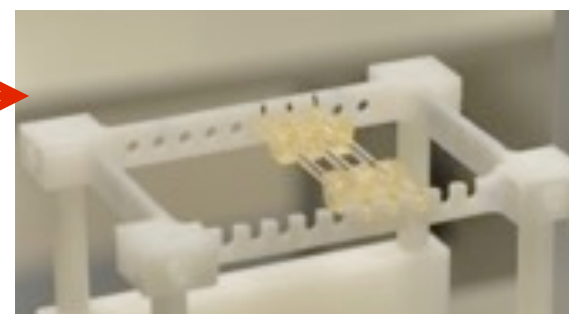
in-situ cyclotron production of the radiotracer.

- Phantoms filled with **F-18** based **tracers** (F-18 in water solution)
- **$t_{1/2} \sim 110$ mins**
- Concentration diluted in water; **A_0 : few MBq up to ~ 100 MBq**

Phantoms for reconstruction

(1) capillaries

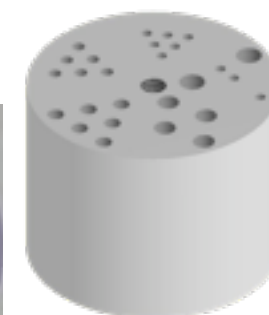
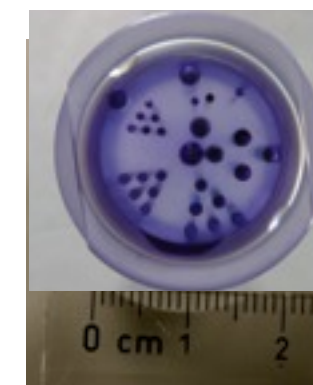
L = 3cm ;
Diam = 1.4 mm ;
Pitch = 5 mm



pictures not on scale!

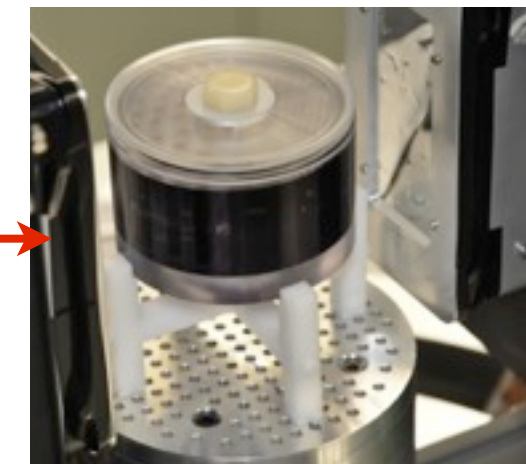
(2) micro Derenzo

H = 1.5 cm ;
Diam = 2 cm;
Rods_Diam = 0.8÷2 mm



(3) mini DeLuxe

H = 5 cm ;
Diam = 7.5 cm;
Rods_Diam = 1.2÷4 mm



(4) homogeneous cylinder

H = 9 cm ;
Diam = 6 cm;



(5) NEMA phantom

H = 6.3 cm ;
Diam = 3.3 cm;

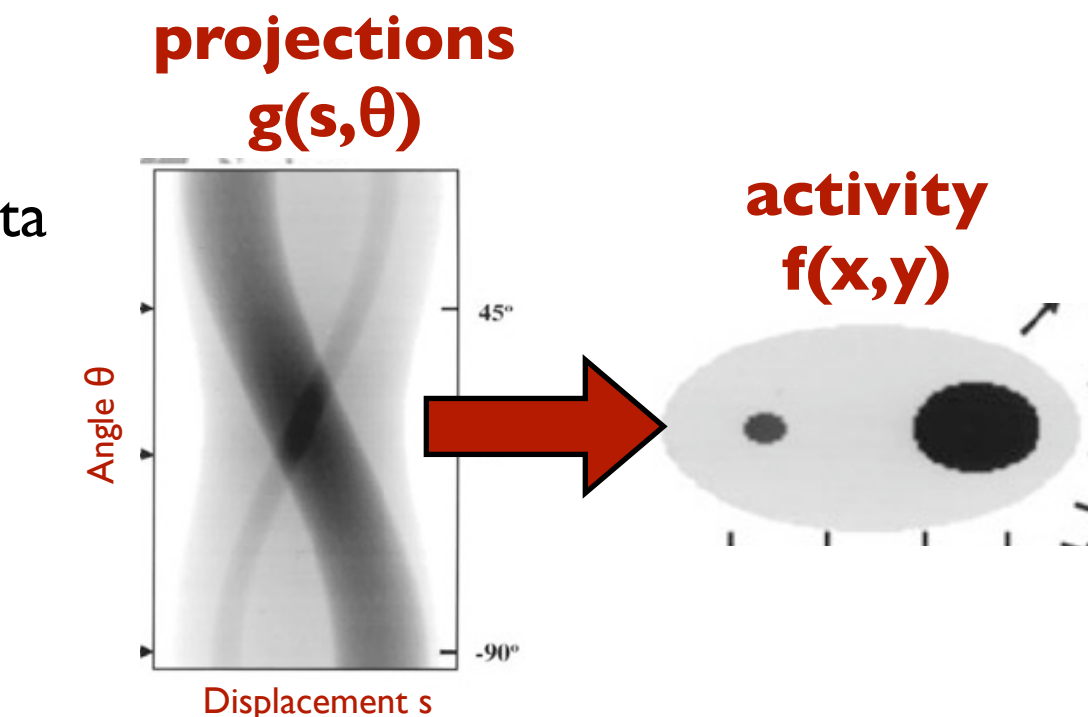
Image reconstruction

Goal :

recover the activity distribution, starting from the acquired data

Data :

LOR of the various coincidence events i.e. **projections**
(typically organized in “sinograms”)



Two different approaches :

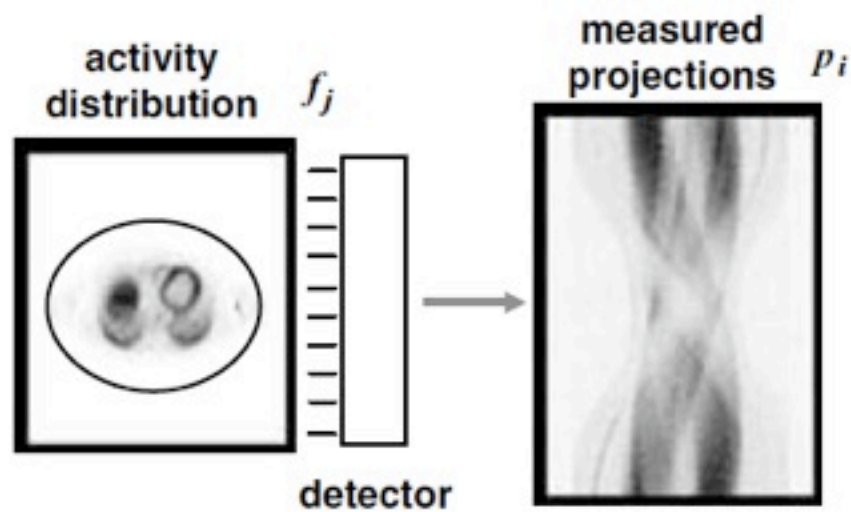
ANALYTICAL METHOD

- Filtered Back Projection (FBP) :
 - 1) Fourier analysis of the projection data
 - 2) Different weight to different frequencies (“filtering”)
 - 3) “Back-Project”
- **simple and fast** ☺
- **not extremely accurate** ☹
- assumption : measured data are perfectly consistent with the source object (never true: e.g. noise, gaps between detector...)

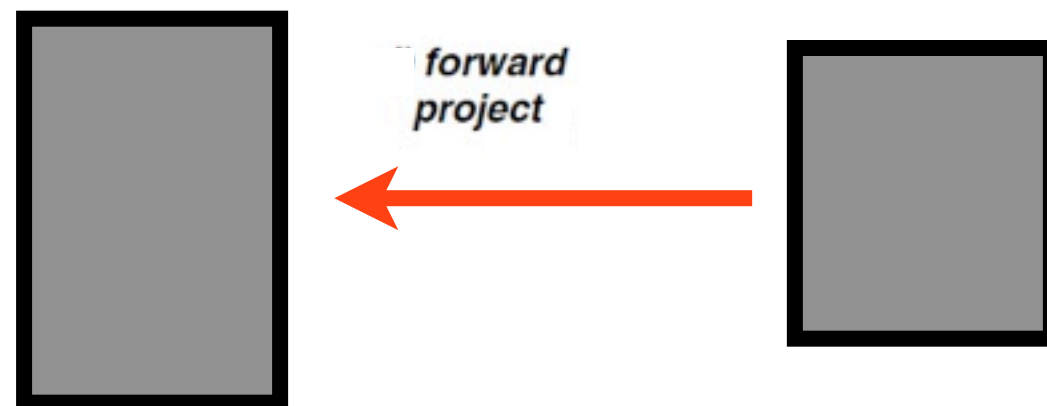
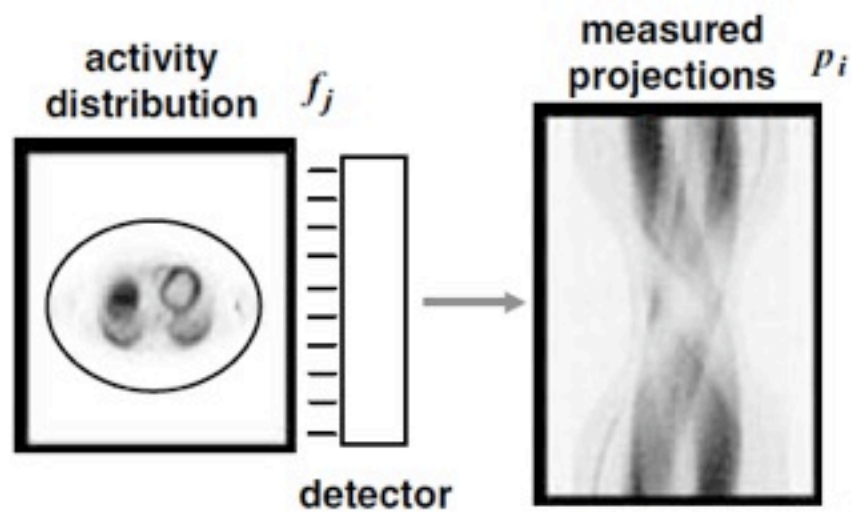
ITERATIVE METHOD

- **slow and CPU consuming** ☹
- accurate model of the emission and detection processes
- **accurate reconstruction** ☺
- optimization procedure until the best estimate is found
- several optimization strategies exist

Iterative reconstruction method



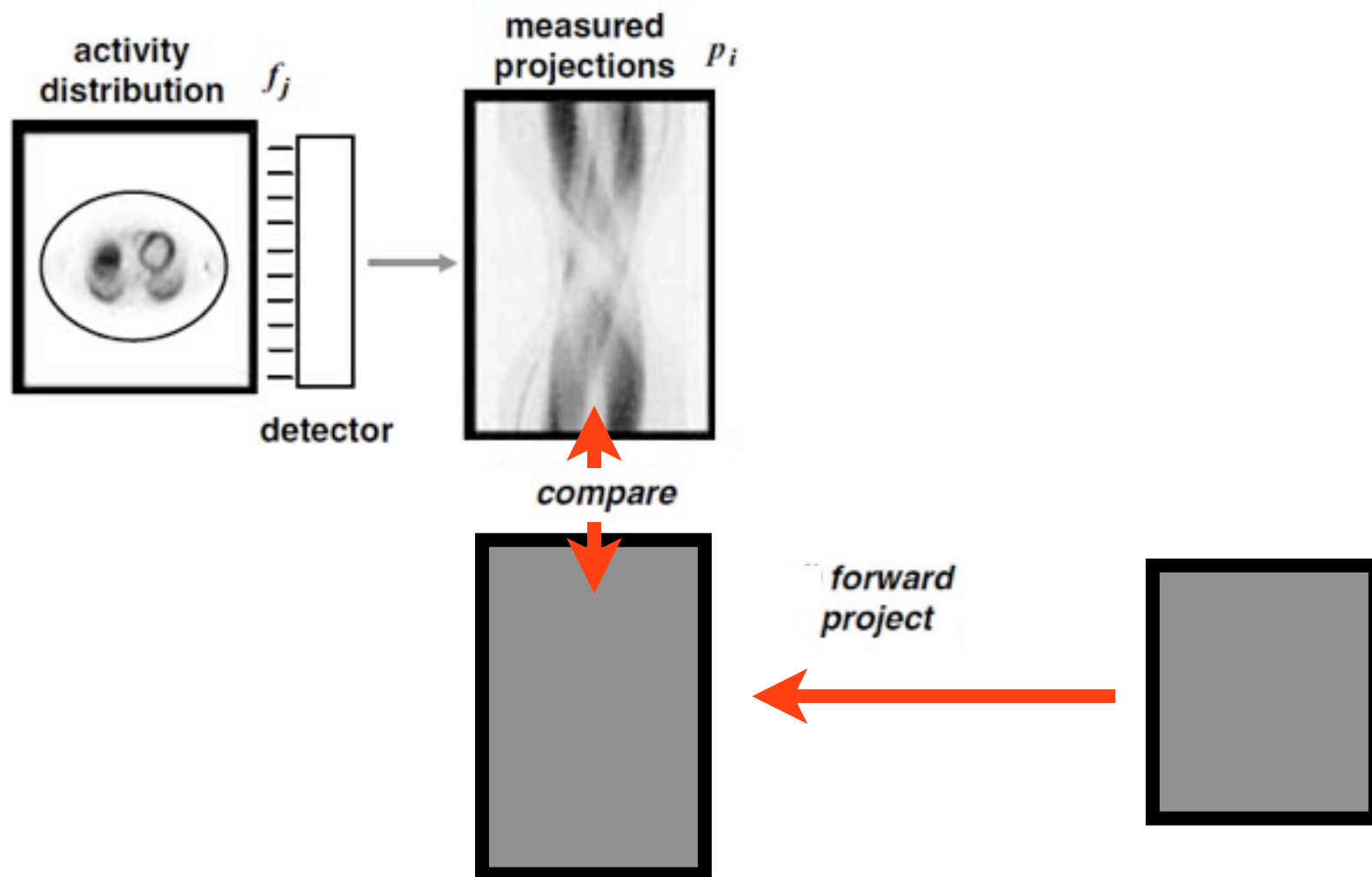
Iterative reconstruction method



(1)
initial estimate of the
object count distribution
(typically: uniform)

(2)
obtain the projection that would
derive from such an object

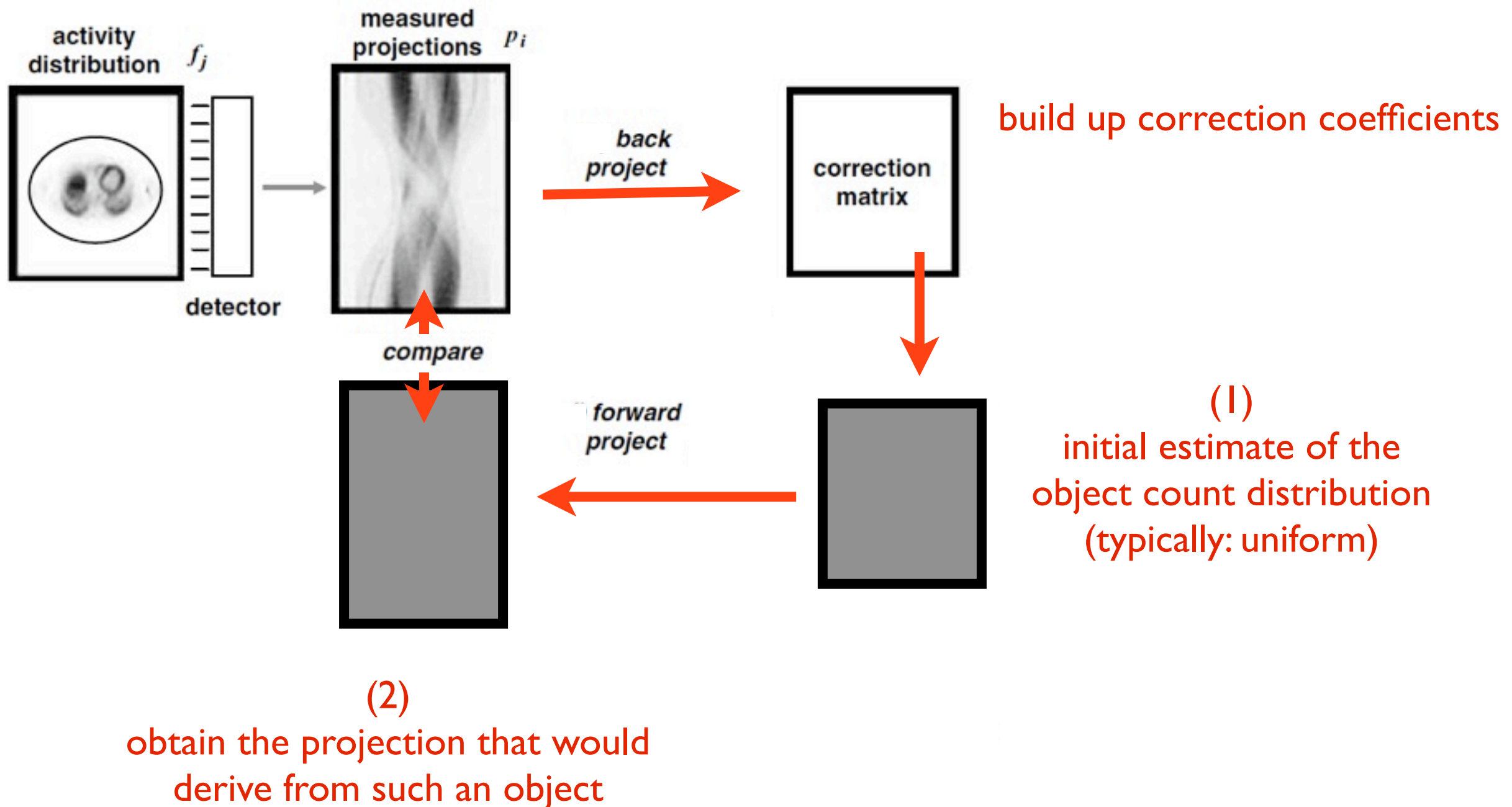
Iterative reconstruction method



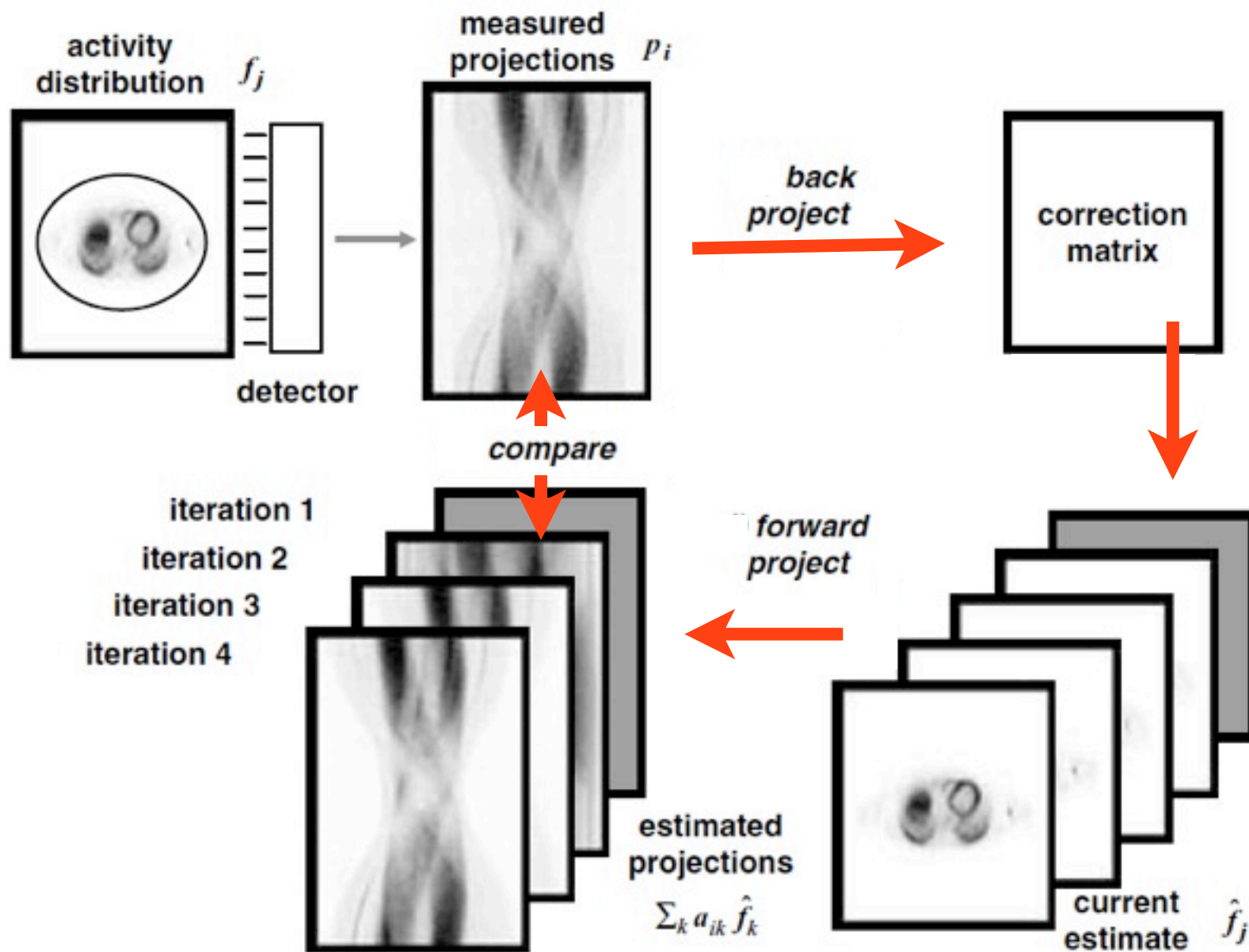
(2)
obtain the projection that would
derive from such an object

(1)
initial estimate of the
object count distribution
(typically: uniform)

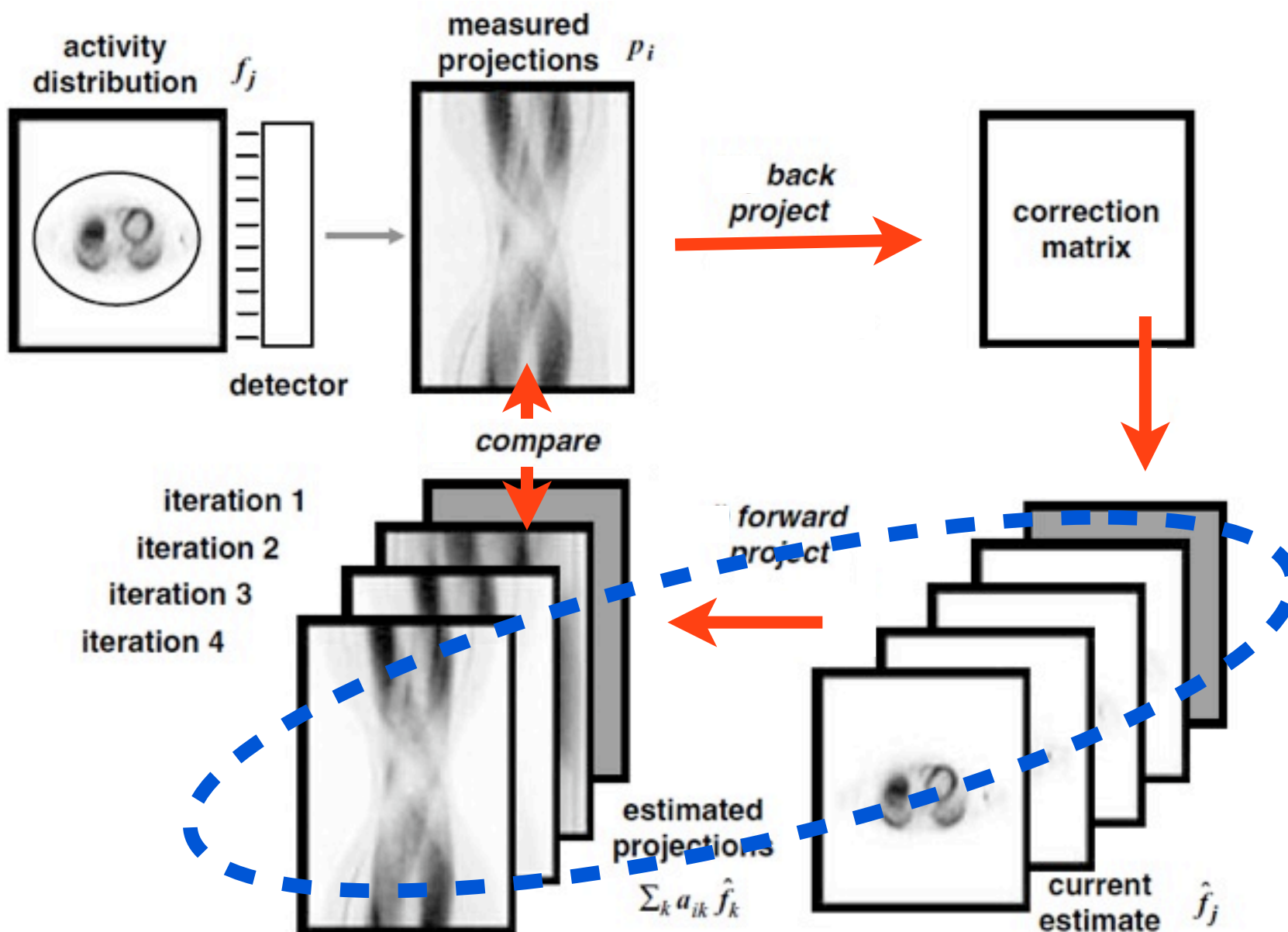
Iterative reconstruction method



Iterative reconstruction method

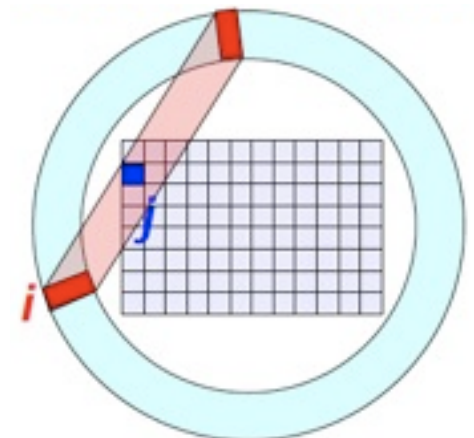


Iterative reconstruction method



requires a description of the physical model of emission and detection processes :

SYSTEM MATRIX M_{ij}

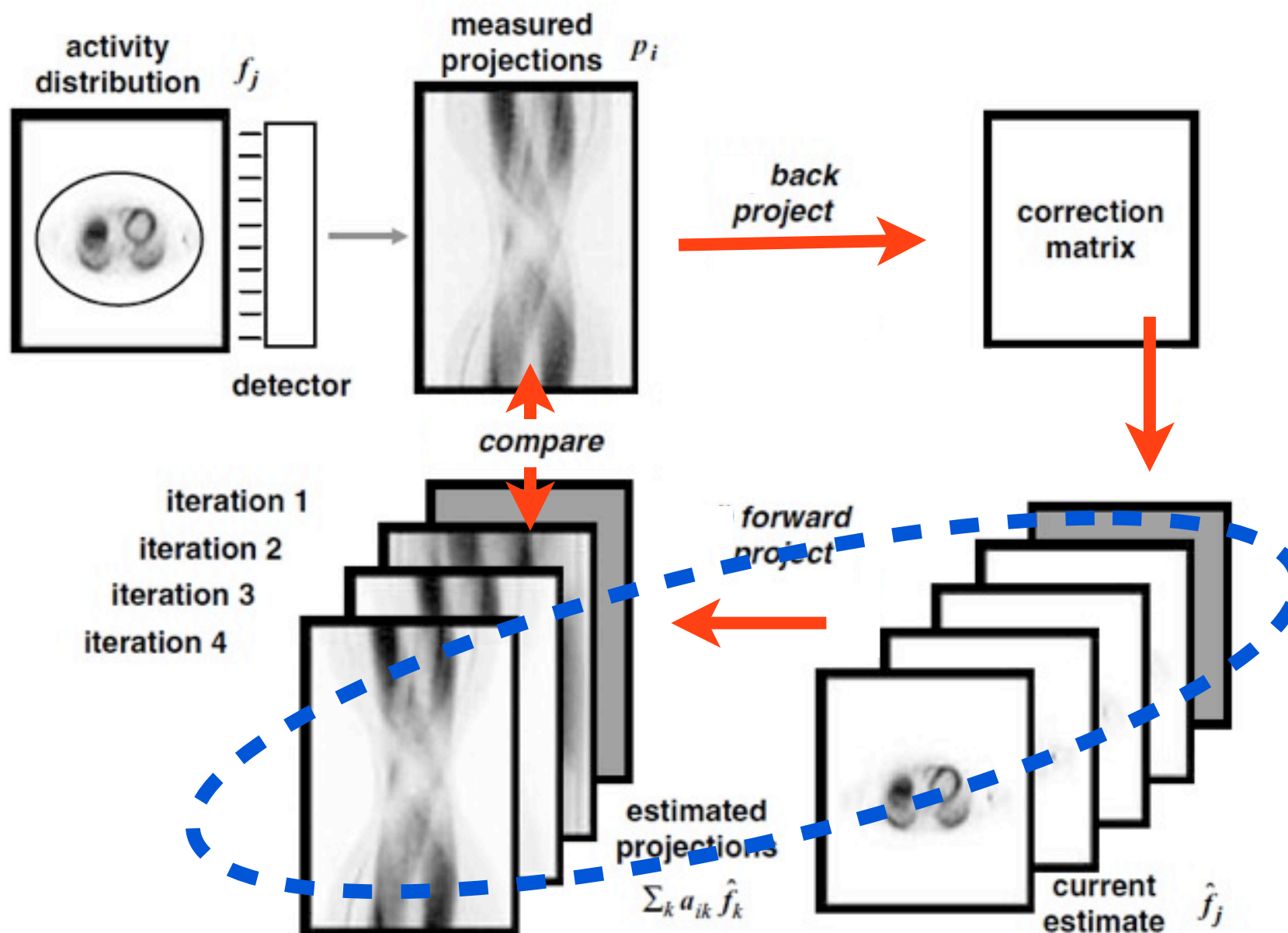


probability of the activity in the j -voxel to be detected by the i -LOR

includes :

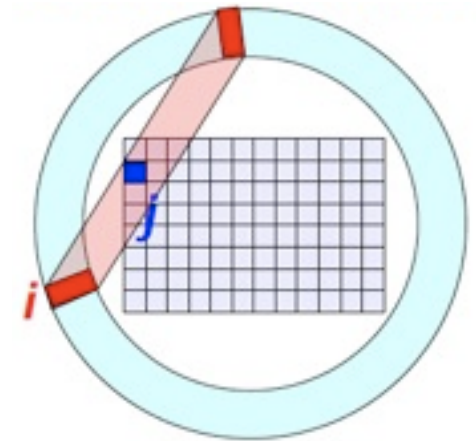
- **geometry** description
- **physics** (e.g.: attenuation)
- **variable fraction of the voxel contributes to the counts**
- ...

Iterative reconstruction method



requires a description of the physical model of emission and detection processes :

SYSTEM MATRIX M_{ij}



probability of the activity in the j -voxel to be detected by the i -LOR

includes :

- **geometry** description
- **physics** (e.g.: attenuation)
- **variable fraction of the voxel** contributes to the counts
- ...

out of the many possible iterative methods

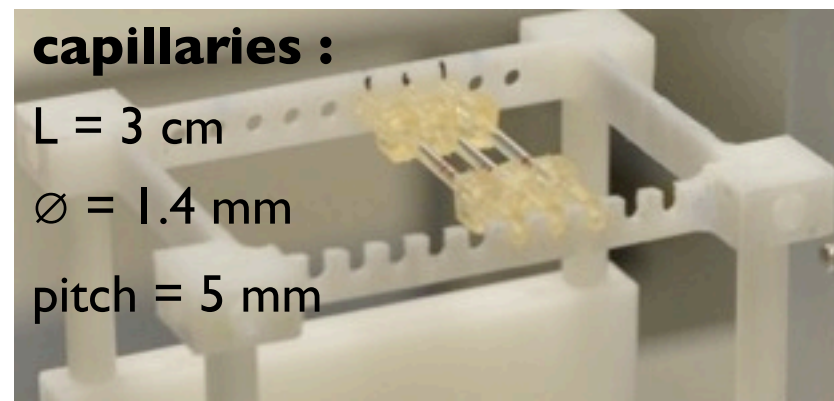
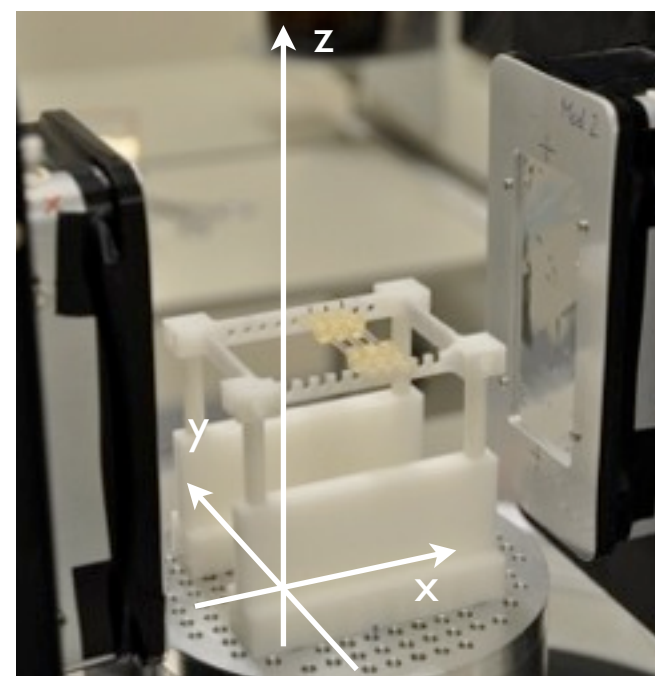
AX-PET uses **ML-EM**

Max Likelihood

Expectation
Maximization

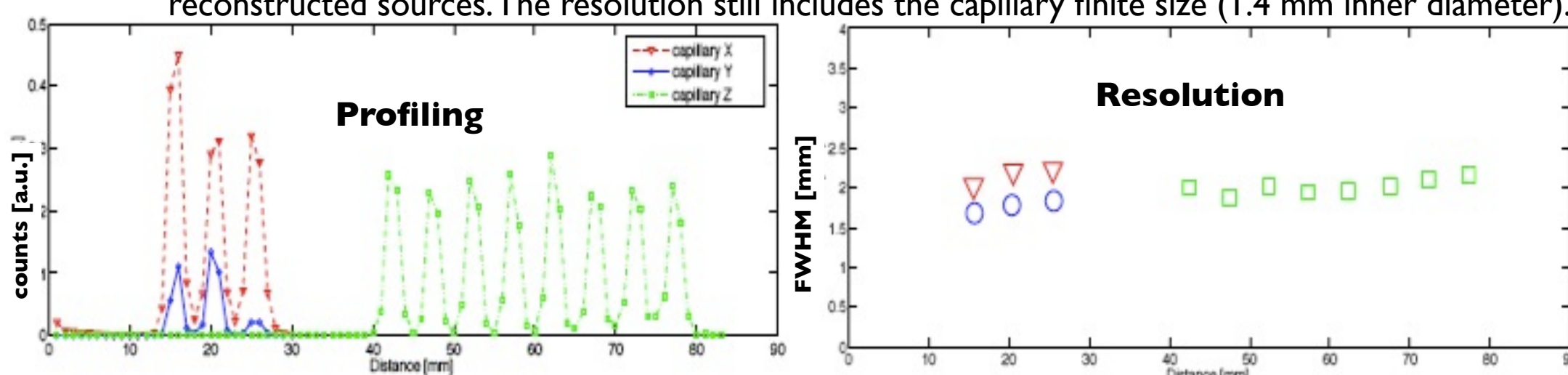
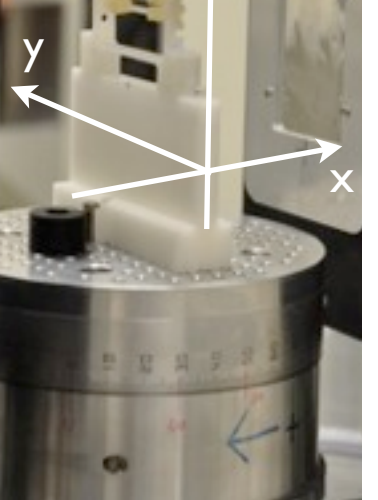
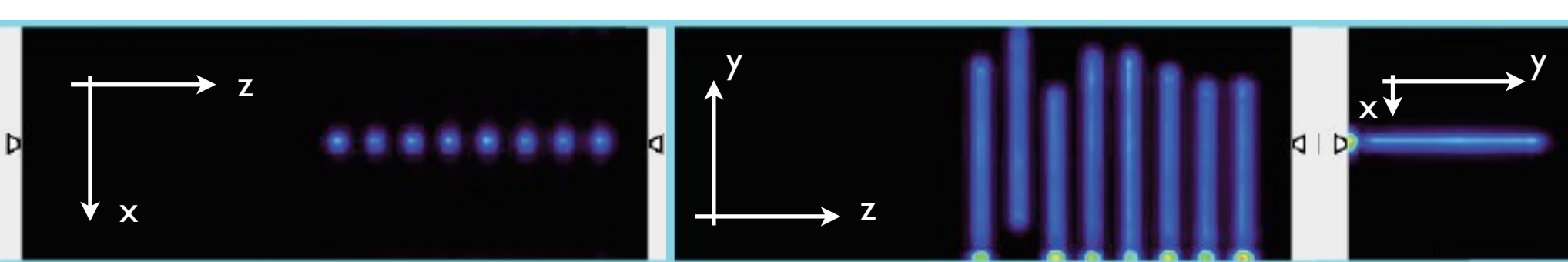
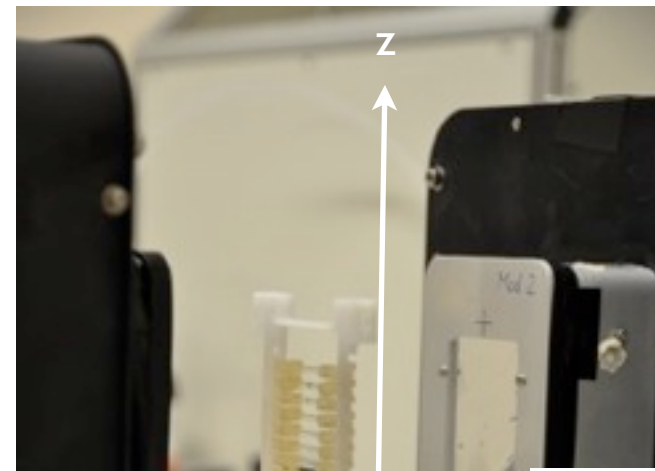
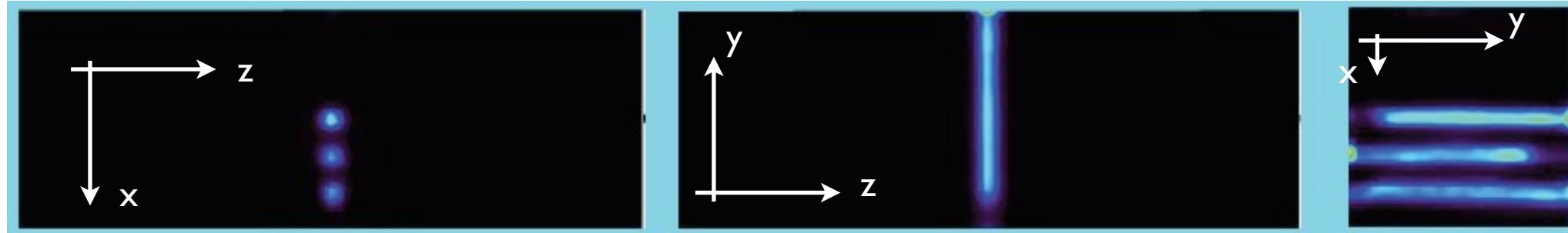
two steps per iteration :
(1) Expectation step : form the likelihood of any reconstructed image given the measured data
(2) Maximization step : find the image with the greatest likelihood

Simple reconstructed images : capillaries



**central FOV
no modules rotation**

ETH 2010



NEMA phantom

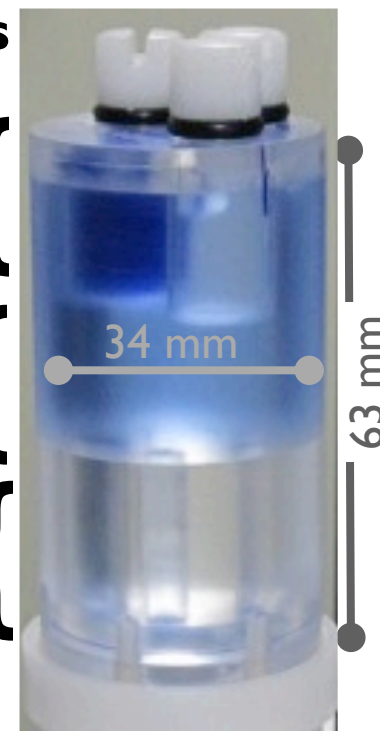
extended FOV
2nd module rotation

Three regions in the same phantom to address three different aspects

Hot & Cold rods for **contrast**

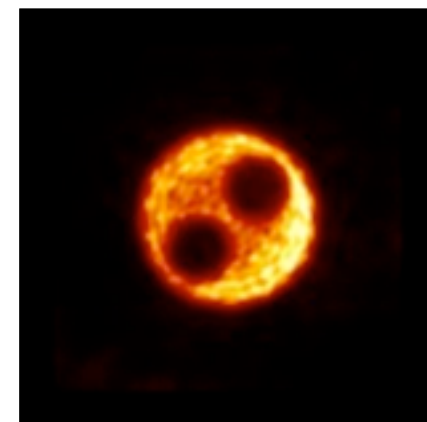
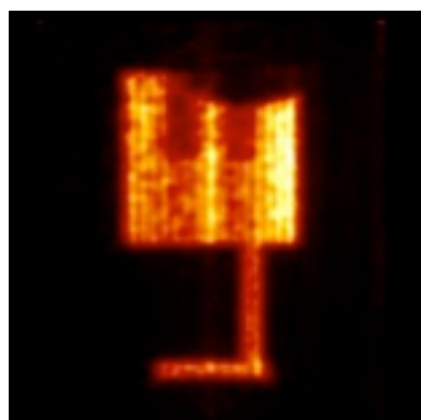
Homogeneous cylinder for assessing the **ability to reconstruct homogeneous distributions**

Series of small rods for **resolution**



NEMA phantom

extended FOV
2nd module rotation

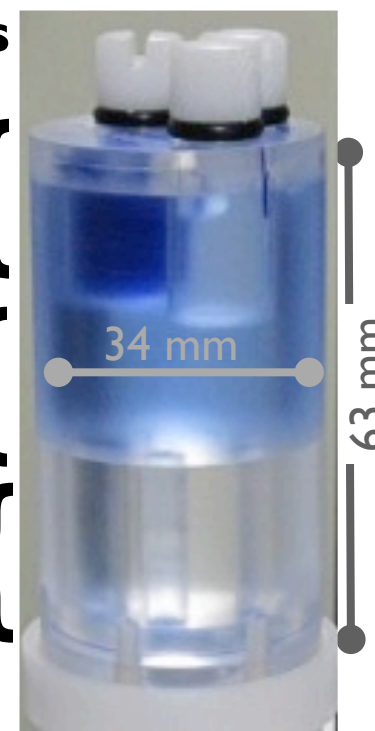


Three regions in the same phantom to address three different aspects

Hot & Cold rods for **contrast**

Homogeneous cylinder for assessing the **ability to reconstruct homogeneous distributions**

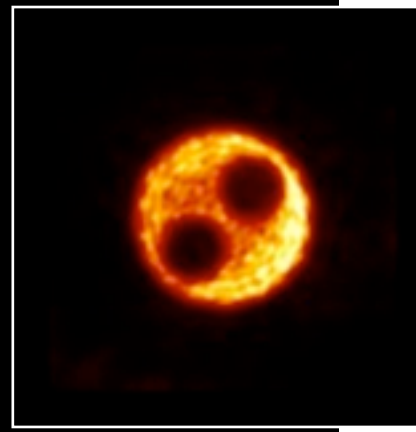
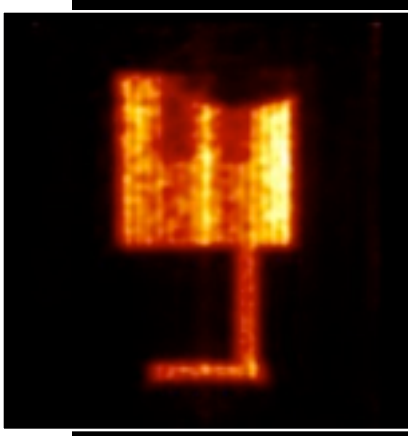
Series of small rods for **resolution**



NEMA phantom

**extended FOV
2nd module rotation**

NEMA phantom uniformly filled - AAA 2010

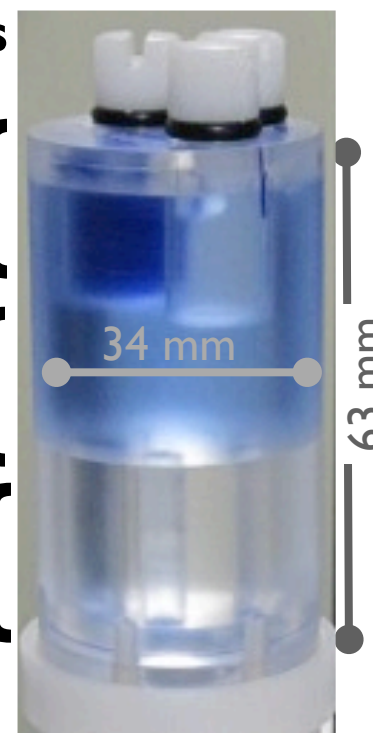


Three regions in the same phantom to address three different aspects

Hot & Cold rods for **contrast**

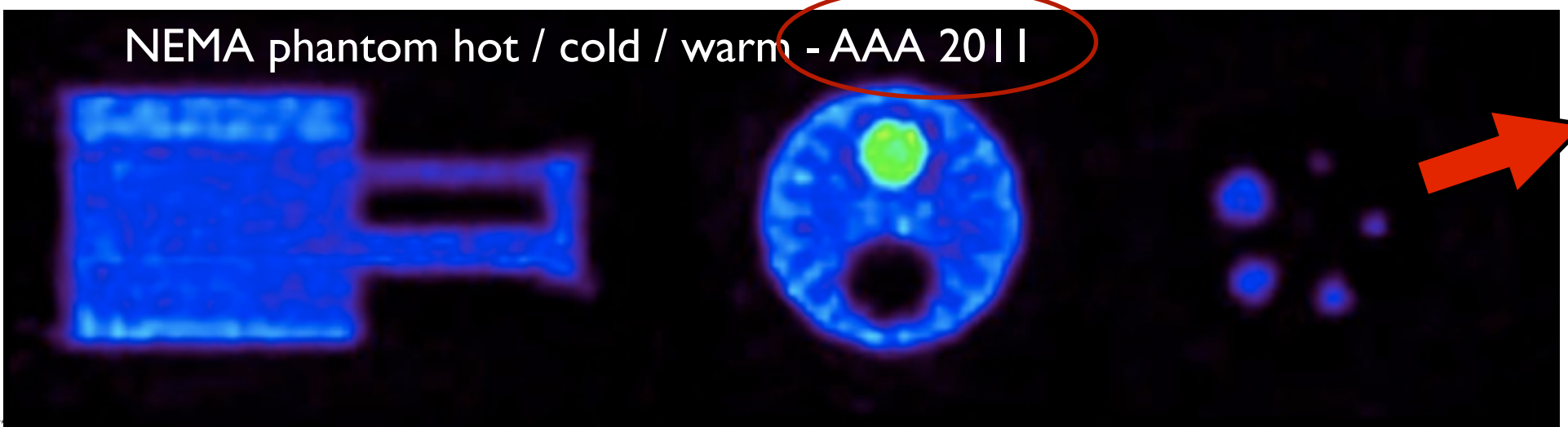
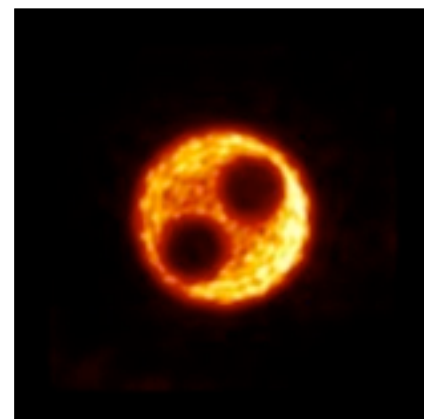
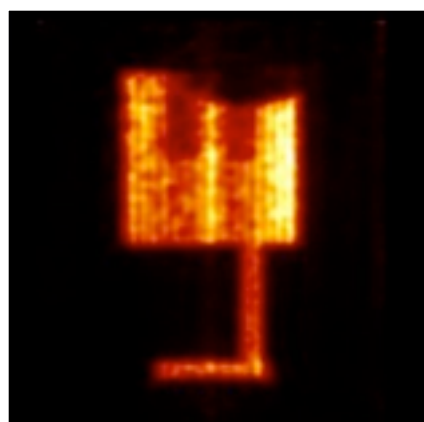
Homogeneous cylinder for assessing the **ability to reconstruct homogeneous distributions**

Series of small rods for **resolution**



NEMA phantom

extended FOV
2nd module rotation

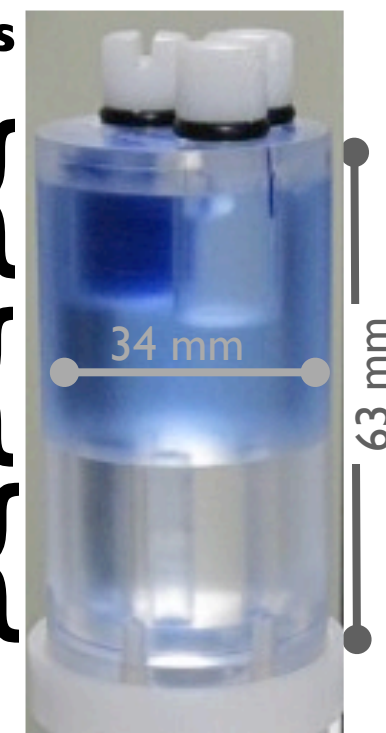


Three regions in the same phantom to address three different aspects

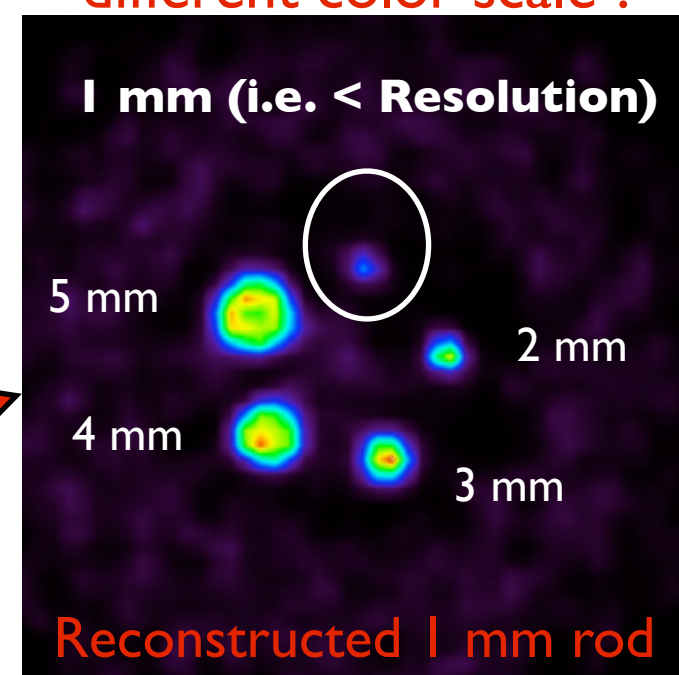
Hot & Cold rods for **contrast**

Homogeneous cylinder for assessing the **ability to reconstruct homogeneous distributions**

Series of small rods for **resolution**



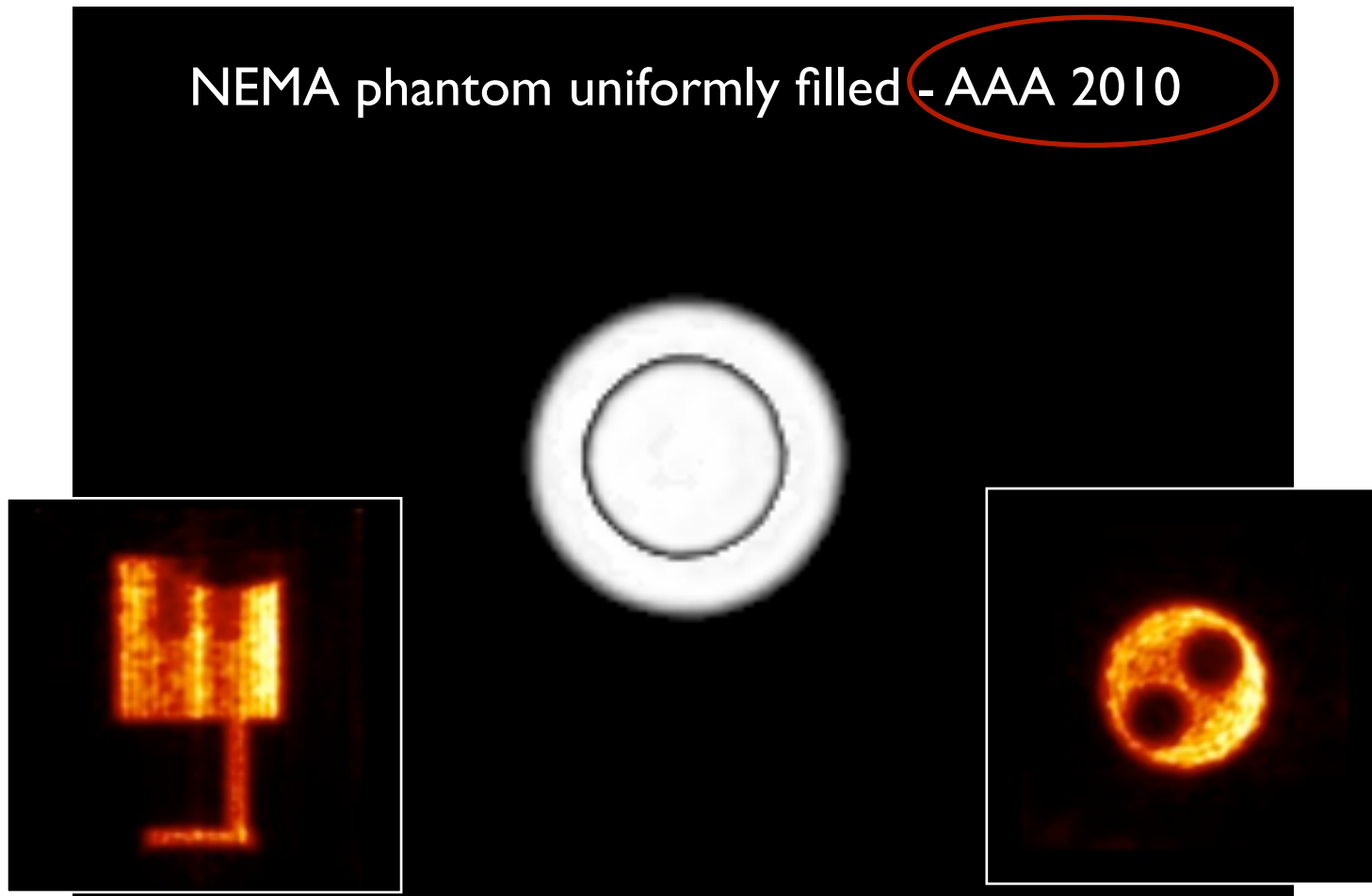
different color scale !



NEMA phantom

extended FOV
2nd module rotation

NEMA phantom uniformly filled - AAA 2010

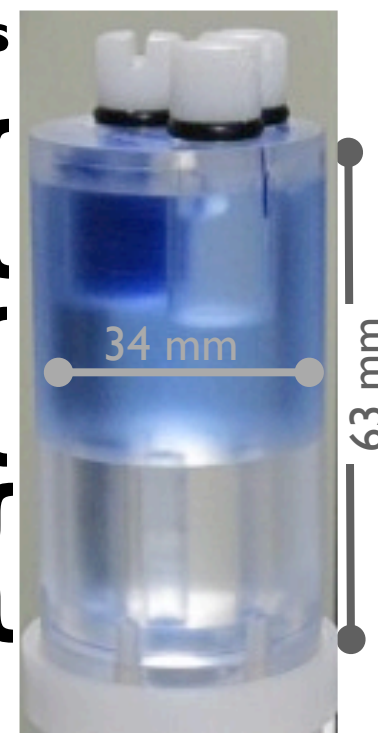


Three regions in the same phantom to address three different aspects

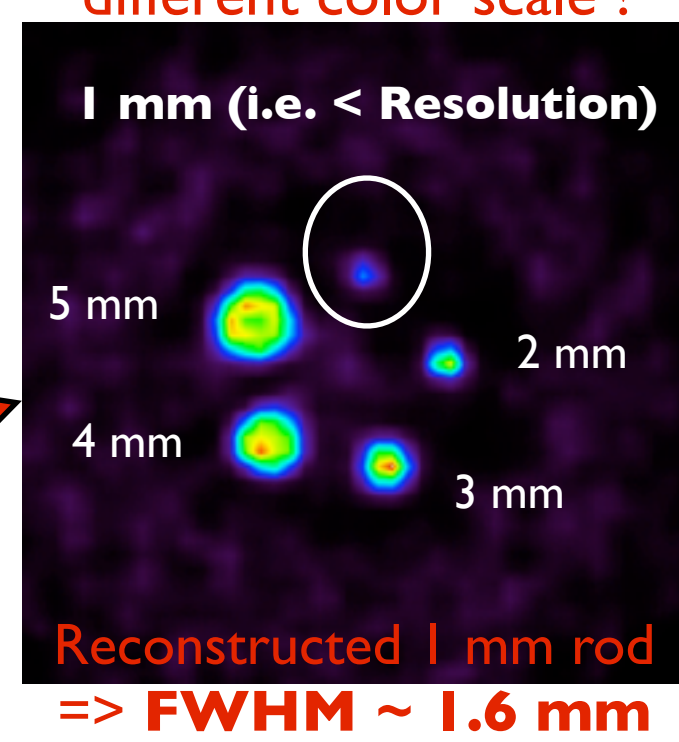
Hot & Cold rods for **contrast**

Homogeneous cylinder for assessing the **ability to reconstruct homogeneous distributions**

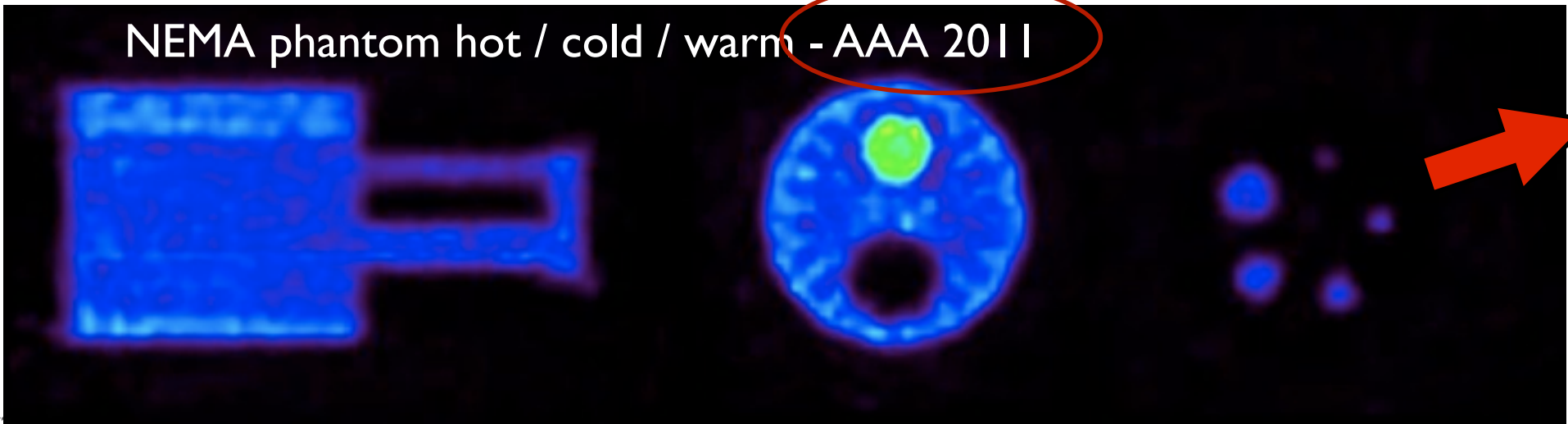
Series of small rods for **resolution**



different color scale !

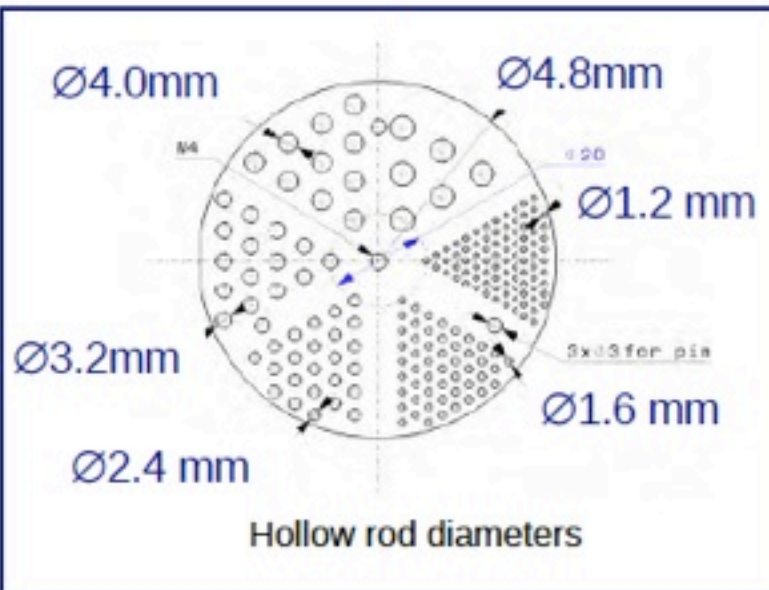


NEMA phantom hot / cold / warm - AAA 2011



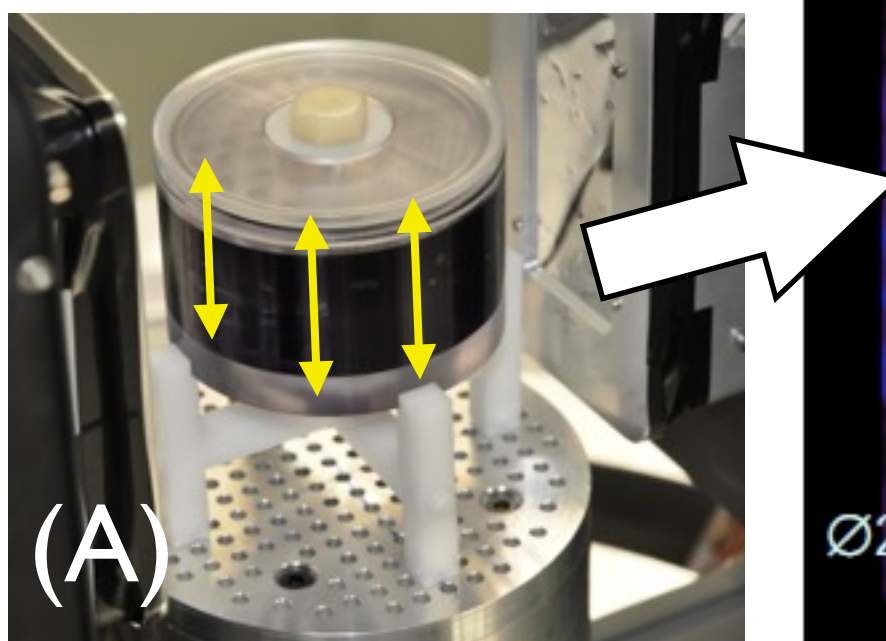
Resolution phantom : Mini Deluxe

Mini Deluxe phantom

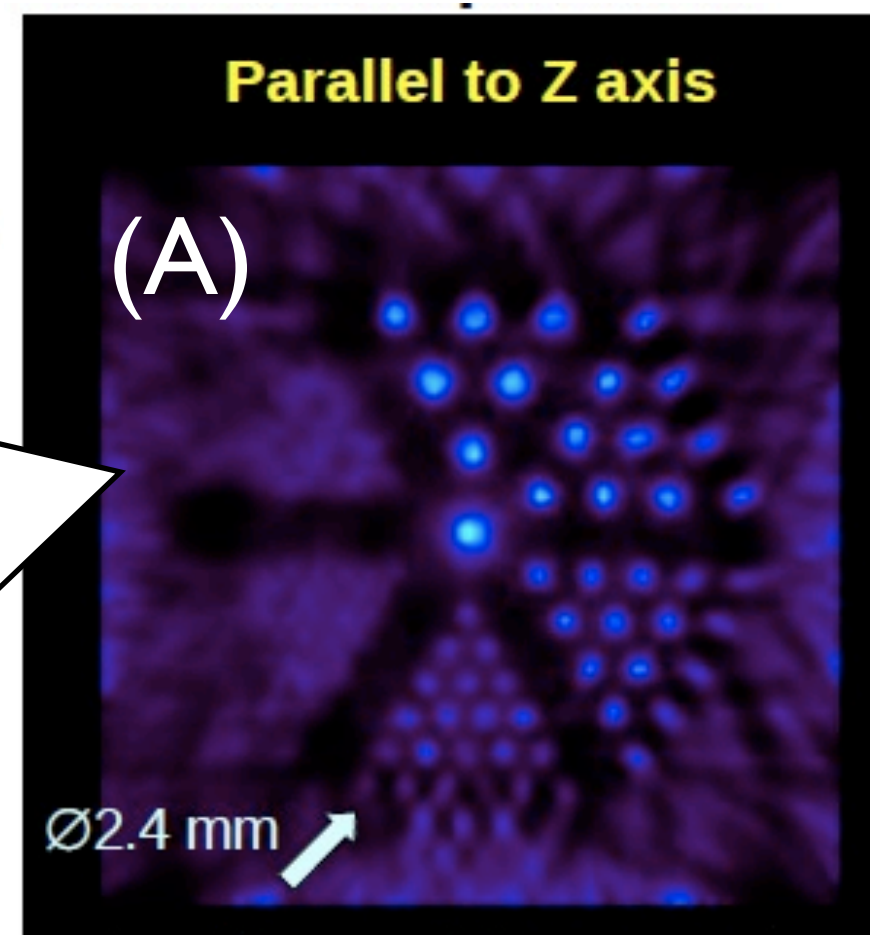


extended FOV
2nd module rotation

AAA 2011



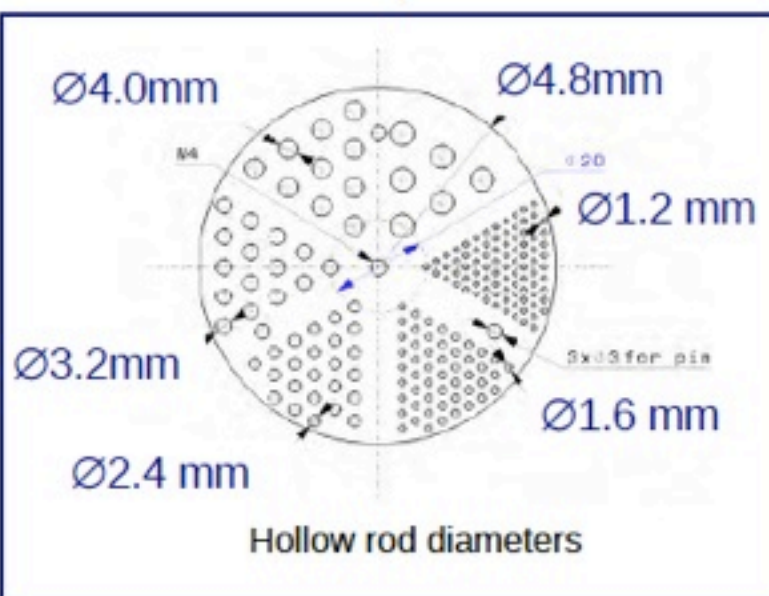
(A)
Rods oriented parallel to Z axis



- Fixed time acquisition: 120 s /step
- 60 iterations + post-reconstruction smoothing
- No corrections
- Artefacts due to data truncation (FOV too small...)

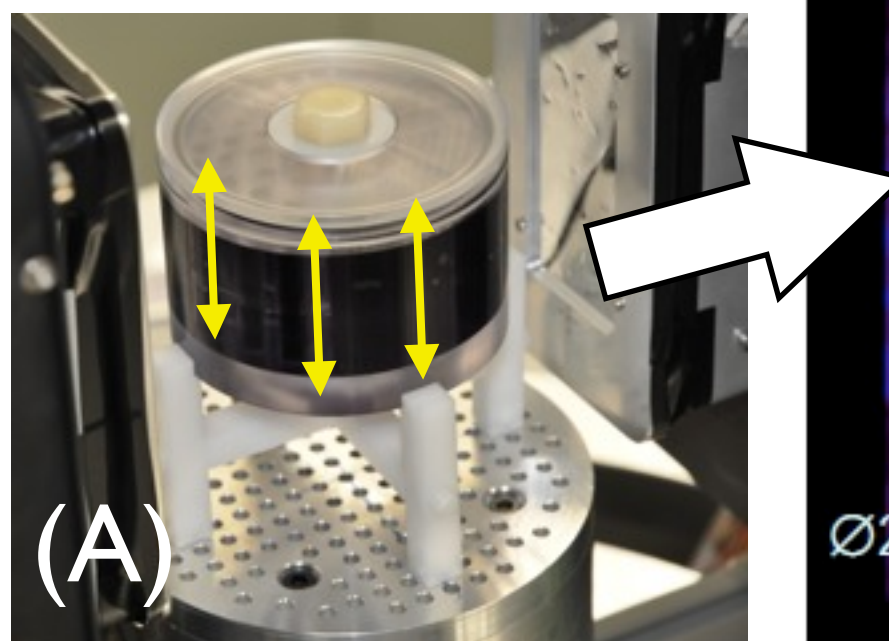
Resolution phantom : Mini Deluxe

Mini Deluxe phantom



extended FOV
2nd module rotation

AAA 2011

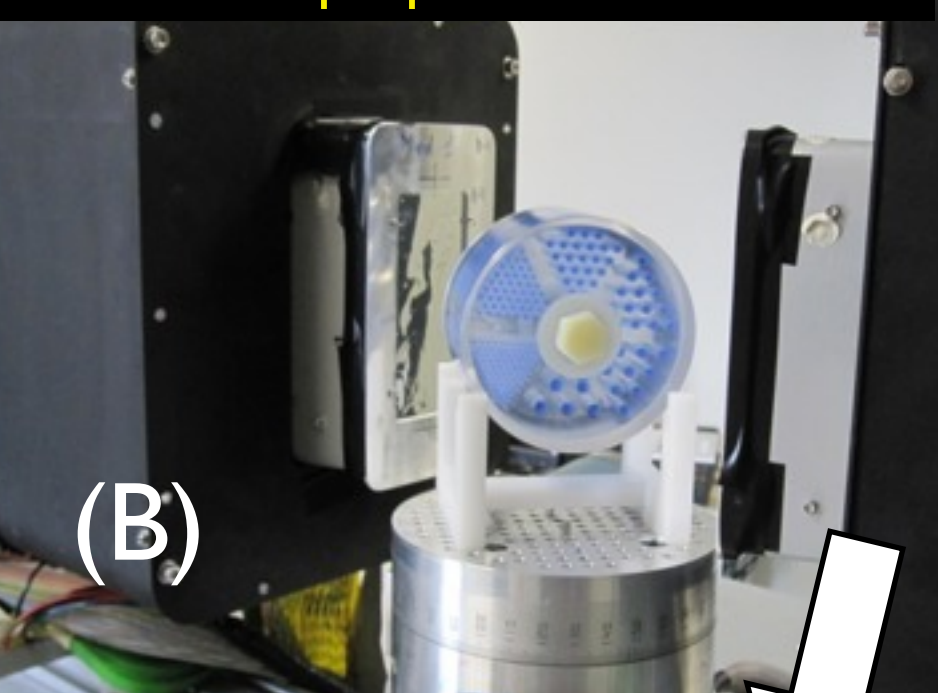
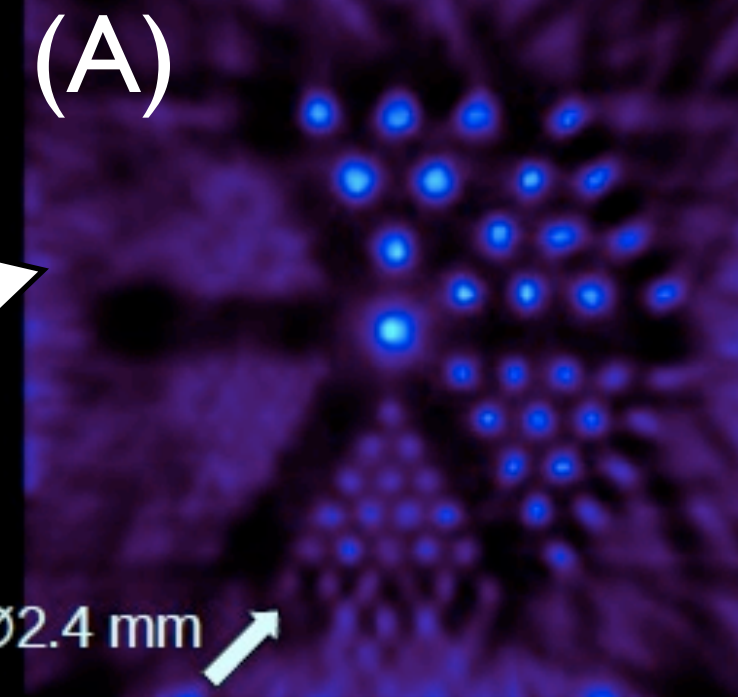


Rods oriented parallel to Z axis

Parallel to Z axis

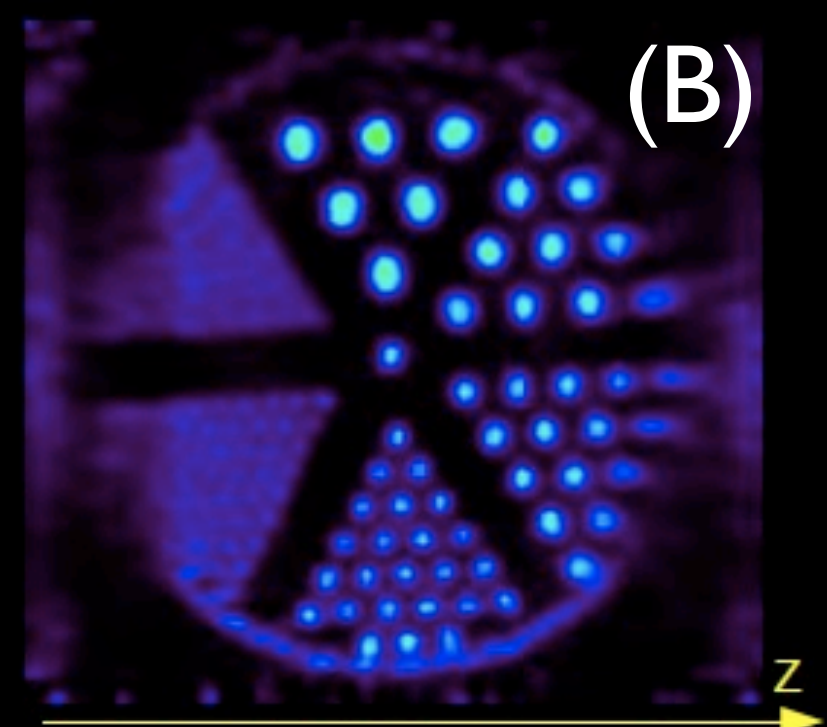
(A)

$\varnothing 2.4\text{ mm}$



Perpendicular to Z axis

(B)



- Fixed time acquisition: 120 s /step
- 60 iterations + post-reconstruction smoothing
- No corrections
- Artefacts due to data truncation (FOV too small...)

Results presented in Valencia, IEEE 2011

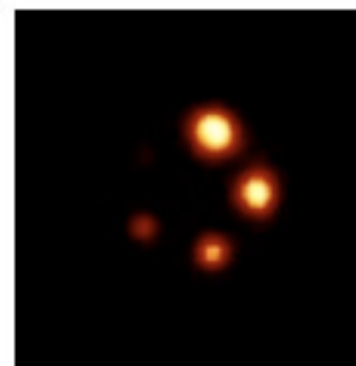
What's next (I/3) ?

What's next (1/3) ?

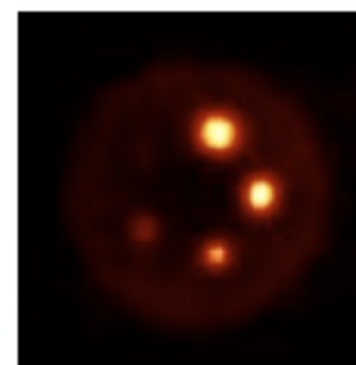
- **improve the reconstruction algorithms**
- **include ICS (Inter Crystal Scattering) events in the reconstruction**

preliminar!

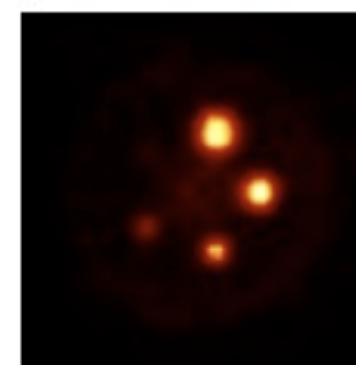
- ICS included:
 - only “triple” coinc. (1+2)
 - simplest weighting (50% ; 50%)
- Simulated One-Pass List-mode reconstruction (SOPL)
- No image deterioration when ICS events are included!



SOPL + ICS



SOPL w/o ICS

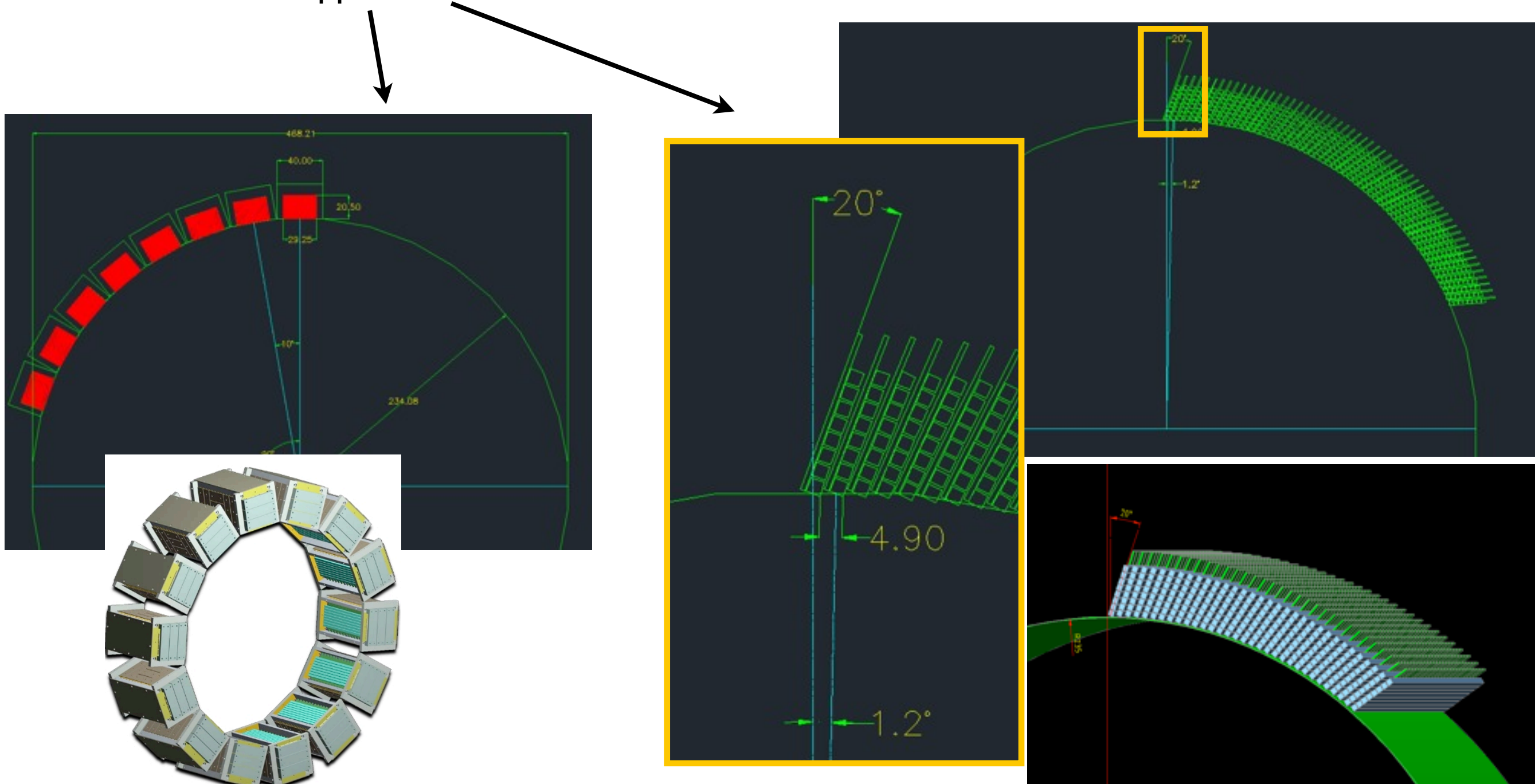


MLEM + precomputed SRM

What's next (2/3) ?

- **full ring simulations:**

- performance of (hypothetical) full ring (e.g. resolution, sensitivity, NEC...)
- two different approaches



What's next (3/3) ?

- **images of (probably dead) small animal**

- new measurement campaign
- @ETH Zurich, Radiopharmaceutical Institute
- Spring 2012 ?
- F-18 (bone scan) or FDG ?

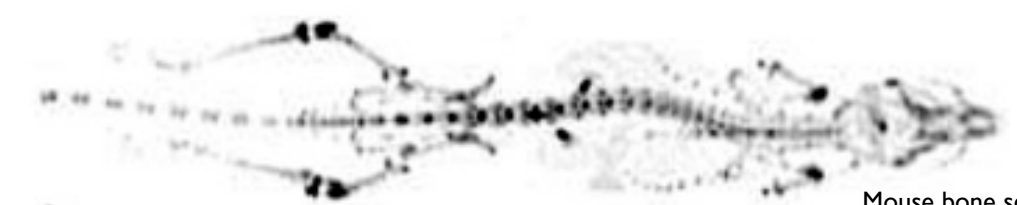


Mouse bone scan,
NanoSPECT (Bioscan)

What's next (3/3) ?

- **images of (probably dead) small animal**

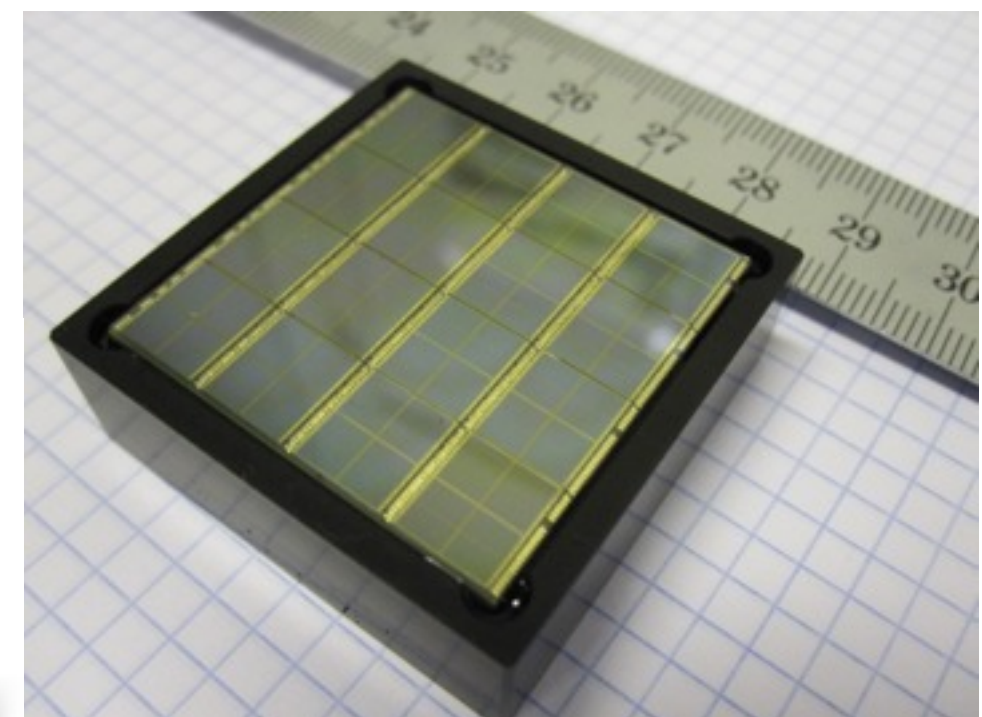
- new measurement campaign
- @ETH Zurich, Radiopharmaceutical Institute
- Spring 2012 ?
- F-18 (bone scan) or FDG ?



Mouse bone scan,
NanoSPECT (Bioscan)

- **test digital Silicon Photomultipliers (from Philips)
as alternative photodetectors**

- extremely good timing performance
- GOAL : demonstrate the possibility
a TOF-PET with the axial concept

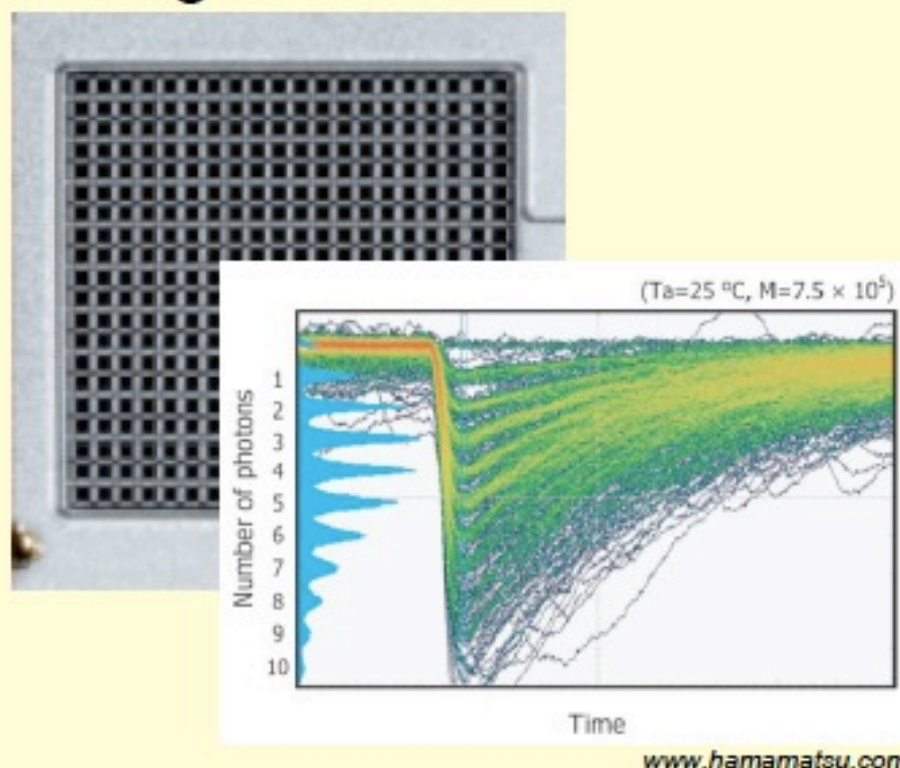


Digital Silicon Photomultiplier (D-SiPM)

PHILIPS

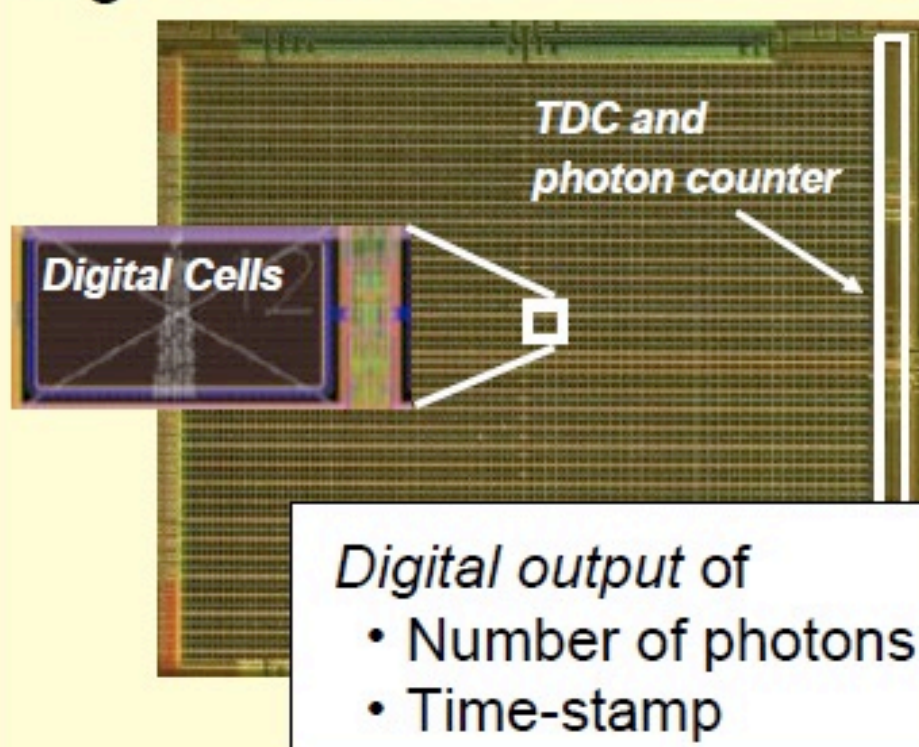
Digital SiPM – New Type of Silicon Photomultiplier

Analog SiPM



- Cells connected to common readout
- Analog sum of charge pulses
- Analog output signal

Digital SiPM



- Each diode is a digital switch
- Digital sum of detected photons
- Data packet

D-SiPM :

Single Photon Avalanche Photodiode (SPAD) integrated with conventional CMOS circuits on the same substrate.

All SPADs (including their corresponding electronics) connected together

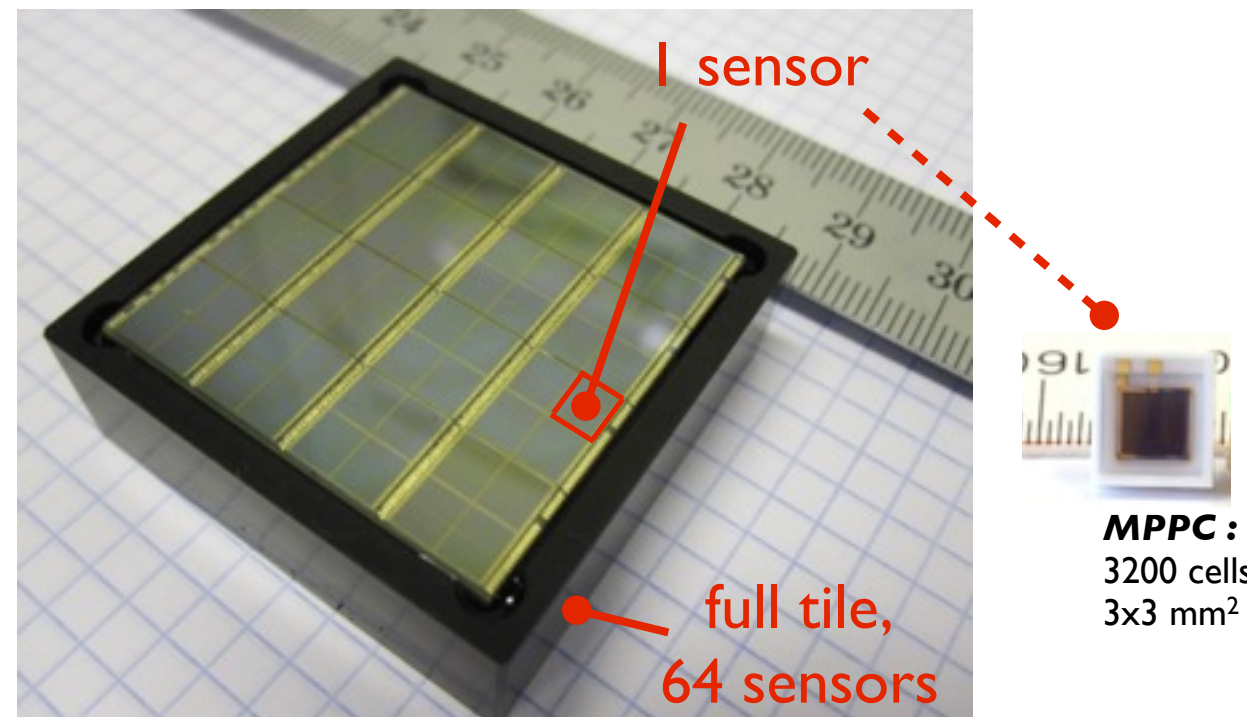
- to photon counter
- to TDC

Thomas Frach,
CERN Detector seminar, Oct 2011

Digital Silicon Photomultiplier (D-SiPM)

Advantages of D-SiPM for AX-PET:

- Intrinsically very fast photodetector ($\sim 50\text{ps}$).
=>Great potential for TOF-PET.
- Small size. High level of integration.
- Compactness.
- Interesting concept of simplifying the readout chain. Bias supply included.



- Early digitization of the cell output; integrated electronics on chip => low noise.
- Digital => Temperature and gain stability is less critical than in analogue SiPM.
- Possibility to disable cells with high Dark Count.
- MRI compatible.

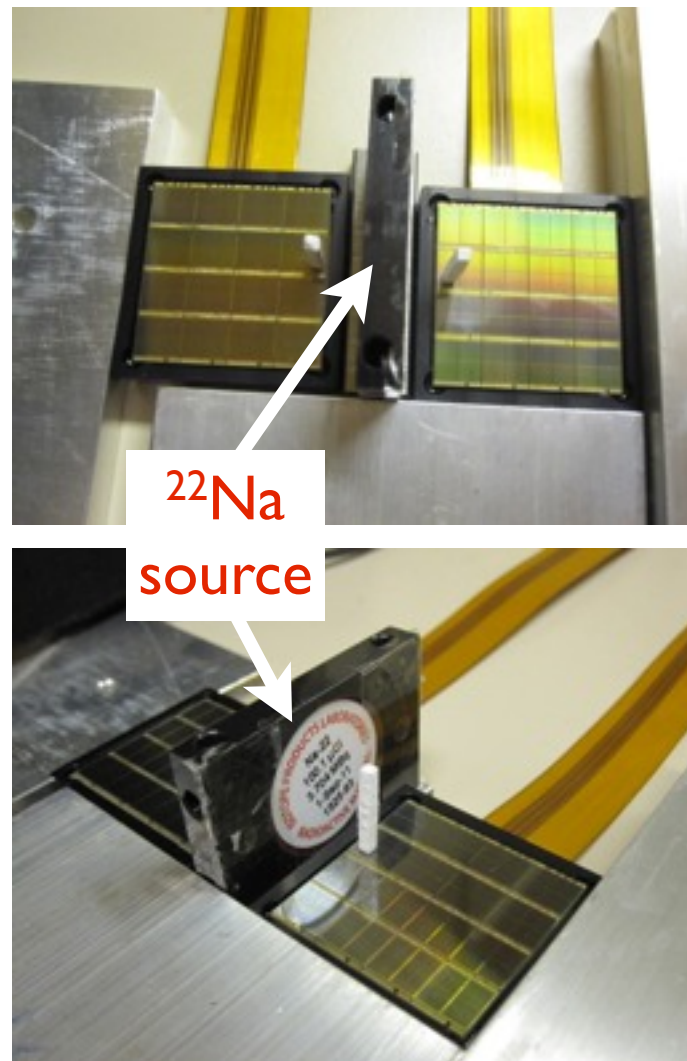
Technology Evaluation Kit (TEK) :



- 4 tiles :
 DLS_6400 (x2 tiles) ; 6400 cells/sensor
 DLS_3200 (x2 tiles) ; 3200 cells/sensor
- each tile : 8x8 sensors
- 1 sensor : $3.9 \times 3.3 \text{ mm}^2$

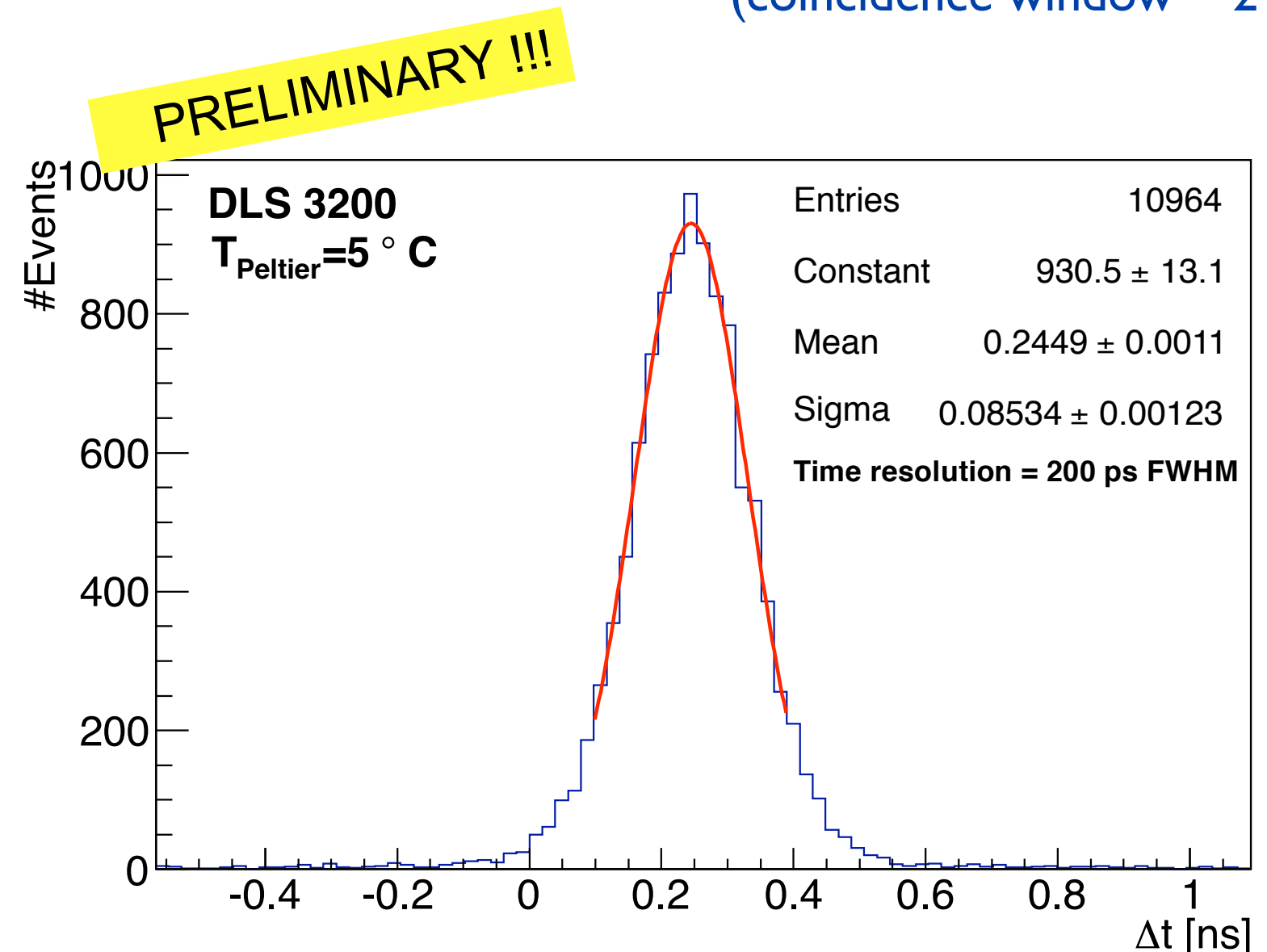
received at CERN on Jan 12th, 2012

D-SiPM: first preliminary results



- 2 LYSO scintillator crystals
 - **non AX-PET standard**
 - $(2 \times 2 \times 12) \text{ mm}^3$ and $(2 \times 2 \times 15) \text{ mm}^3$
 - wrapped with teflon
 - coupling done with optical grease
- LYSO crystal placed in the center of the pixel
(no precise mechanical alignment)

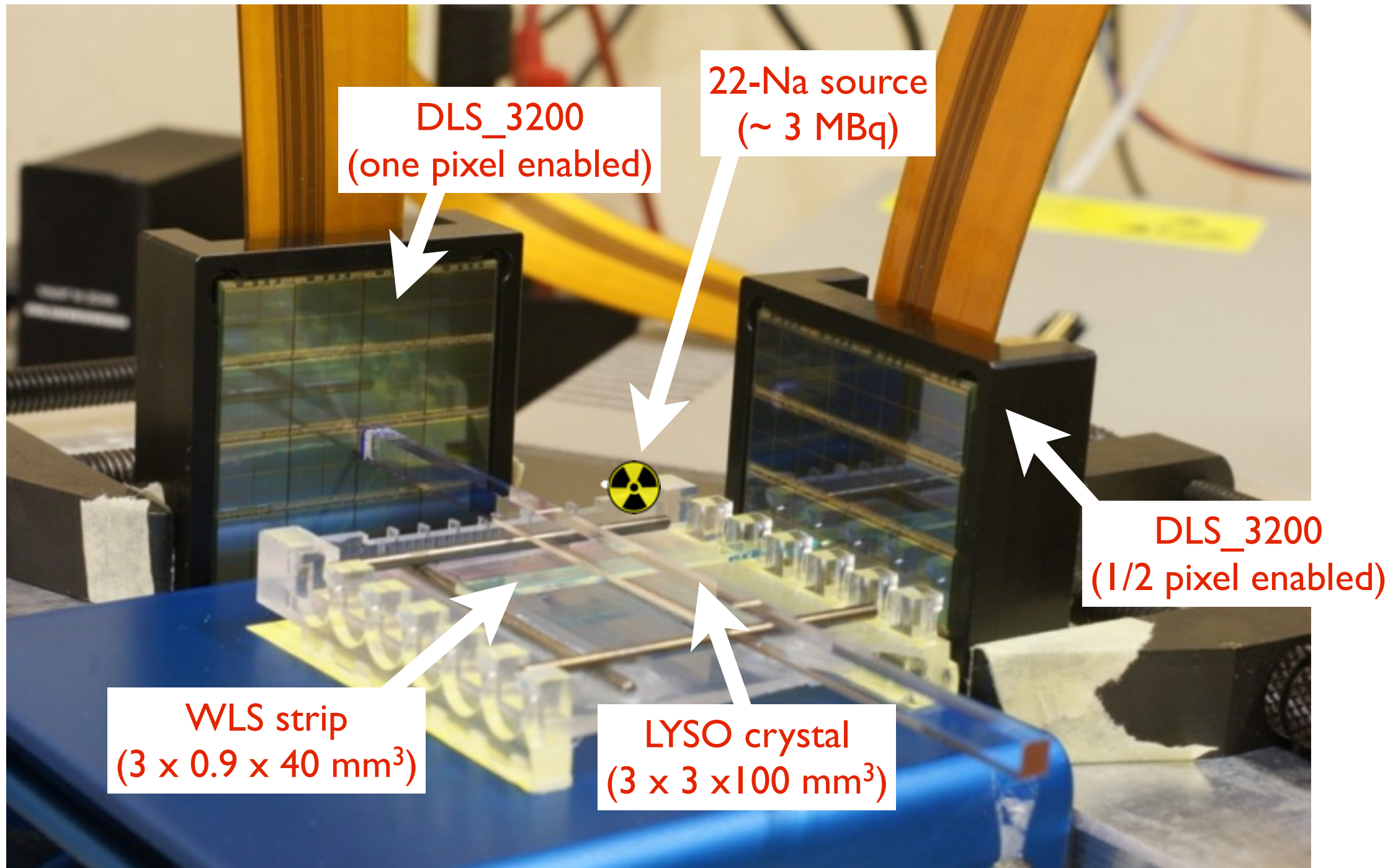
time difference between the two tiles for coincident events
(coincidence window = 2 ns)



FWHM ~ 200 ps
(cutting on events at the photopeak)

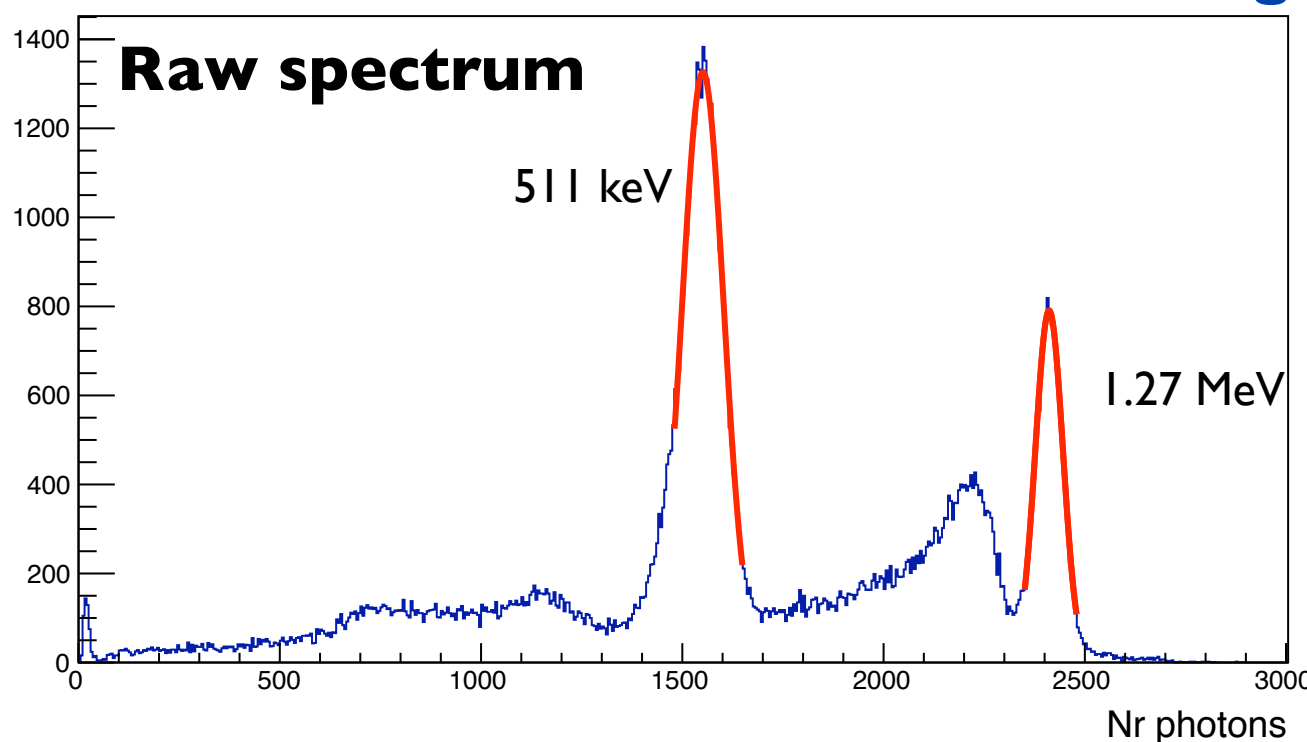
D-SiPM: first preliminary results

Minimal AX-PET like set-up

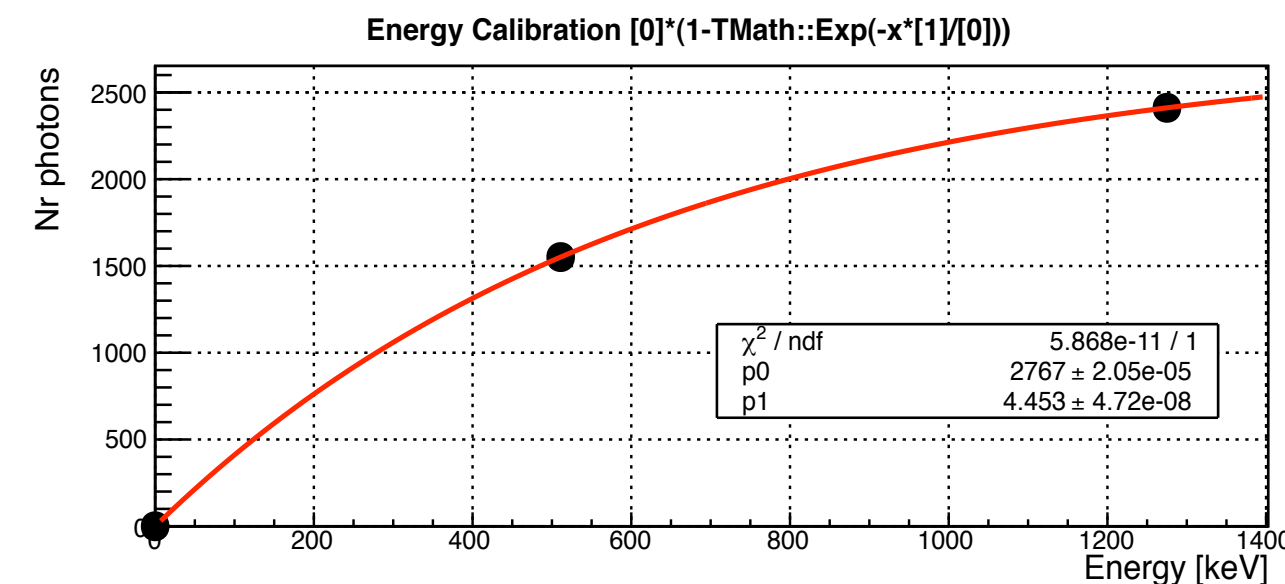


D-SiPM: first preliminary results

Raw LYSO spectrum, Na-22 source



LYSO light yield

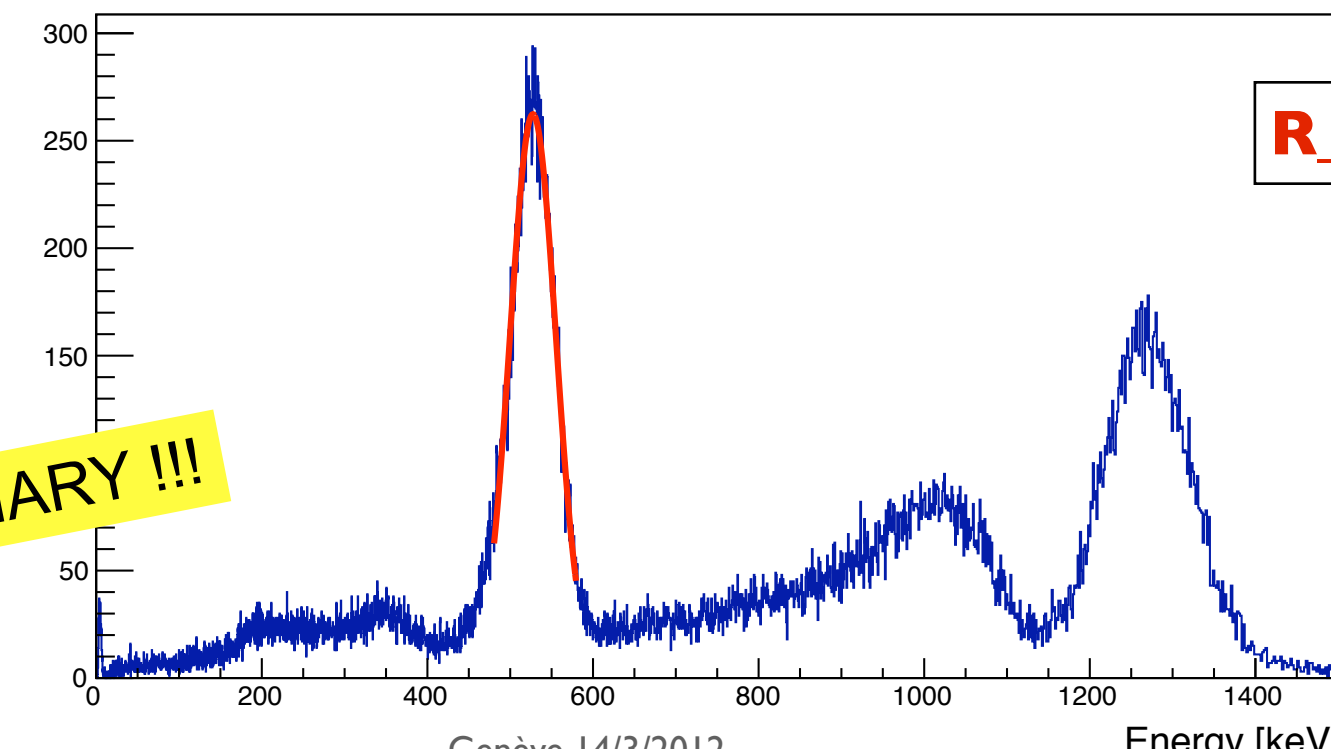


LYSO energy spectrum, Na-22 source

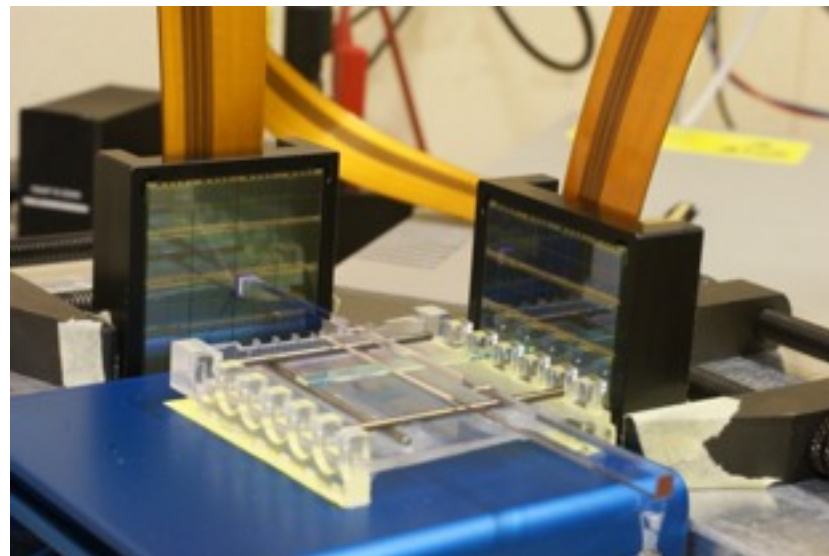
Energy spectrum
(calibrated, corrected
for saturation)

PRELIMINARY !!!

R_FWHM ~ 12.3%



D-SiPM: first preliminary results

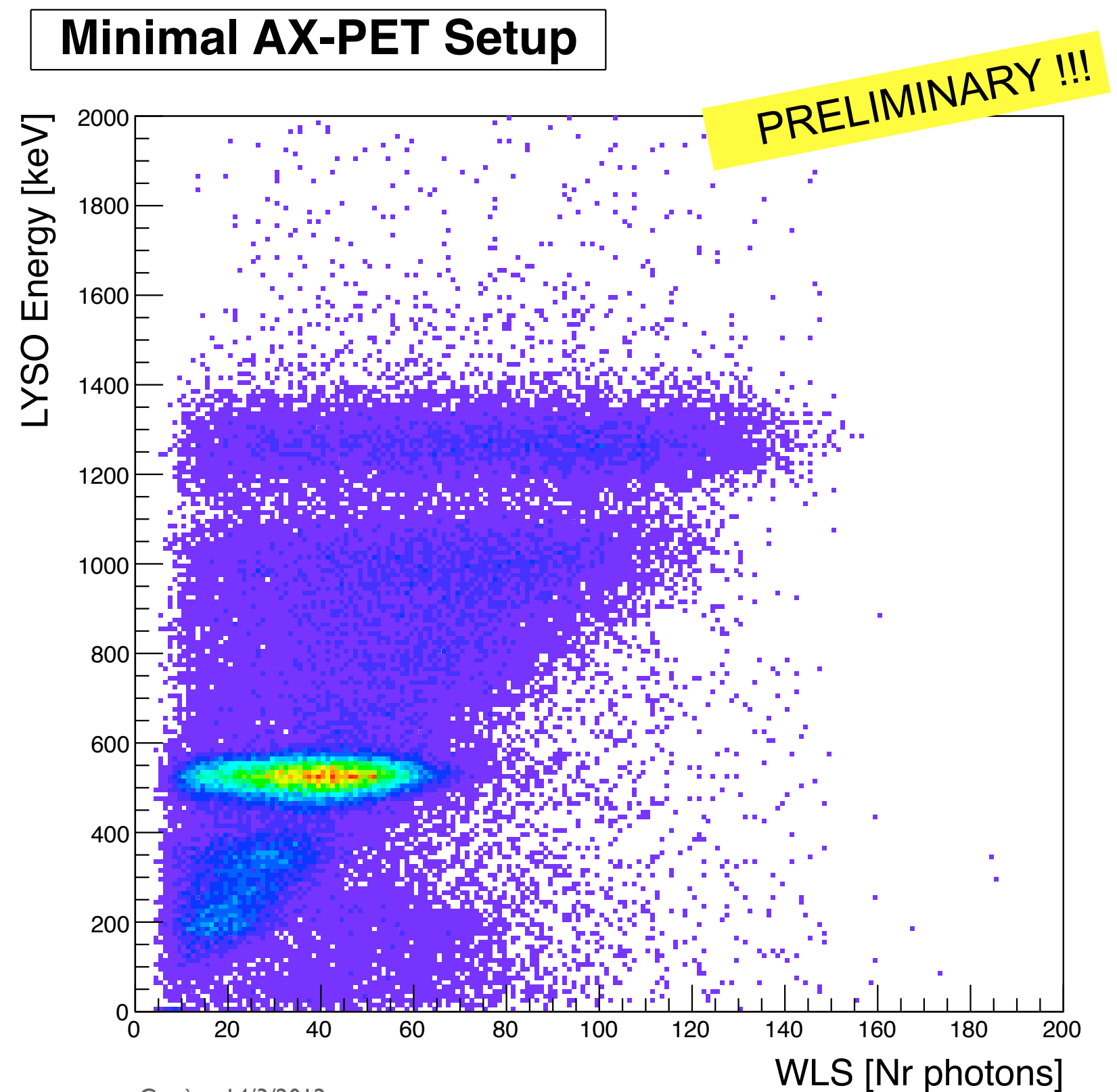


- 2 tiles operated **in coincidence**

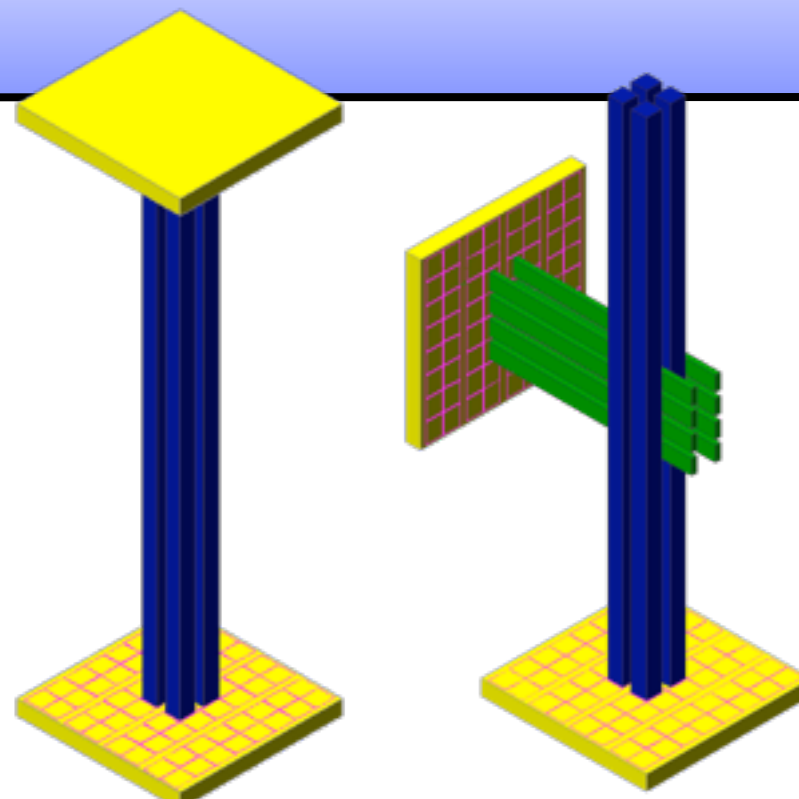
Correlation LYSO / WLS response

Still to do :

- add more WLS strips
- full WLS cluster
- extract axial coordinate



D-SiPM: Outlook



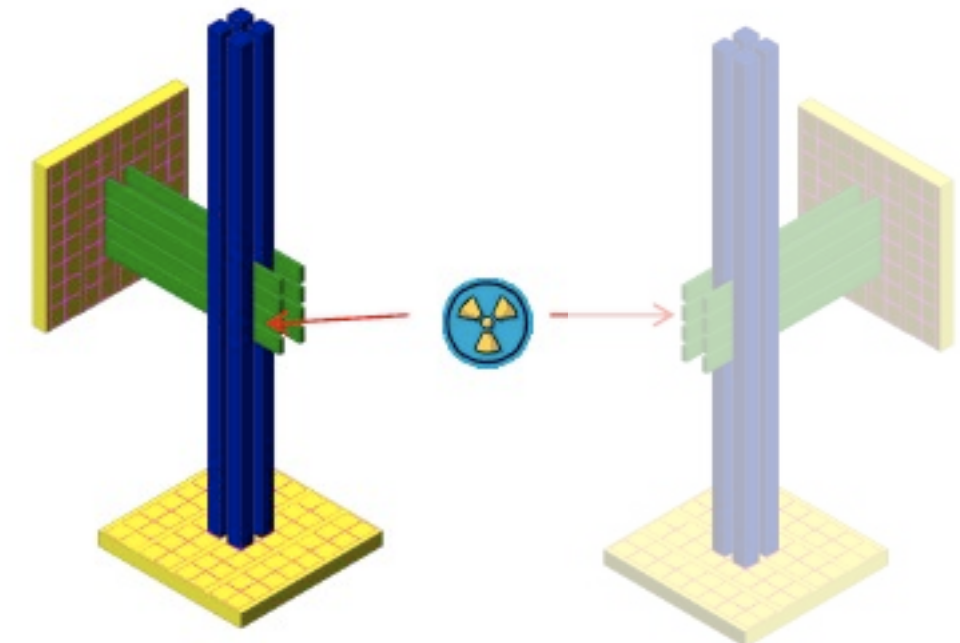
two needed arrangements

Questions to be answered :

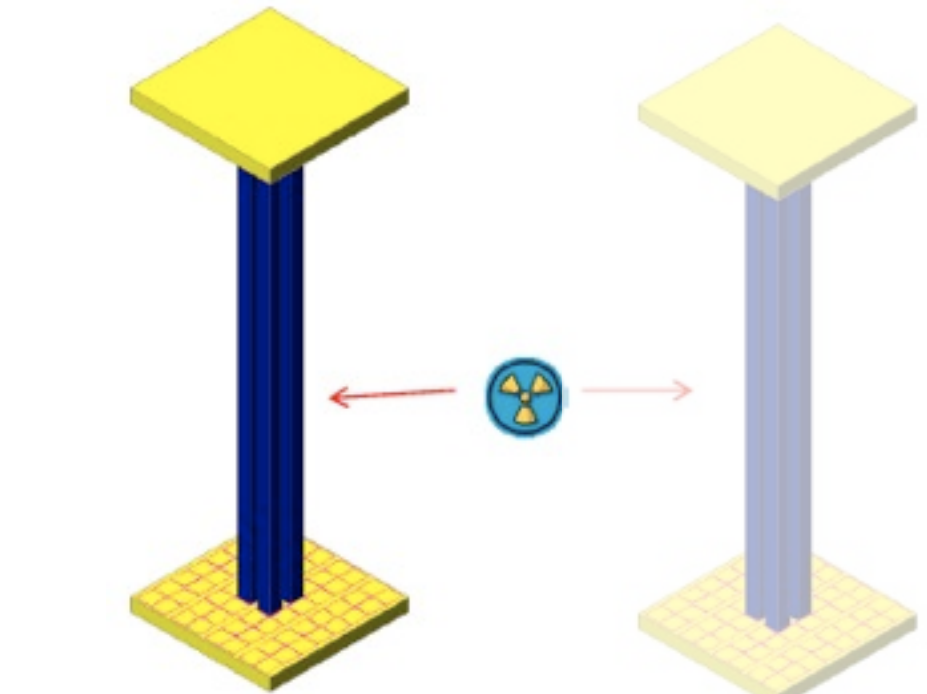
- light yield and $\Delta E/E$ from LYSO crystals ?
- axial coordinate reconstruction: does it work ?
- axial resolution through WLS readout ?
- time resolution (long crystals) ?

coming soon...

AX-PET performance demonstration



timing performance demonstration



Conclusions

Axial concept for a PET scanner :

i.e. long and axially oriented scintillation crystals

Intrinsically parallax free system (DOI information directly from the axial geometry)

Spatial resolution and sensitivity could both be optimized

AX-PET implementation :

3D spatial information of the photon interaction point with :

matrix of LYSO crystals and WLS strips

individual readout of each channel (Si-PM)

Two modules built (i.e. **AX-PET demonstrator**)

Energy resolution ~ 12% FWHM, @ 511 keV

Spatial resolution ~ 1.35 mm FWHM

(competitive with state of the art PET)

► **calorimeter with tracking capabilities (granularity)**

► **novelty as a PET detector :**

- geometry

- WLS implementation

- module sum / trigger

- Compton scattering reconstruction

Fully simulated device

Simulations - fully validated on the demonstrator - will assess the final performance of an hypothetical full ring scanner. **Flexible design:** scalable in size / dimensions / nr. layers....

=> flexibility in the final target of AX-PET (small animal PET / brain PET)

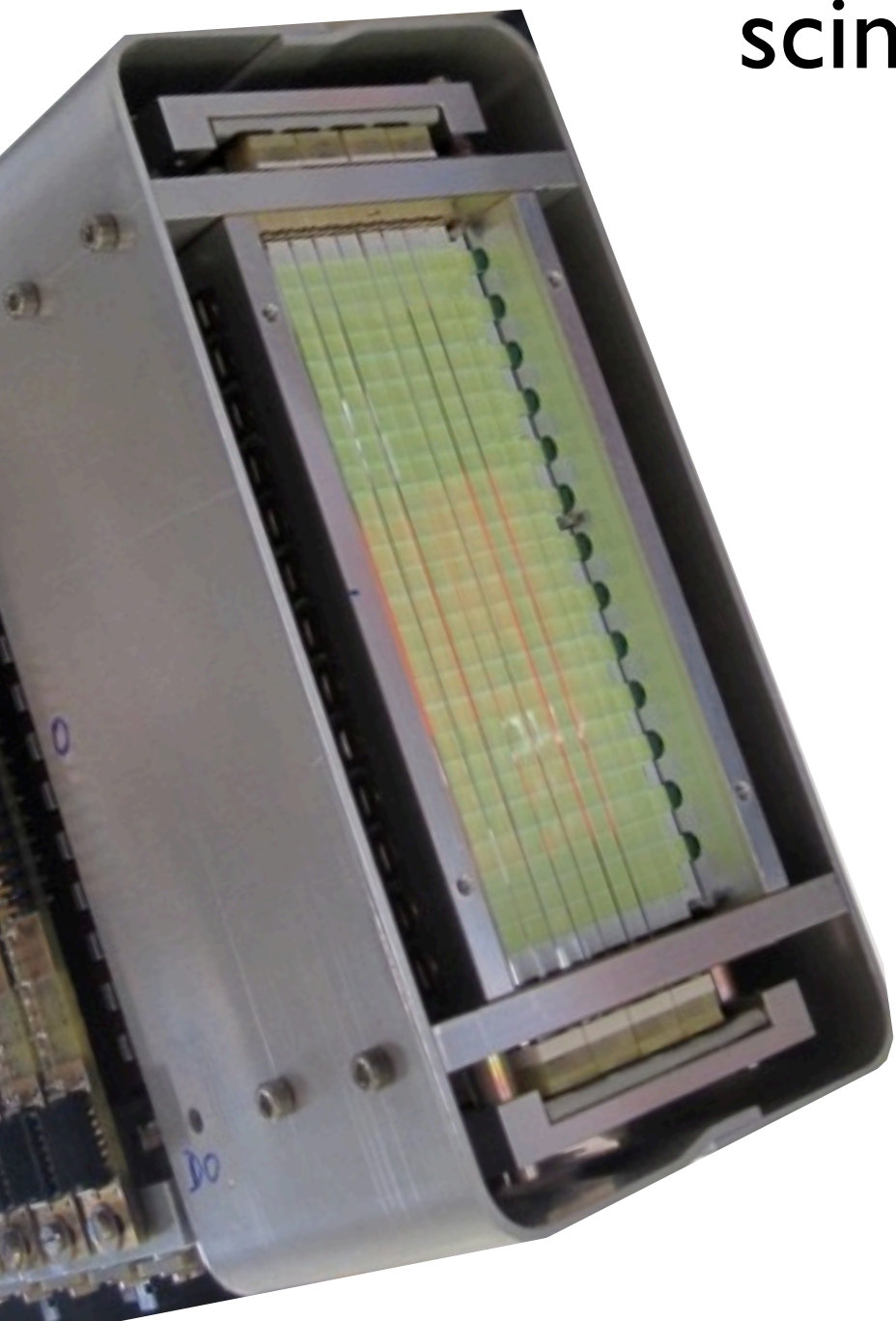
AX-PET demonstrator :

Extensively tested with sources and successfully used with phantoms !

Currently under test :

Digital SiPM as alternative for photodetector for AX-PET (TOF capabilities)

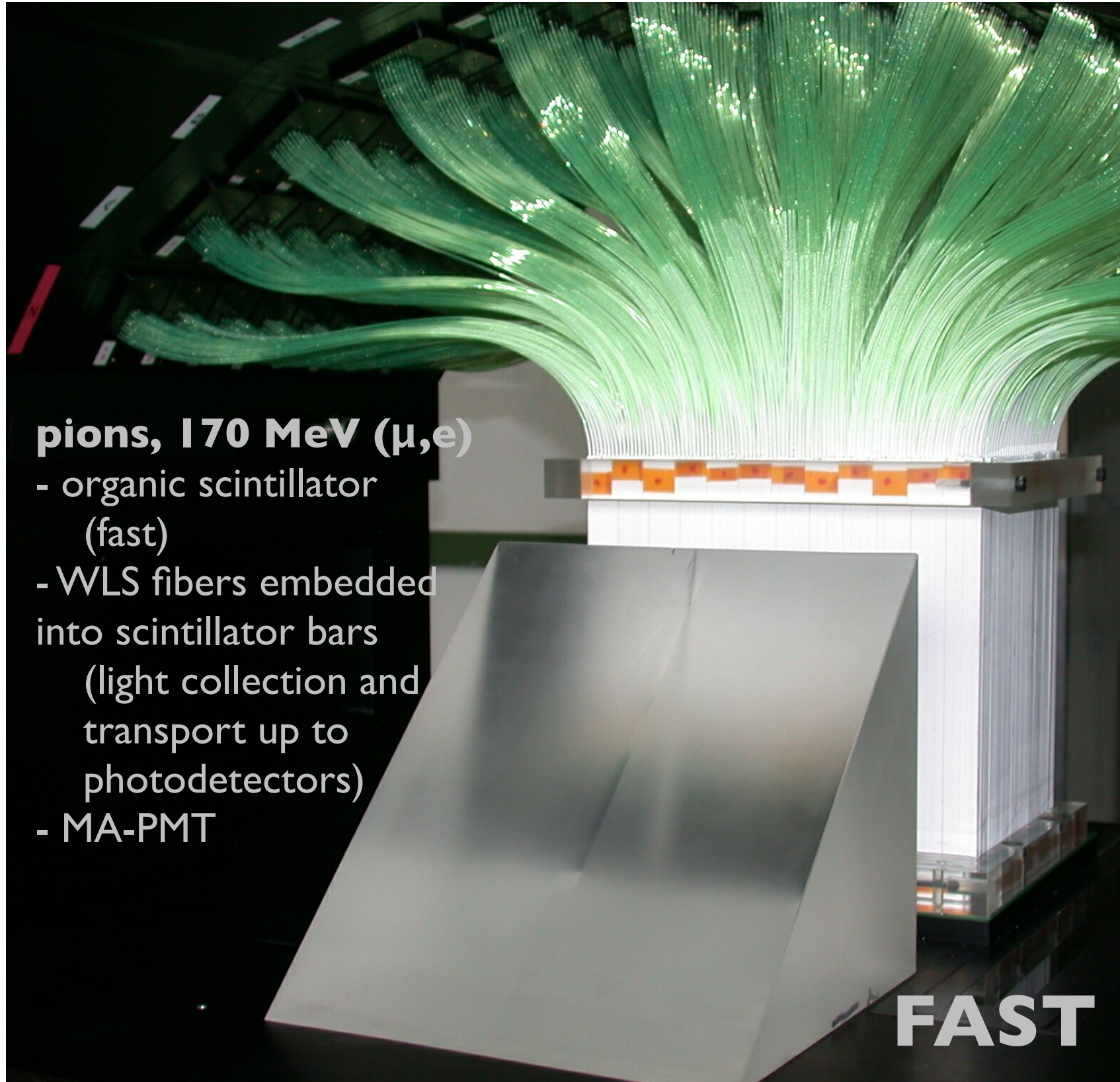
scintillator bars and WLS...



AX-PET

photons, 511 keV

- inorganic scintillator
(high Z, high ρ , high light yield)
- unwrapped scintillator bars
- WLS strips (for axial coord.)
- Si-PM



FAST

Conclusions







AX-PET collaboration

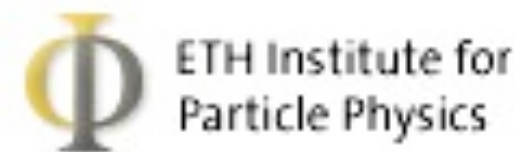
A. Braem, M. Heller, C. Joram, T. Schneider and J. Séguinot
CERN, PH Department, CH-1211 Geneva, Switzerland

V. Fanti
Università e Sezione INFN di Cagliari, Italy.

C. Casella, G. Dissertori, L. Djambazov, W. Lustermann, F. Nessi-Tedaldi, F. Pauss, D. Renker¹, D. Schinzel²
ETH Zurich, CH-8092 Zurich, Switzerland

¹ Currently with Technical University München , D-80333 München, Germany

² Currently with Massachusetts Institute of Technology, Cambridge 02139-4307, USA



J.E. Gillam, J. F. Oliver, M. Rafecas, P. Solevi
IFIC (CSIC / Universidad de Valencia), E-46071 Valencia, Spain

R. De Leo, E. Nappi
INFN, Sezione di Bari, I-70122 Bari, Italy

E. Chesi, A. Rudge, P. Weilhammer
Ohio State University, Columbus, Ohio 43210, USA

E. Bolle, S. Stapnes
University of Oslo, NO-0317 Oslo, Norway

U. Ruotsalainen, U. Tuna
Tampere University of Technology, FI-33100 Tampere, Finland

